Defence Research and Development Canada
Recherche et développement pour la défense Canada

Project to Study Soil Electromagnetic Properties

Final Report

R.C. Bailey and G.F. West, Department of Physics, University of Toronto

Contract Scientific Authority: Y. Das, DRDC Suffield

Defence R&D Canada

Contract Report

DRDC Suffield CR 2009-051

September 2007

Canada

Project to Study Soil Electromagnetic Properties

Final Report

R.C. Bailey and G.F. West
Department of Physics, University of Toronto
60 Saint George Street
Toronto ON M5S 1A7

Contract Number: W7702-03-R942

Contract Scientific Authority: Y. Das (403-544-4738)

Defence R&D Canada – Suffield

Contract Report

DRDC Suffield CR 2009-051

September 2007

PROJECT TO STUDY

SOIL ELECTROMAGNETIC PROPERTIES

Final Report

Contract # W7702-03-R942

R.C. Bailey & G.F. West

30 September 2007

Department of Physics

University of Toronto

Project duration:

1 Sep. 2003 - 31 Mar. 2007

Scientific Authority:

Y. Das, Defence R&D Canada, Suffield, Alberta.

Summary/Abstract

The research covered in this contract is directed to improving the effectiveness of EMI mine detectors of the kinds typically used in humanitarian demining. More specifically, it focuses on the effect of "difficult" (ferromagnetic mineral containing) soils on performance of the detectors. It began with a period of exploratory studies and goal identification; with the objectives then being specified more clearly. Originally, the main objective was a computer modelling code which could also model the problematic soils. The chief variation from that plan was inclusion of an instrument development and a sample measurement phase. Originally, the program was intended to finish by 31 March 2006, but because of the success of the instrument phase, it was extended an additional year to allow for construction of two additional instruments for delivery to the Scientific Authority, and also to allow results of earlier phases to be incorporated into the modelling code.

The overall purpose of the project is to facilitate the design of electromagnetic induction (EMI) mine detectors for humanitarian demining purposes. The specific aim is to help designers optimize the ability of these devices to detect low metal, anti-personnel mines in what are called "difficult" soils (considered here mainly to be those soils that contain appreciable quantities of electromagnetically lossy ferromagnetic minerals).

Present day EMI mine detectors are already very refined devices. If one is to improve them appreciably, one must not only be able to simulate a hypothetical instrument's response to typical target objects but also be able to simulate typical kinds of interference arising from the earth environment. From a theoretical point of view, creation of the simulation code is a technically complicated but feasible task. However, the code can only serve its purpose if enough quantitative information is available not only to describe the metal objects typically found in anti-personnel mines but also the electromagnetic properties of the soils in which they are found. It was to get some initial observational data for this that an instrument development part was included in the project.

Deliverables provided by the project are the following:-

1) A simulation code (called University of Toronto EMI Simulator, or UTEMIS) which is written in and (currently) runs in the MatLab R14 programming environment, and is controlled from a versatile MatLab Graphical User Interface (GUI).

2) Two EMI spectrometers for measuring the EMI properties of small objects or soil samples in the frequency range 70 Hz - 70 kHz. (University of Toronto EMI (UTEMI) spectrometers).

3) A suite of measurements made using the prototype version of the above instruments on

soil samples and metal mine simulants supplied by the Scientific Authority.

4) Three open scientific publications, given at SPIE conferences and published in the SPIE Proceedings, and delivered as electronic documents.

5) Various project reports to the Scientific Authority, and manuals and reports ancilliary to items 1-4 (delivered as electronic documents).

6) This overview (Final Report).

CONTENTS

Outline of Project Components

1. UTEMIS Code

This is a MatLab code (Utemis) which is run via a MatLab Graphical User Interface (GUI). It has been written almost entirely by R. C. Bailey, although it does use some algorithmic methods suggested by G. F. West. Code testing was done by summer student J. Saarimaki.

The code provides a means of simulating the response of a specified EMI metal detector due to a magnetic and/or conductive ground that may contain small ferromagnetic and/or electrically conductive objects. It is a flexible system that allows a variety of computational components to be integrated with a variety of graphic displays, enabling a researcher to explore various EMI scenarios. With some elaboration it could be turned into a training module for users of EMI detector.

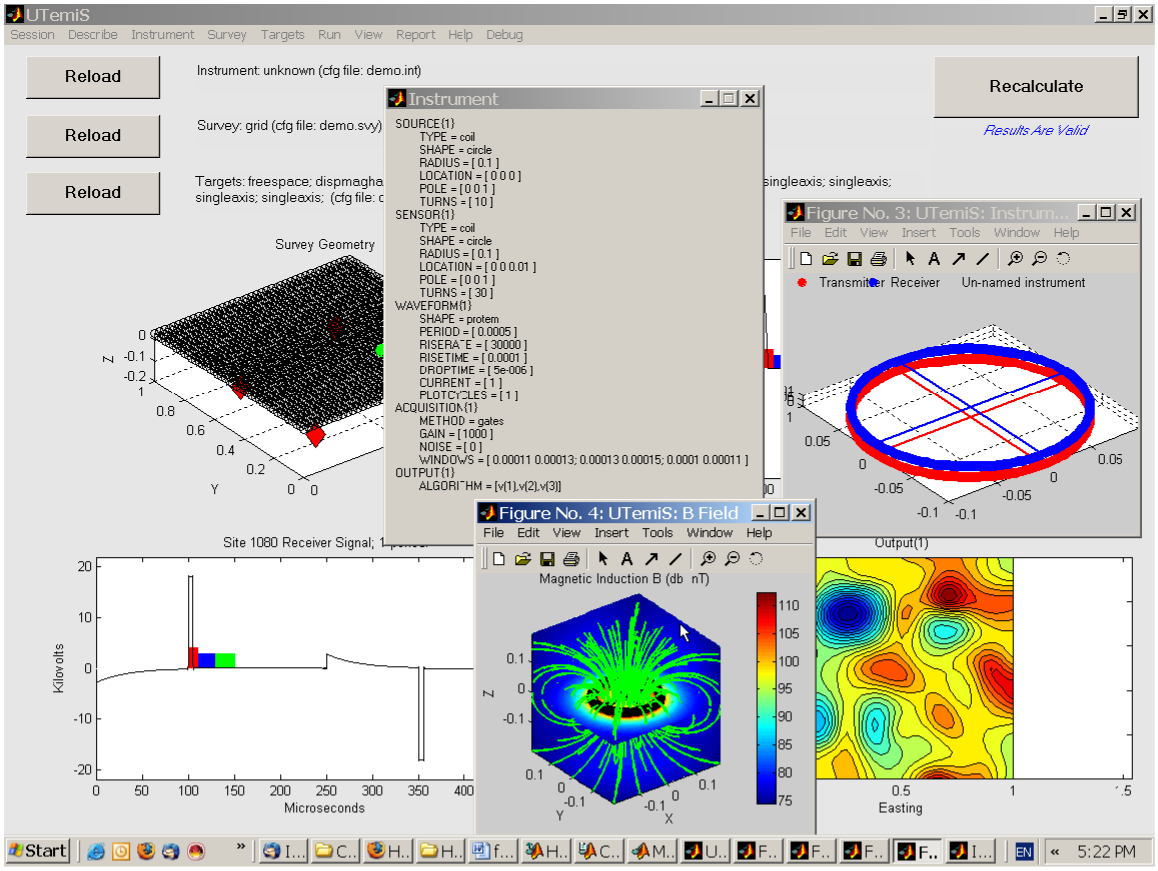

Figure 1.1 *Screenshot of the UTemiS Graphical User Interface, with some auxiliary information windows.*

In UTEMI simulation, an EMI detector is considered to consist of one or more loops of thin conducting wire. The loops may have arbitrary shape. A time-varying current is impressed in one or more of them (called the transmitter or Tx loop) by some sort of electronic signal generator, thereby generating a time-varying magnetic field in the vicinity (called the primary magnetic field). The primary magnetic field then may induce magnetizations and /or eddy currents in the nearby earth (or parts of it) which will create their own (secondary) magnetic fields. In a standard EMI detector, secondary magnetic field is observed by the voltage it induces in an unloaded receiver (Rx) loop. The Rx loop may be the same as, or distinct from the Tx loop. It is assumed (with good evidence) that practical primary and secondary EMI responses are linear in the Tx current. Thus, response of a detector may be characterized by the primary and secondary transimpedances (V_{Rx} / I_{Tx}) of the detectors Tx and Rx coils.

In general, the primary magnetic field is much stronger than any secondary magnetic field, and it can induce a much stronger voltage in the Rx loop than the secondary field. Thus, practically all EMI detectors incorporate a means for separating the secondary and primary signals. A common scheme is to make the Tx current vary in a transient fashion, and to search for secondary field signal shortly after the transient primary current has ended, i.e., at a time when the primary current vanishes or is accurately constant. Another is to use an alternating Tx current and somehow cancel (buck out) the normal primary Rx signal with a signal derived from the Tx current. If the bucking is sufficiently complete, small secondary signals can be fairly easily observed in the residual signal. A third method is to arrange that the Rx and Tx are null-coupled to one another (in free space).

In the UTEMIS modelling algorithms, loops are considered to be single or multiturn, thin filaments, and to be circular, or of arbitrarily polygonal shape, or of limitingly small diameter (dipoles). The simulator permits the Tx excitation current to be alternating at a list of frequencies, or described by an arbitrary (specified) periodic waveform that may include discontinuities. Since practical EMI metal detector loops have dimensions of a meter or less, and the time-variation of the Tx loop current is always relatively slow (usually < 1MHz), delays associated with the propagation of fields are entirely negligible (~3.3 ns/m). Thus, anywhere within the useful range of an EMI detector, the Biot Savart law may be used to calculate the magnetic field of the current in the Tx loop and Faraday's law of induction to calculate the induced voltages in the Rx loop.

Conceptually, the UTEMI simulation concentrates on two types of EMI target models:- a) a background half-space earth medium which is approximately uniform or stratified in its properties and which may be somewhat conductive and/or ferromagnetic, and b) discrete, small objects located in the host half-space that may respond to a primary magnetic field by induced magnetization and/or by eddy current induction. The EMI-detectable content of an actual low metal mine may need to be described as a group of several, differently positioned

and oriented, small objects. The response of the EMI detector to the targets and host space is considered to be accurately enough represented simply by adding the responses of individual targets calculated as if they were in free space. Because, for realistic ranges of earth parameters, host space secondary field as a fraction of primary field is very weak, any electromagnetic interactions between target and host usually can be neglected. Similarly, interactions between the various different objects in a target are not likely to be very significant unless the parts are very intimately associated (e.g., a metal spring surrrounding a metal rod), and then they can be considered together as a single object.

The response of a small target is calculated from the free space, vector magnetic field, Green's functions for the Rx and Tx at the target centre. Target response (induced magnetic moment / inducing magnetic field, or **m/H** --- here called target "magnetance") is a second rank Cartesian tensor at any single frequency, and for objects with orthorhombic or higher symmetry, each principal component of the tensor may respond with an different frequency spectrum. In the most general case, the orientation of the principal axes may also be frequency dependent and the tensor spectral characteristics more complicated. The program provides for the input of measured spectral responses of real objects or for estimation of these responses by using simple models like a loop, a sphere, or an ellipsoid. The simulator can generate maps or profiles of (target+ host) response versus detector position as well as waveform details or frequency spectra of the responses at specific detector locations.

Response from the host environment is calculated using one of two methods. Both initially treat the host medium as a half space having uniform or uniformly layered properties. From this response, the response of a somewhat heterogeneous host medium can be estimated.

The first (and simplest) method treats the medium as a uniformly magnetically susceptible half space whose susceptibility may be frequency dependent and complex, and it is based on an image solution of the half space magnetostatic boundary value problem.

The second treats the host space as a conductive and susceptible uniformly layered half space (in which susceptibility and conductivity may be complex and frequency dependent) and uses the well known layered half space formulation of the full EM boundary value problem in frequency and radial wavenumber (Hankel transform) domain.

The full calculation is a much larger task and therefore slower than the magnetic solution, and is limited in the present software to the case of circular Rx and Tx coils that lie horizontally. It is useful for checking whether any conductive effects can be expected. Except when the host medium is very porous and sea-water saturated, and for ordinary EMI detector frequencies, the first method is likely to be sufficient.

The effect of a heterogeneous host medium is estimated by statistically based modification of the uniform host medium response. Specific heterogeneities within a host medium such as the void response created by a nonmagnetic and nonconductive boulder can be simulated using the algorithms for target objects.

An important feature of the UTEMI Simulation software is its treatment of response spectral characteristics. Certain of the modelling algorithms are more easily formulated in frequency-domain than any other, while the EMI detector of interest may operate with a complicated waveform and the measurement operations may involve time-domain waveform sampling.

UTEMIS uses a systematic and complete description of the instrument geometry and the Tx current waveform, and of those specific aspects of the Rx voltage waveform that determine each "output" from the detector, and it combines this with an economical spectral representation of the modeled earth response that embeds the diffusive nature of the physics. The earth response of an instrument is its secondary trans-impedance (the transfer function describing the secondary Rx voltage due to a given Tx current). UTEMIS describes it with a restricted sub-class of the widely used pole -zero representation of realizable transfer functions; one in which all poles are on the damping axis and all zeros are at the origin because the relevant physics is purely diffusive. We call this an NDP spectral model (after the usual symbols for three types of parameter employed by the representation) or a "damped pole" representation. Usually only 6-15 coefficients are necessary to represent a physical EMI response accurately over more than 3 decades of frequency. In UTEMIS, all measured target responses are directly handled in this manner. However, certain theoretical model responses (such as the conductive stratified earth model) are calculated directly in frequency-domain (or what ever domain is most computationally convenient), and then that result is least squares-fitted by an NDP representation in order to connect it to the instrument's spectral description.

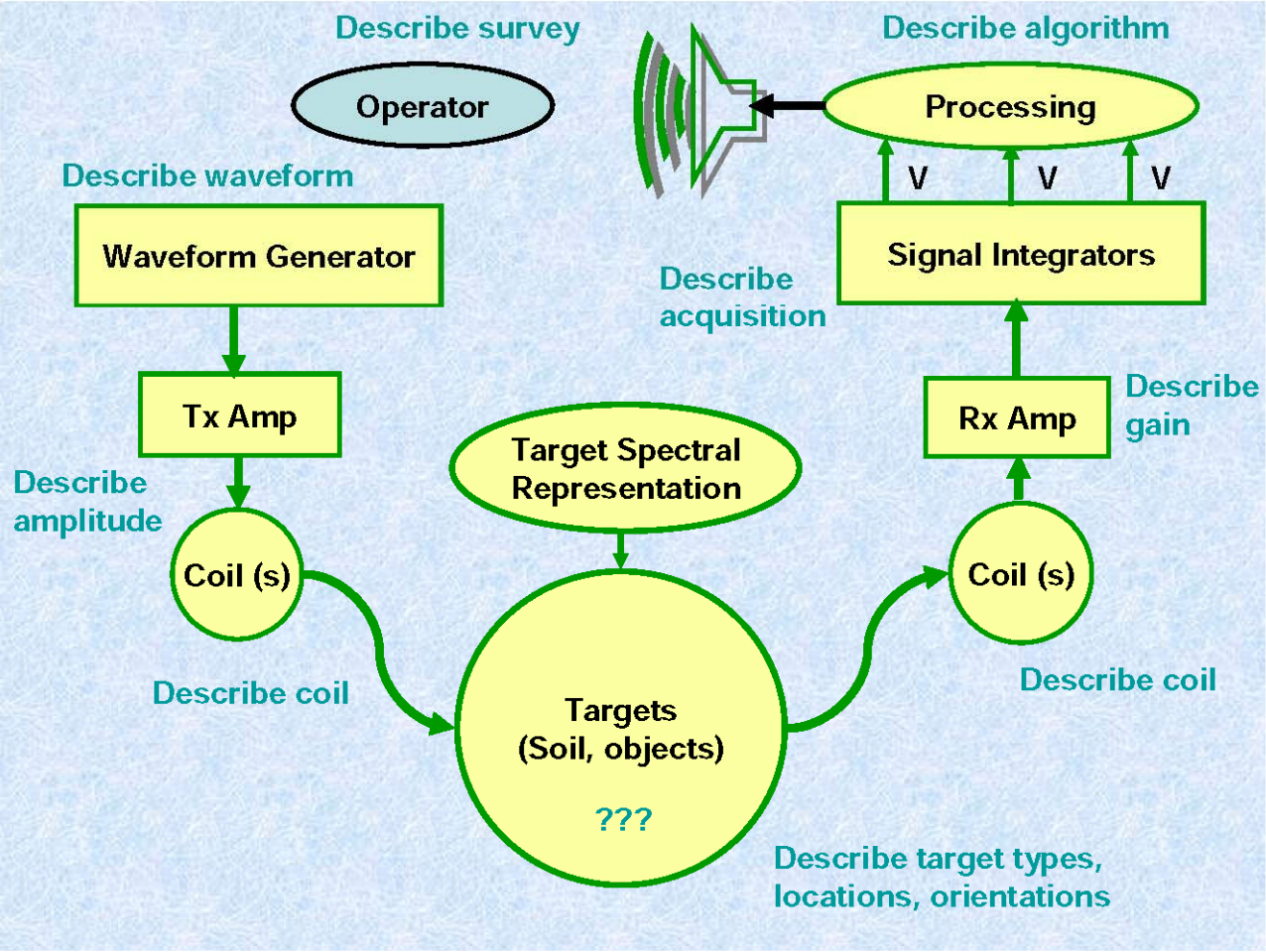

Figure 1.3 A schematic view of the conceptual view of the computational sequence and relationships discussed in the text.

The UTEMIS code is run from a MatLab GUI (graphical user interface) with a plethora of display and control capabilities. The code is modularized, and is extensible to treat other modelling situations. Information is input to the code mainly via three user-supplied and user-editable text files; one for describing the EMI instrument(.int), one for the survey performed by the instrument over the target space (.svy), and one for describing target parameters and geometry (.tgt). In the ".tgt" description of the various target items, each item includes a key word that couples that target's sets of parameters to a specific modelling module in the simulator code. The modelling module takes survey and coil geometry information from the ".svy" and ".int" files and delivers results in NDP form to output modules of the GUI so that results can be displayed on the screen in one of the many possible forms, or output files can be created for further processing of the results.

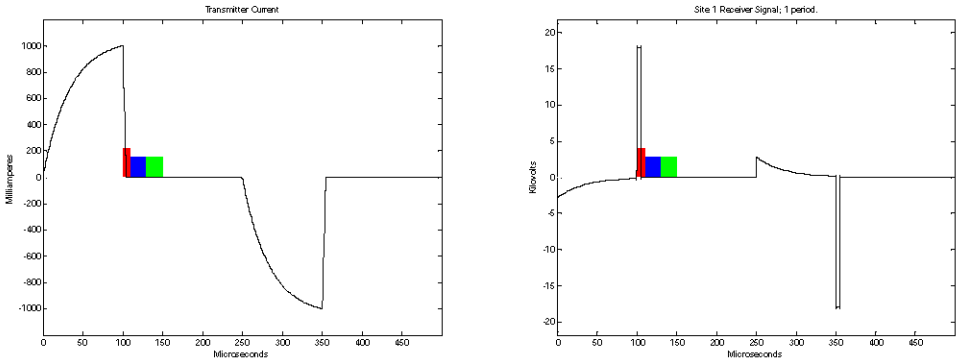

Figure 1.3 *GUI detail: a time-domain instrument waveform and its calculated response. Instrument measurement time-gates are shown in colors.*

2. UTEMI Spectrometer

The University of Toronto EM induction spectrometer (Utemis) is a transportable tabletop instrument for measuring the time-varying magnetic moment induced in small, laboratory-scale samples by a time-varying, spatially uniform, magnetic field. Specimen dimensions (optimally) are ~ 3 cm; the spectral range of measurements is 80 Hz to 70 kHz. The instrument measures what we call the axial magnetance of the specimen:-(induced magnetic moment/ exciting magnetic field strength = m/H, both vectors on same axis) at ~ 35 frequencies, or its volume-normalized equivalent, volume magnetic susceptibility (= K). For a usual 12.5 ml sample, the noise level is about 0.02 mSIU of volume susceptibility or ~0.2 microlitres of magnetance. Sample magnetances over 10 ml and volume susceptibilities over 1 SIU can be measured. Provision is made for rotating the sample about one axis, to enable full tensor measurement.

The instrument was conceived and designed by G. F. West, as was the first prototype that remains at U. of T. Programming of the MatLab GUI that runs the instrument was mainly by summer student Xiaoyu Yu. The two instruments delivered under this contract are very similar to the first prototype, but the main components were custom manufactured by Geosensors Inc of Toronto.

The spectrometer consists essentially of a set of six coaxial coils symmetrically disposed about the sample point. It is shown schematically in Fig. 2.1 and a picture is shown in Fig. 2.2. The inner pair are the principal sensors of the magnetic moment induced in the sample. The middle pair generate the exciting magnetic field, the outer pair are auxiliary sensors whose roles are to provide a primary field reference signal and to cancel most of the primary field coupling between the transmitter coil pair and the set of receiver coils. The symmetric pairing makes it possible to achieve a high degree of uniformity in the excitation field and the sensitivity to an axial dipole source in the sample region as well as cancellation of sensitivity to external noise fields.

The Utemi Spectrometer works by comparison of two signals; measuring the complex ratio of a sample and a reference signal. Its calibration is thus not dependent on excitation level or gain setting and is "built in" to the coil design. Tests on high quality ferrite samples and on a manufactured wire loop show that maximum calibration errors are less than a few percent and that variation of spectral amplitude over the whole observation range is accurate to within about 1% for easily measured materials.

The support electronics consist of a power amplifier unit to drive the transmitter coils and a pair of preamplifiers for the signal and reference sensor coils. A two channel (stereo), 24 bit,

192 kHz sound card in a small computer allows digital generation and analysis of transmitted and received signals via MatLab built in functions.

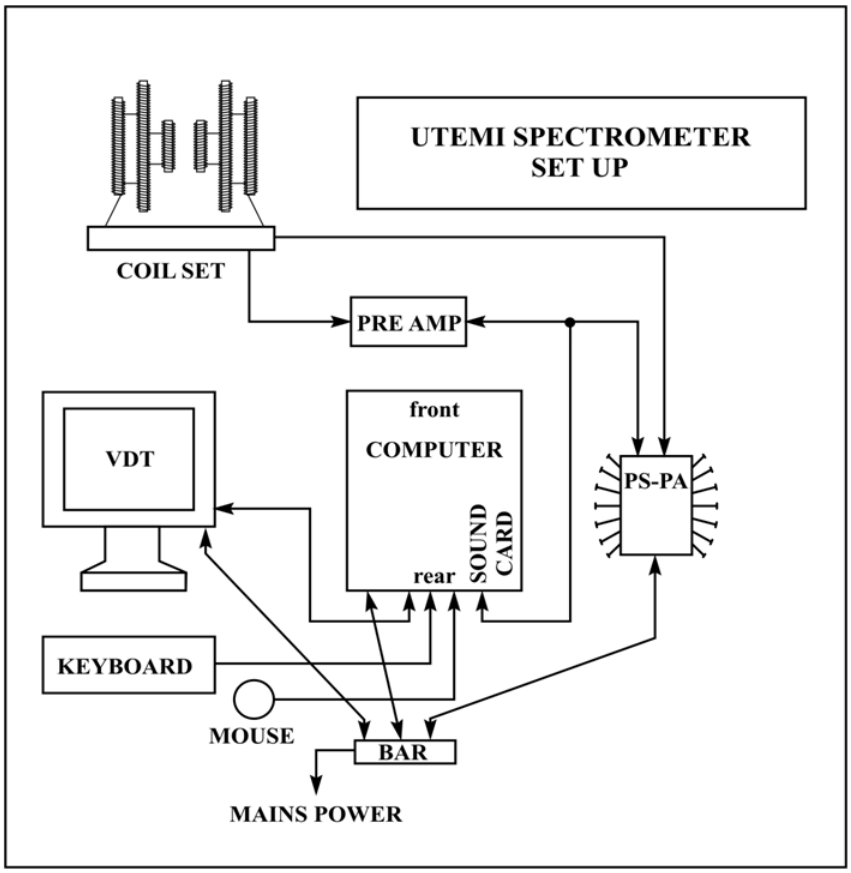

Fig. 2.1 Schematic diagram showing interconnection of the UTEMIS components

.

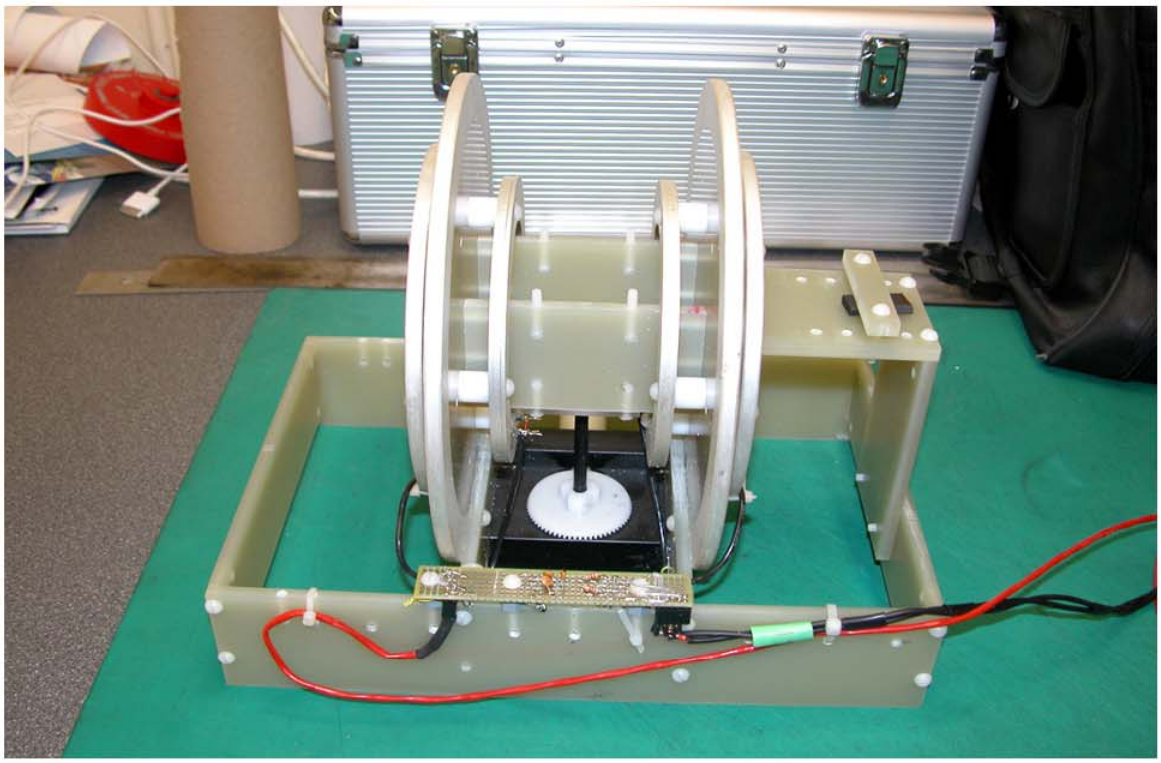

Fig.2. 2: UTEMI Spectrometer Coil Set; view from rear.

The UTEMI Spectrometer is run from a GUI operating on the associated computer. In the present prototype form of the instruments, the software must be run directly in MatLab R14 (or higher). Thus, the instrument user must licence MatLab from MatWorks in order to run the spectrometer. For future systems, it is expected that it will be possible to compile the operating software, so a general MatLab licence will not be required. A Windows XP OS software is employed and a basic set of utility programs for servicing and testing the spectrometer are provided.

The Utemis 1.1 prototype instruments delivered under the contract consists of a Penguin 1630 ABS foam-lined packing case containing the following items:-

1. Spectrometer coil-set, with connecting cables to preamp and power amplifier (Coil Set).
2. Sample holder rotation actuator (Sample Rotator)
3. Power Supply and Power Amplifier (PS-PA) module.
4. Preamplifier module (PreAmp).
5. Shuttle AMD64 WinXP computer (Computer) containing one RME Hammerfall sound card.
6. A 17'" liquid crystal TFT Video Display Terminal (VDT)
7. A compact format ASCII Keyboard
8. USB Mouse

9. Interconnecting and power cables for the above.
10. Box holding samples, sample containers and ancillary components
11. 2 Folders containing instructions, software CD's, component documents
12. Power bar extension cord

3. Sample measurements (Soils and mine EMI simulants)

The scientific authority (Y. Das) supplied a set of bottled sample materials to the project. These included (sterilized) soil samples from EMI mine detector test sites in five countries, four synthetic ferromagnetic soils made from magnetite and construction grade sand, and a suite of standard metal objects that are considered to approximate those found in various types of AP blast mines. Aliquots of these materials were set up in standard polystyrene "pill box" vials for use in the spectrometer. In some cases it was necessary to dry and crush the original sample in order to get a fine enough grain material that the volume would be meaningful. The mine simulant objects were premounted in small styrofoam blocks. At the susceptibility or magnetance level of these samples, the vials and styrofoam are non magnetic.

Figures 3.1 to 3.3 give some example results.

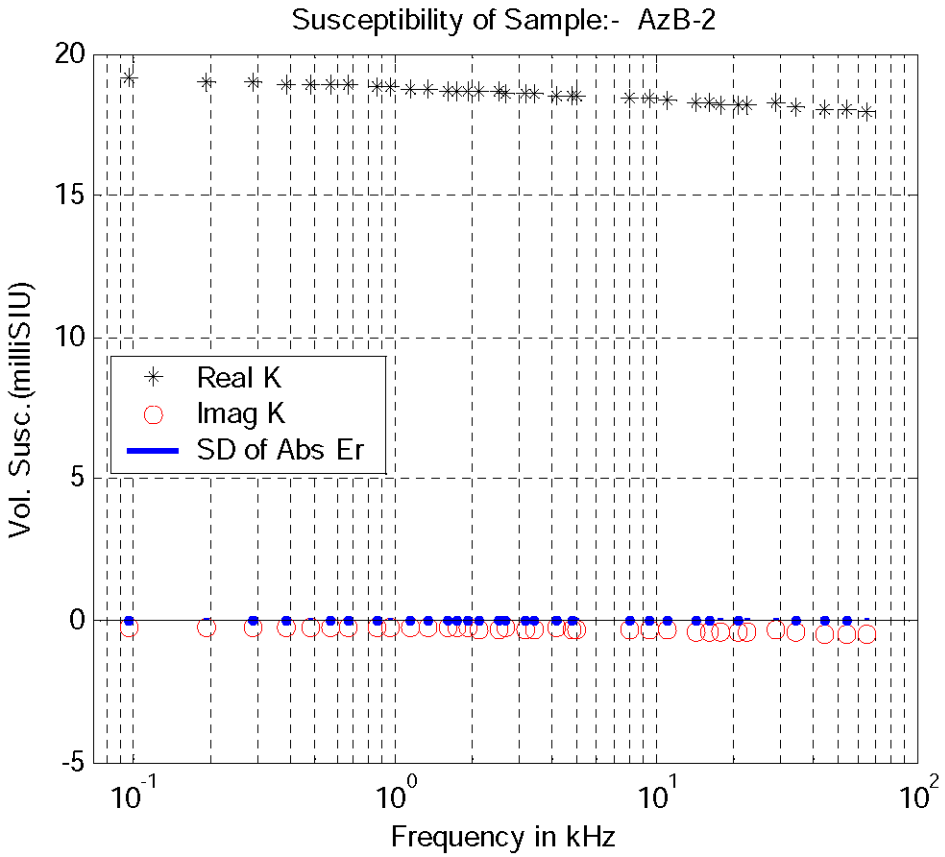

Figure 3.1 *Australian soil from test range; moderately magnetic but only slightly dispersive.*

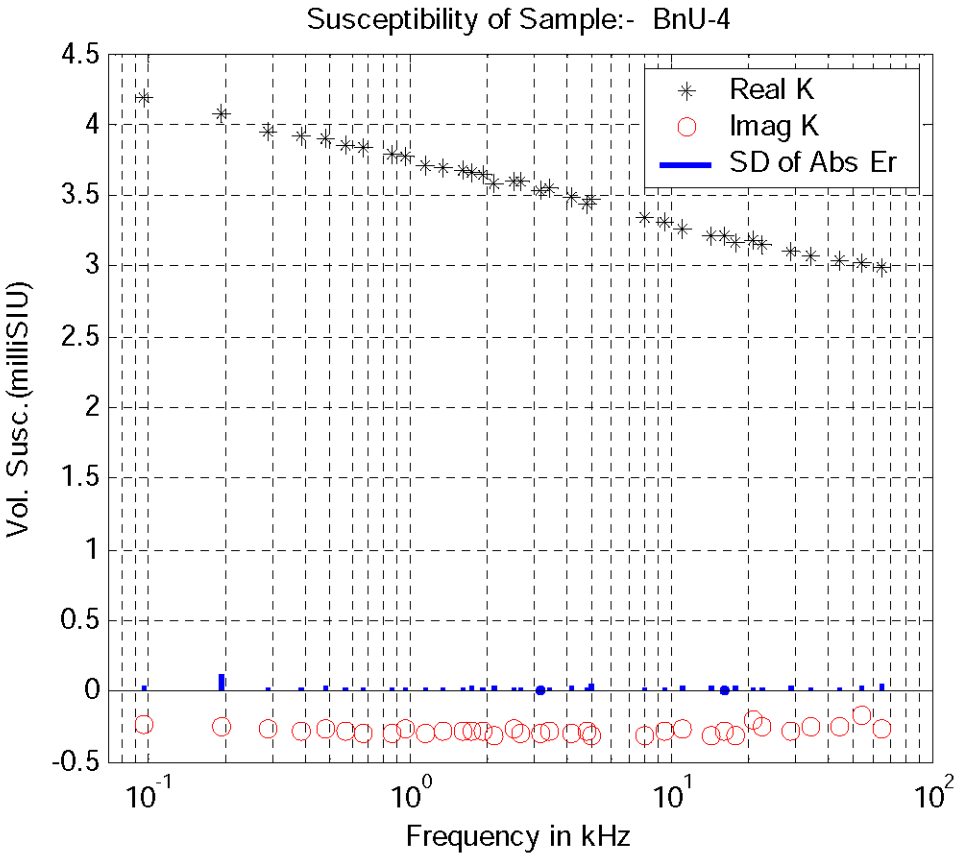
Susceptibility of Sample:- BnU-4
Real K
Imag K
SD of Abs Er
Vol. Susc.(milliSIU)
Frequency in kHz
4.5
4
3.5
3
2.5
2
1.5
1
0.5
0
-0.5
10^-1
10^0
10^1
10^2

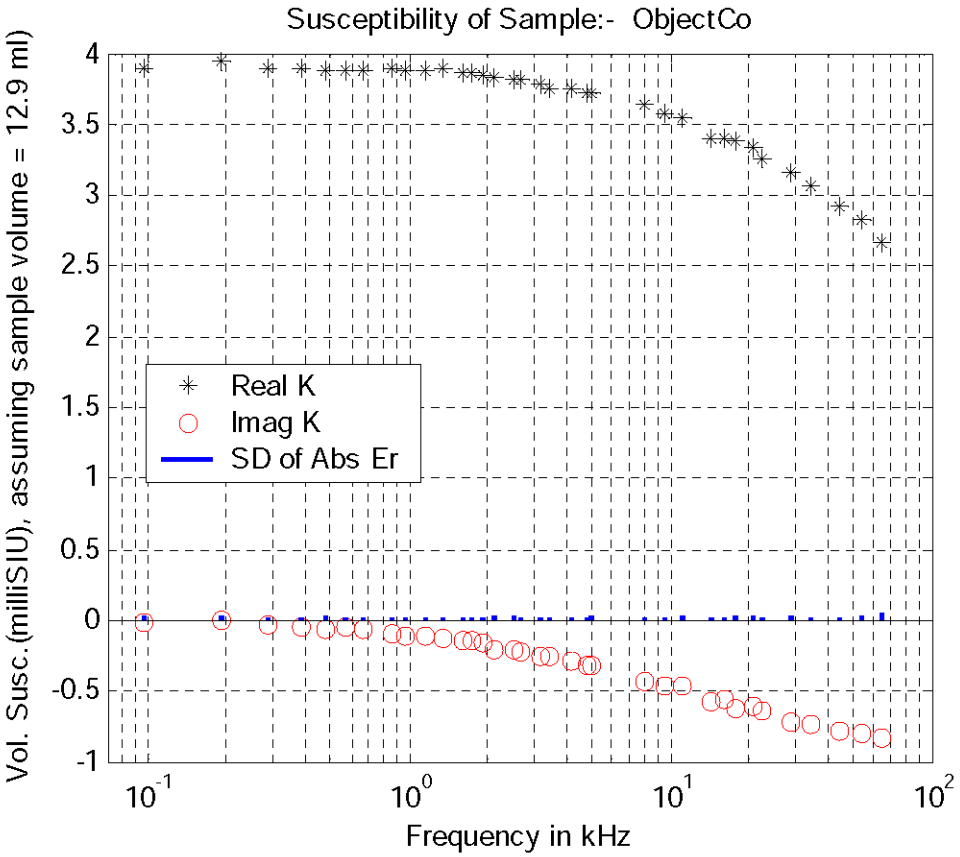

Figure 3.2 Top*: - BnU-4:- Bosnian soil from test site, modestly magnetic strongly dispersive*
Bottom*: ObjCoSpectrum:- ITOP metal detector test object Co, "very difficult to detect", 1/8 in dia carbon steel ball*

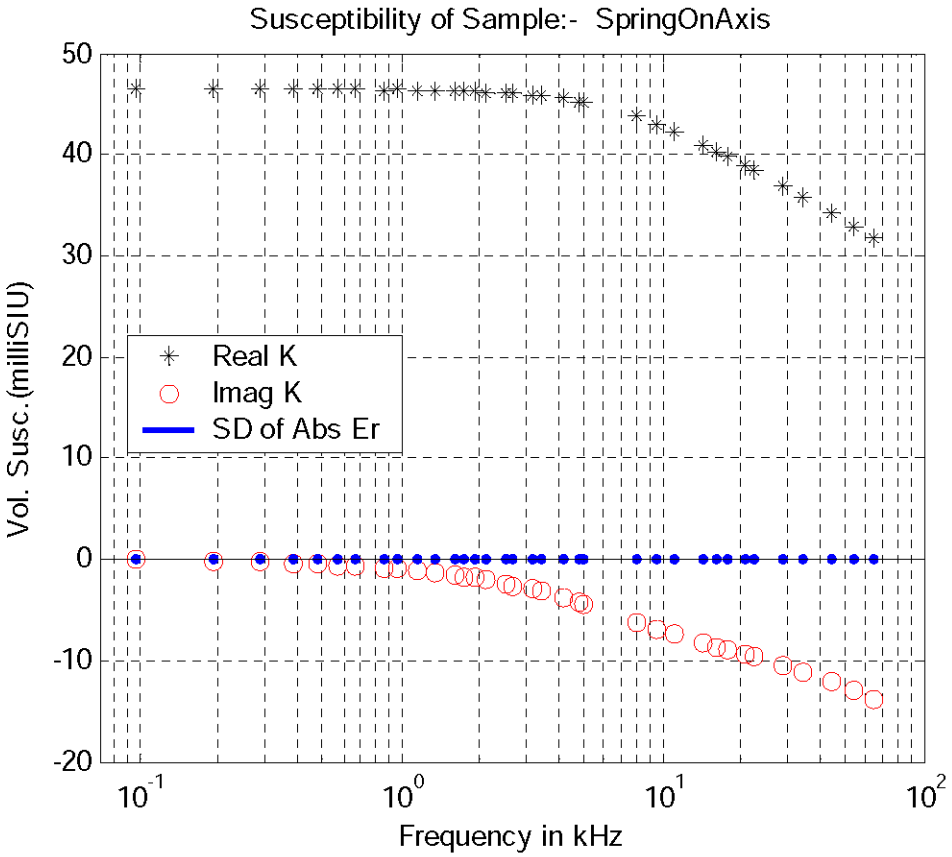
Susceptibility of Sample:- SpringOnAxis
Vol. Susc.(milliSIU)
Frequency in kHz
Real K
Imag K
SD of Abs Er
50
40
30
20
10
0
-10
-20
10^-1
10^0
10^1
10^2

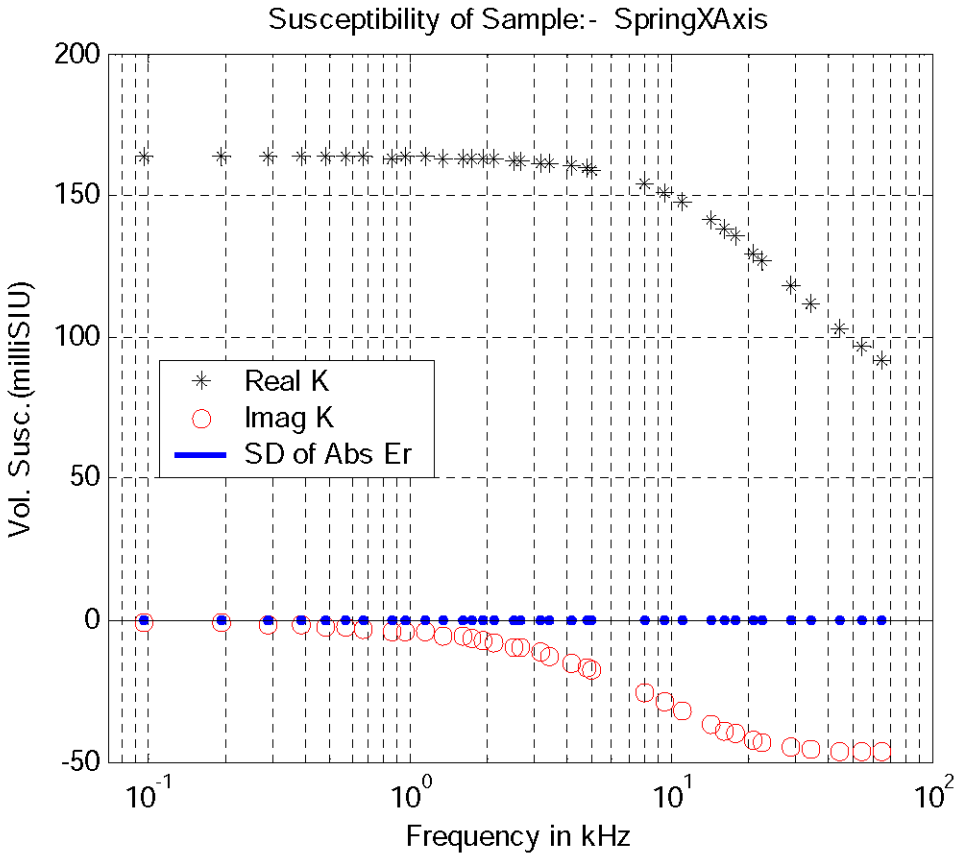

Figure 3.3 Top*: SpringOnAxis:- Part of ITOP metal detector test object Oo, "easiest to detect", Carbon steel spring.* Bottom*: SpringXAxis:- Part of ITOP metal detector test object Oo,"easiest to detect", Carbon steel spring*

4. Scientific publications

Four publications arose out of this work. Three papers, attached as appendices 1, 2, and 3, were presented at the spring SPIE Defense and Security Conferences (in 2005 and 2006) in Orlando, Florida, and printed in the conference proceedings. A fourth was presented orally and as a program abstract at the 18th International Electromagnetic Induction Workshop in El Vendrell, Spain in September 2006. They are listed below, and attached in full as Appendices.

West, G. F. and R. C. Bailey, "An instrument for measuring complex magnetic susceptibility of soils", Proceedings, SPIE Defense and Security Symposium, 17-21 April, 2006, Orlando, Florida USA, 12 pp.

R. C. Bailey and West, G.F., "Characterizing mine detector performance over difficult soils", Proceedings, SPIE Defense and Security Symposium, 17-21 April, 2006, Orlando, Florida USA , 12 pp.

West, G. F. and R. C. Bailey, "Spectral representation, a core aspect of modelling the response characteristics of time-domain EMI mine detectors", Proceedings, SPIE Defense and Security Symposium, 17-21 April, 2006, Orlando, Florida USA, 12 pp.

R. C. Bailey and West, G.F.," Improving electromagnetic induction detector technology in humanitarian demining" IUGG 18th International Workshop on Electromagnetic Induction in the Earth, El Vendrell, Spain in September 2006.

Observations and Conclusions

The contracted program has been successfully accomplished. It has confirmed that several soils known to be problematic for EMI detection of mines are indeed lossy ferromagnetic materials that exhibit a dispersive complex magnetic susceptibility (at least in the frequency range 100 Hz to 100 kHz and likely over a much wider range) wherein the real (in-phase) component of susceptibility decreases almost uniformly with increasing frequency by several percent per decade, and the imaginary part is negative and almost constant with frequency.

Empirically, this dispersive behaviour is intermediate between the classic susceptibility (or magnetance) of an ideal ferromagnetic substance (positive and constant with frequency) and the apparent susceptibility (or magnetance) of a conductive and possibly ferromagnetic object subject to Foucault (eddy current) induction. In the Foucault case, the apparent susceptibility is constant and entirely real at low frequency with a zero or a positive value. But, as frequency is increased, it decreases rapidly over 1 or 2 decades until a negative real plateau value is reached (called the inductive limit). At this limit, the object is excluding magnetic field by induction of a current sheet on its surface. A substantial negative imaginary component appears throughout the transition which, below the transition frequency is proportional to frequency The imaginary component of the field is indicative of ohmic energy loss in the object.

A Foucault induction process usually exhibits a fairly distinct characteristic transition frequency or time constant. For a real discrete object, the transition may not be as abrupt as for an ideal lossy inductor (i.e., single pole response of an ideal resistive wire loop that exhibits only a single time constant), but the time constant range of the response of a single simple object is usually limited. Thus, the response of a lossy soil generally will differ qualitatively from that of a small conductive object, but it is like that of an assemblage of many small ferromagnetic and conductive objects that have a wide range of Foucaualt time constants.

It has further been confirmed that not all ferromagnetic earth materials are lossy. Material containing magnetite in large (> 100 micron) grains behaves as a classic ferromagnetic material having no visible frequency dependence in the measured range. It seems likely that this is at least partly because the intrinsic susceptibility (relative permeability) of the grain magnetite significantly exceeds 10 SIU, so the apparent susceptibility of the grains will be limited to a much lower, frequency independent value (usually ~ 3) by grain shape demagnetization, even if the intrinsic susceptibility were to drop somewhat with frequency.

The dispersive soils susceptibility spectra are consistent with the hypothesis that their

magnetic properties are due to single domain or pseudo single domain, fine grain, thermally activated, viscous induced magnetization as described in Dunlop and Ozdemir, 1997 and , for example, John K. Eyre (1997) .

Magnetance spectra of the mine EMI simulants are qualitatively consistent with predictions based on theoretical modelling of simple objects. It should be noted that the Foucault transition frequencies of the simulants for hard-to-detect minimum metal mines tend to be at or above 100 kHz, the limit of our spectral measurements. It may be that it is partly this aspect, not just the small volumes of these objects, that makes them "very difficult" to detect with typical detectors.

Although we have not yet run full simulations of realistic mine models in realistic model ground, it is apparent that current standard detectors are not using all possible discriminants both spectral and geometrical. A combination of geometrical and spectral response is likely to be able to discriminate mine-like, soil like, and even soil heterogeneity -like responses. To our knowedge only the Minelab detectors incorporate a reasonable system for modelling the response of a lossy ferromagnetic soil and using it as a kind of base level for detecting anomalies. Even it appears to be a fairly primitive compensation system.

Nevertheless, it is difficult to deal optimally with all search scenarios with single detection algorithm. It would seem that there is a need to convey more information from the detector to the operator about the earth response. Of course, practical detectors for use by demining crews need to be very simple to operate. However, although deminers often may be illiterate, this is not an impediment to their becoming very good craftsmen in use of their tools. There is anecdotal evidence from Minelab of demining operators learning to differentiate different types of mines on the basis of EMI scan signature. Thus, it is not necessary that ouput from a detector be just a binary acoustic alarm, although some kind of acoustic output is likely to continue to be the most effective. It needs only to function in a reliable and intuitive manner so an operator can learn to interprete its information output by his training experience.

Recommendations

If further research is to be directed towards optimizing EMI detection tools for humanitarian demining, we would suggest the following as an effective path to follow:-

1. Continue the program of measuring the EMI spectral properties of soils and mine metal components begun in this project.

2. Conduct some pathfinding research on ways of encoding more types of information on an aural signal. Someone with music background and experience with synthesizers would be best for this. It is already established that, for safety reasons, an EMI detector should give a more or less continuous aural signal whenever the device is properly operating. Information about ground response can possibly be encoded in tone variation, tone interruptions, vibrato or warbling tones with possible rate and intensity variation, multiple signals in various tone ranges, etc. Hopefully, this would suggest simple ways that a few different aspect of the ground response could be conveyed to the operator.

3. Design and build a quantitative research EMI spectrometer for in-situ, field studies on real soils and real mines. The instrument should be designed so it can thoroughly scan an area of at least 1 meter square at constant ground clearance, and record all the results quantitatively within a few minutes. Repeatable physical scanning could perhaps be accomplished by using a very light pair of tracks or a counterbalanced pole manipulation system. The coil system should be wideband, like that of the Utemis spectrometer, so all coil system responses are determined over a broad spectrum. The goal is field results that could confirm and also permit elaboration of the modelling of various critical detection scenarios. Particularly to be sought is information about typical soil response, especially its heterogeneity, (e.g., effects of suface roughness, roots, boulders, etc.,) and the geometrical signatures of real mines in whatever situations they are likely to be found . This instrument might evolve into a pathfinder instrument for testing new clearance sites to see what problems EMI detectors may encounter. If newer detectors incorprate more sophisticated discrimination algorithms, this might provide the information for setting optimum algorithm parameters.

4. With the aid of simulation studies and incorporating the results of 1 an 2, design and build a "concept demonstration" EMI metal detector for humanitarian demining that either can convey to the operator a more meaningful, subtle and sensitive "picture" of what is in the ground by aural means, and/or can incorporate more refined detection algorithms that can be set to suit the local circumstances.

References:

Rock Magnetism:- Fundamentals and Frontiers, 1997; David J. Dunlop & Özden Özdemir, University of Toronto; Cambridge Press, Cambridge Studies in Magnetism (No. 3).

John K. Eyre (1997) Frequency dependence of magnetic susceptibility for populations of single-domain grains, Geophysical Journal International 129 (1), 209–211.

APPENDIX 1

An instrument for measuring complex magnetic susceptibility of soils

Gordon F. West* [a] and Richard C. Bailey [b],
[a] Geophysics Lab., Dept. of Physics, University of Toronto, Toronto, ON, Canada, M5S1A7
[b] Physics and Geology Depts., University of Toronto, Toronto, ON, Canada, M5S1A7

ABSTRACT

To improve the success of electromagnetic induction (EMI) metal detectors in identifying anti-personnel land mines buried in slightly ferromagnetic natural soils, we need to know what range of soil physical properties must be dealt with. We have therefore built a laboratory instrument for measuring complex magnetic susceptibility in inch-sized samples over a frequency range from 100 Hz to ~ 70 kHz with errors of a few percent of the sample susceptibility in a sample of ~1 milli-SIU volume susceptibility, (i.e. ~30 micro-SIU). The instrument is a symmetrical, six coil, induction spectrometer. A pair of transmitter coils in Helmholtz configuration generates a uniform magnetic field over the sample region. The magnetic moment induced in the sample is detected (mainly) by a pair of receiver coils which are closer to the sample than the transmitter pair and also (nearly) in Helmholtz configuration, so as to provide uniform sensitivity over the whole sample region. The coupling of the main receiver pair to the transmitter pair is annulled with a second pair of coils (called the reference receiver pair) situated outside the transmitter pair. The transmitter coils are energized with a wideband current. Data acquisition is by a PC computer with a 192 kHz, 24 bit, 2 channel sound card using software in written in MatLab. Although our instrument is still a prototype and its design continues to evolve, we have measured susceptibility spectra of some samples from de-mining projects in areas where false alarms are a problem and have found dispersive susceptibilities.

Keywords: EMI, metal detector, land mines, demining, induction spectrometer, complex susceptibility

1. INTRODUCTION

With support from Defense Research and Development Canada's program on humanitarian demining, we are developing software tools to help simulate the performance of electromagnetic induction (EMI) metal detectors of arbitrary design. In order to make valid simulations, we need quantitative descriptions of the induction response of mine-like target objects and of the electromagnetic properties of the soils in which the mines may be hidden. The information must be valid in the spectral range employed in typical mine detectors, 1 to 100 kHz, and should preferably cover from 0.1 kHz to 1 MHz. Unfortunately, with the exception of a few susceptibility amplitude measurements[1] at two frequencies (465 and 4650 Hz) using the Bartlington susceptibility meter[2], few direct spectral measurements are available in the scientific literature.

* west@physics.utoronto.ca; phone 1 416 978-3155; fax 1 416 978-7606

Modern anti-personnel mines typically contain only a few grams or less of electrically conductive metal; often only ~ 1 mm to ~ 1 cm in extent. Thus, it has become necessary to increase the basic sensitivity of mine detectors to a level where discrimination between the desired EMI response from a significant target object and the unwanted responses from magnetic minerals naturally present in the soil is often the key issue --- not just simple target detectability. Furthermore, in wet locales such as marine beaches, the bulk electrical conductivity of the environment may possibly generate significant interference. Therefore, most modern detectors are designed to be unresponsive to ideally permeable, non conductive materials and they use a spectral window below about ~100 kHz to minimize possible response from the bulk conductivity of the soil.

Although experience with the best modern EMI metal detectors has been relatively favorable, it has also revealed that many naturally magnetic soils do not behave as ideally permeable materials. Some may exhibit a frequency dependent, complex, magnetic susceptibility capable of confusing most detectors (sometimes termed *viscous magnetization* or VM). In the few cases where the effect has been investigated seriously, it usually is attributed to the presence of very fine grained ferromagnetic material close to the Nèel superparamagnetic transition[3]. The problem was first noticed[4] in Australia where EMI metal detectors are widely used in prospecting for gold nuggets in weathered soil, and at least one instrument is already on offer there that can be trained to reject a VM background signal[5].

It is, of course, possible to estimate by theoretical methods the EMI response characteristics of conductive and permeable objects like those present in mines. However, the metal objects in actual mines may have poorly known compositions and odd shapes, so direct experimental confirmations seem necessary. Likewise, the volume magnetic susceptibility of typical soils (real or complex) can be estimated from the limited available studies, and electrical conductivity can be estimated from porosity and water salinity data. However, because reality often differs from prior expectations, we believe that direct observation would be better.

To a typical EMI mine detector with coils of order 20 -30 cm diameter, any object less than ~ 2.5 cm in extent is small, and any point more than ~1 m from the coils is (essentially) infinitely far off. The space of main interest can be considered (roughly) to be a 40 x 40 x 20 set of $(2.5\text{cm})^3$ voxels centered beneath the detector coils. We may call it the search region. The detector system may not be totally insensitive to material outside this volume, but it cares little about anything but bulk average properties there.

The response of an EMI detection system to material in the search space is of two types:- *local* and *global* induction. Separate small target objects (conductive and/or magnetic) and weak-to-moderately magnetic materials in the soil act locally, i.e., each voxel of the search volume acts independently of its surroundings. Then, the detector's total response may be calculated by integration over all the locally induced magnetic moments.

Only if electric current can flow from one voxel to another or when local induced magnetizations are so strong that they generate secondary magnetic fields in neighboring cells comparable in strength to the primary field from the detector will the soil (or target objects acting in concert with the soil) produce a global type inductive response of

appreciable magnitude. In practice, global response is only significant in special cases, for example, when working on saline water saturated high porosity soils, or black (magnetite-concentrating) beach sands, etc. Therefore, in most simulation cases, it is only necessary to show that any global response is negligible. Furthermore, if it is necessary to model global response quantitatively, a very sophisticated knowledge of earth and target properties may be needed (e.g., the local distribution of moisture near the soil surface, the presence or absence of insulating layers on target objects, moisture wetting of surfaces, etc.; and this may be impossible to learn without detailed in-situ investigations. If sufficient need arises, an *in situ* EMI spectrometer with additional capabilities for directly measuring earth conductivity via contacting or capacitative electrodes could also be built.

At this point, it is necessary to mention a further assumption. We shall assume that all EMI response mechanisms are linear in primary magnetic field amplitude. This allows us to use standard Fourier techniques on all the spectral measurement data. This is certainly valid in most cases, but there could be exceptions; for instance in clusters of highly permeable ferromagnetic grains or where conductive paths involve interfaces with special properties.

For the above reasons, our EMI spectrometer has been designed to measure the local EMI response of materials in laboratory sample form. It measures the magnetic dipole moment **m** that is induced in a sample when a uniform alternating magnetic field **H** is applied to it. Assuming linearity, the result can be expressed as a frequency domain complex transfer function relating $\mathbf{m}(f)$ to $\mathbf{H}(f)$ (time variation expressed as $exp(2\pi\, i\, f\, t)$) or, alternatively, as a time-domain system function $\mathbf{m}(t)$ for a step or impulse variation in $\mathbf{H}(t)$. Where the result is expressed in terms of unit sample volume, it is magnetic susceptibility, $\kappa(f) = \mathbf{m}(f) / (V\, \mathbf{H}(f))$ that is measured. Susceptibility (i.e., "magnetic moment per unit sample volume per unit primary magnetic field intensity" or $Am^2 / m^3 / Am^{-1}$) is a dimensionless ratio. Unfortunately, the cgs and SIU definitions differ ($\kappa_{SIU} = 4\pi\, k_{cgs}$).

2. BASIC DESIGN DECISIONS

2.1 Samples

We want our spectrometer to measure the EMI response of friable soils, small rock fragments and shrapnel, and a variety of possible target objects from mine detonators. The selected sample size is thus a compromise. Although hectagram to kilogram sized samples would provide better estimates of average properties of soils, heterogeneity of the soil on a few-centimeter scale may contribute to false detections, so we want to be able to study that as well. Furthermore, the target metal objects in minimum metal, anti-personnel mines are often of sub-centimeter dimensions. These would be hard to measure accurately in a large sample space. We therefore chose the 2.5(4) cm (~1 inch) diameter by 2.5(4) cm high cylindrical sample as our standard specimen shape (volume ~12.(9) ml), in part because specimens of this size have been widely used in geophysical rock magnetic studies.

However, the sample space was designed to be larger than 25 mm, so somewhat bigger target objects can be accommodated. Within the standard sample volume, sensitivity variation was required to be negligible and not exceed about 5 % anywhere in a region about twice the standard sample size. Although granular soil samples are unlikely to exhibit anisotropy because the grains mix in the sampling process, solid objects certainly may do so.

Target objects are especially likely to have directional properties. We have therefore made it possible to measure susceptibility as a function of sample rotation angle so tensor susceptibility may be determined. Theoretically, the most complicated form the EMI response of small object can take on is that of second rank tensor with complex, frequency-dependent elements.

2.2 Sensitivity requirement

Magnetic soils that present a serious problem for mine detection usually have susceptibilities of 1 milliSIU or greater. Thus the sensitivity objective for the instrument is an ability to delineate accurately the susceptibility spectrum of a standard 12.9 ml specimen with a susceptibility of about 1 milliSIU. This implies that base level drifts and noise should not much exceed 0.01 milliSIU over the measurement bandwidth.

2.3 Spectral Characterization

Many modern EMI metal detectors operate in the time-domain, measuring the transient secondary response that follows a pulse of transmitter current. However, none measure a pure discontinuity response (step, impulse, derivative impulse, etc. Since our simulation software is expected to handle any form of time variation, e.g., arbitrary transmitter waveforms and receiver gates as well as frequency domain measurement, we decided that it would be simplest if all data were archived in frequency domain.

2.4 Spectral Coverage

For economy and simplicity, we decided to use a standard PCI bus sound card (24 bit, 192 kHz sampling rate, 2 channels in + 2 channels out, Hammerfall 9632) sound card in a PC computer to provide the signal generator -signal analyzer unit of the spectrometer. This had the additional advantage of enabling a direct interface to MatLab for easy software development. However, the decision does limit the maximum useable frequency of our spectrometer to about 70 kHz (about 0.7 of the 96 kHz Nyquist frequency). Although higher would be better, it is not just a matter of sampling frequency. It becomes difficult to design a coil system that is sufficiently sensitive at low frequency and sufficiently free of phase/amplitude error due to skin effect and self resonances at high frequency if it is expected to cover more than a 1000:1 frequency band. Because we wanted have useable sensitivity down to at least 100 Hz, we decided that a 70 kHz high frequency limit was acceptable.

2.5 Coil configuration and expected sources of error and noise

Many successful metal detectors employ only a single coil --- thereby combining the transmitter and receiver functions. However, this is problematic when the free space current-to-voltage response of that coil must be cancelled out or subtracted off to very high precision over a broad spectrum. Furthermore, we require a paired coil configuration, symmetric about the sample, to obtain uniform sensitivity in the sample space; and the number of turns in the coils had to be kept low so self resonances remained above ~ ½ MHz. We therefore decided to use the six coil configuration shown in Figure 1.

Two transmitter coils in Helmholtz configuration generate a uniform inducing field through the sample volume; the inner pair of receiver coils (called the "sample receiver coils" and also ~ in Helmholtz configuration) senses the induced magnetic moment uniformly over the sample

volume. Then, an outer pair of receiver coils (called the reference receiver coils) provides a signal that can annul the primary signal in the main receiver coils. This arrangement also makes it possible to null the receiver system to any uniform spurious external magnetic field. Using a MATLAB program for the mutual coupling of thin wire loops, the diameters, locations, and turns-ratios of the coils were adjusted so as to achieve both null conditions simultaneously. The program also calculates the sensitivity constant of the accepted coil set.

It is relatively easy to predict the basic level of noise in the spectrometer due to coil resistances and the specified noise levels of the amplifiers after making some plausible assumptions about levels of transmitter current. This exercise shows that a sensitivity of ~ 1 μSIU might possibly be achieved with our coils at 100 Hz. However, the key factor limiting sensitivity is not the level of internally generated noise --- it is the short term mechanical and electrical stability of the nulling arrangement for the transmitter - receiver coil coupling.

3. IMPLEMENTATION

3.1 Coils + preamplifier system

Forms for the spectrometer's 6 coils were lathe cut from ½ inch thick G4 epoxy-fiberglass sheet and supported with a frame of ¼ inch G4. The coil windings are 2 or 6 layers of 5 turns each of # 22 formel-insulated copper wire laid in a wide groove cut in the top of each form. Dimensions are given in Figure 1. The coil windings are covered with tape and painted with a layer of silver "print" to provide electrostatic shielding.

The right and left transmitter coils are connected in series so their magnetic field will add at the sample location and are driven by a pair of IC audio amplifiers connected in a bridge configuration (National semiconductor LM4675, 30W dual amplifier). The 4 receiver coils are similarly connected in series, with the midpoint of the set grounded, the nulling coils in the centre of the set and the sample receivers on the outside. The polarities of the sample receiver and the nulling coils are opposite. (the connection order is R1, -R3, (gnd pt), -R4, R2).

With this coil configuration, the susceptibility measurements can be made simply by comparing the voltage signal available across the full set of 4 coils (sample signal voltage) with that available across the inner pair (reference voltage). All the individual coils have impedances < 10 kΩ at the highest spectrometer frequency, and they are operated essentially unloaded. However, a damping resistor is connected across the whole set to attenuate self resonance -. Because it is essential that the comparison process be free of even small amplitude and phase error anywhere in the 100 kHz band, it is desirable to use identical amplifiers for the two signals. However, the reference signal is huge in comparison to the sample signal, so we attenuate it by a factor of 3300 at the input to the reference amplifier. This attenuator also serves as damping resistor on the reference coil set. The amplifiers are three stage devices with gains of 2500 and with differential input and differential line driver outputs. The amplifier outputs are fed directly by balanced lines to the balanced inputs of the sound card in the computer.

In reality, only about a 1% null level is achieved using the designed dimensions, and this is

improved to about 1 in 1,000 by appropriate positioning of a ferrite rod near one reference coil. All remaining coupling is then highly frequency dependent, and it arises from the different diameters and number of turns on the sample and reference receiver coils. Much of this signal is cancelled by means of a moveable, heavily damped coil near the other reference coil, to reach a null level of order 1: 20,000. Then, by differencing each sample measurement from a background measurement (no sample) made just before and/or just after the sample measurement, most of remaining primary signal is removed. We have found that we can reduce the residual null signal level to close to 1 in 15 million, which is the fractional level that corresponds to a susceptibility error of about 0.01 milliSIU.

3.2 Excitation and signal processing

There are many possible ways to use the basic spectrometer system. For example, the transmitter coils can be excited sinusoidally (with the frequency changed sequentially), or with a swept frequency signal, or with square waves, or with a long pseudo random binary sequence.

After a number of preliminary studies, we found that although the performance of the sound card was generally excellent, it did exhibit a variety of very narrow noise peaks directly related to the sampling frequency which grew in amplitude towards the Nyquist frequency. They are probably a direct consequence of the sigma-delta converter algorithm, not faults in the sound card design. In any case, we found it helpful to avoid using any even sub-harmonics of the sampling frequency above a few kHz. Consequently, it was better to use periodic signals of selected fixed frequency than a swept frequency or other continuous spectrum signal.

We further discovered that null-point stability could be seriously affected by changes in excitation current levels, if the excitation current was high or of long duration. The problem appears mainly at high frequency, and it likely arises from transmitter coil heating and cooling, which changes coil resistance and/or inter-turn mutual inductance and capacitance. The problem appears in the sample signal only because these high order inductive effects in the transmitter are unequally coupled to the sample and reference coils. In hind sight, it would have been better to have required the R3 and R4 nulling coils to be of exactly the same construction as the R1, R2 sample coils. This would have made the coupling between the transmitter and the reference and sample receiver coils similar, even though it would have sacrificed some uniformity of the coil system sensitivity in the sample region. We may implement this change in a Mark II model.

Currently, we excite the spectrometer sequentially with six periodic signals that are each composed of about 6 odd harmonics of the signals base frequency. The excitation power amplifier applies a voltage waveform to the transmitter coils that is a frequency-truncated square wave. The spectrometer transmitter coils are inductive above ~ 5 kHz and resistive below. In the inductive range, the reference receiver signal looks like the transmitter voltage; in the low frequency range it is more like a sequence of alternating pulses, i.e., the derivative of the excitation voltage. Frequencies of the six signals and their harmonics are chosen so that a reasonably complete logarithmic sampling of the spectral range is obtained. Signal levels are set to prevent possible overloading of either the transmitter or the receiver channels.

Each of the six compound waveforms is transmitted for a few seconds, during which the reference and sample signals are recorded. The recordings are then analyzed in MATLAB in a few seconds following each acquisition. Usually, the acquisition cycle is repeated a few times so random error levels can be assessed. As mentioned above, "background" measurements are made before (and sometimes after) each sample measurement or short sequence of sample measurements. One complete spectral measurement takes a couple of minutes including data plotting. A set of measurements at 7 angles that can define anisotropy in one plane takes about 5 minutes. Occasionally, a no sample measurement and a calibration sample measurement are performed, in order to check for possible problems.

The spectrometer is run from a graphical user interface written in MATLAB, using the computer mouse and keyboard. Measurement data and sample identification information are all recorded in computer files.

4 EXAMPLE RESULTS

Figure 2 presents six examples of spectral measurements on a suite soils samples provided to us by the Canadian Center for Mine Action Technologies (CCMAT) at Suffield, Alberta. The samples are from mine fields or mine detector test areas around the world. Samples AzC-4 and AzB-2 are light buff-colored soils from the interior of Australia, the first a coarse grained material, the latter a very fine grained material and exceptionally strongly magnetic (~ 18 milliSIU). Both spectra are dispersive, the fine grained material about 3 times less so than the coarse. The spectral form of the dispersion is what is predicted for a Nèel viscous magnetization where the magnetic grains have a very wide distribution of blocking parameters --- the real component declines steadily with proportionate increase in frequency and the imaginary component is negative and nearly constant. Since the discontinuity response of the soil must be causal, the frequency variations of the real and imaginary components should be related by a Hilbert transform.

The middle row of spectra are samples from Bosnia, where EMI metal detectors have had much difficulty. BnU-4 is a dark brown, coarse grained soil, BnM-4 is a mid brown fine grained material. Both are quite strongly magnetic (3.5 and 6 milliSIU, respectively, and both are highly viscous. Sample BnM-4 exhibits the largest imaginary component susceptibility in the 10-100 kHz range of any we have yet measured.

Samples CbA-4 and CI3-3 in the bottom row are from Cambodia and Columbia, respectively. The Cambodian sample is quite strongly magnetic (2.6 milliSIU) and moderately viscous, the Columbian sample is only weakly magnetic (~ 0.3 milliSIU) and only very slightly viscous. The relatively strong negative imaginary values at high and low frequency likely are measurement artifacts because they significantly exceed the estimated standard deviations. This effect has been noted in several weakly magnetic samples, but does not occur when no sample is present. It may possibly be due to non-linearity exhibited when the sample volume may contain an insufficient number of hysteretic magnetization centers so averaging over the sample volume is insufficient to fully smooth out the response.

Figure 3 presents six different spectra. In the upper row are spectra from two test samples. The first (left) is a mixture of crushed magnetite ore and coarse sand used in mine detector

tests at Suffield. It is the least dispersive material we have measured so far (including commercial ferrites), and we use it for calibration purposes. The second (right) is a null measurement showing a measurement floor of about 0.03 milliSIU. Most of the 66 individual point lie within their estimated (one sigma) standard deviations.

The spectra in the middle row and in the lower left are from permeable and conductive objects employed in mine simulators. These are dummy mines use to train operators of EMI metal detectors. The middle row is the response of a carbon steel spring such as could be present in an anti-tank mine and which is considered easy to detect. Spectra are given for the along axis (left) and across axis response (right). A very strong ferromagnetic response is observed up to a few kilohertz. Above this, conduction currents become appreciable. Note that both responses are greater when the inducing and detection axes are parallel to some of the wire in the spring. Also note the very large apparent susceptibility (~165 milliSIU).

On the lower left is the spectrum of a simulation object considered to be very hard to detect (a carbon steel ball-bearing, about 1/8 inch in diameter). The low frequency apparent susceptibility is only about 4 milliSIU, and the imaginary component conductive response does not peak below 70 kHz. (It is likely at about 120 kHz).

On the lower right and for comparison with the object spectra is the spectrum of the Bosnian "difficult" soil, BnU-4. note that a 2.5 cm cube (1 inch) voxel of soil and the Co test object give similar levels of response in both components. However, the spectra do differ in character significantly.

Figure 4 shows the results of measuring anisotropic apparent susceptibility. The upper display is from the spring object whose principal spectra were shown in figure 3. Here, complex apparent susceptibility at one frequency is plotted as a function of specimen angle in the spectrometer. There are three types of plotted data. 1) the absolute amplitude of the apparent susceptibility which is plotted as a solid line with starred observation data point around the whole circle, 2) the real component data points, and 3) the imaginary component data points, both plotted only around one half circle. The polar axis of the graphs is scaled by the stated factor (in milliSIU).

The lower graph is for a similar but much smaller object, considered very hard to detect. This plot is of the 3200 Hz measurements, so the imaginary part is exceedingly small. The object is short piece of carbon steel wire about ¼ inch long (2.7 mm).

The form of the anisotropy plots is the sum of two simple cardoid functions ($\sin^2(\theta)$ & $\cos^2(\theta)$), one for each of the principal susceptibilities. The response takes this form because the measurement involves two projections of the susceptibility tensor; one onto the primary field axis, the other onto the measurement axis.

5 CONCLUSIONS RE APPARATUS

The spectrometer seems to meet our design objectives quite well. It is extremely easy to use, and it can be shipped without much difficulty. Its level of noise and base level error likely can be reduced by a factor of 2-5. A version that could measure with similar performance in the

spectral range 1 kHz to 1 MHz could probably be built using the same basic coil configuration, but it may require a more sophisticated engineering effort than did this model. The present model could also be programmed to look for non-linear behavior in the samples by using intermodulation methods. Apparatus of this type may well be useful in rock magnetism and other technical areas such as the preparation of magnetic powders.

6 CONCLUSIONS RE MINE DETECTION

We have only begun our sample studies, so it is premature to suggest that reliable conclusions can be drawn already. However, those measurements we have done so far do make it clear that viscous induced magnetization (VM) is not rare, and in soils, it is usually is a very wide spectrum phenomenon. Thus, mine detector design must take this fact of nature into account. The measurements also suggest that the conductive objects in minimum metal, anti-personnel mines are likely to give their strongest imaginary component response near or above 100 kHz. This suggests that improved AP mine detection performance might be obtained if some detectors were designed to work to higher frequencies than present models, even though those instruments might only be useable dry, non-conductive terrains.

ACKNOWLEDGEMENTS

This work was supported by the Canadian Centre for Mine Action Technologies (CCMAT) of Defense Research and Development Canada (DRDC) as part of contract No. W7702-03R942/001/EDM. We gratefully acknowledge the assistance and guidance provided by DRDC personnel in at Suffield, Alberta, and especially the help from Dr.Yoga Das, technical authority for the contract. We also acknowledge the assistance provided by computer specialist Dr Rob Moucha, undergraduate student assistants, Xiaoyu Ouyang and Terence Fu, and graphic artist Raul Cunha.

REFERENCES

1. Parsons Engineering, *U. I., Cleanup plan: UXO clearance project, Kaho'olawe island reserve, Hawaii:,* Technical report, Parsons Engineering, UXB International, 1998.

2. J.A. Dearing, J.A.., *Environmental Magnetic Susceptibility: using the Bartington MS2 System*, Chi Publishing, Kenilworth, pp.104, 1994.

3. L. Néel, *Théorie du trainage magnétique des ferromagnetiques en grains fins avec application aux*
terres cuites, *Ann. Geophys.*, Vol. 5, pp. 99-136.

4. G. Buselli, G., The *Effect of Near-Surface Superparamagnetic Material on Electromagnetic Measurements*, Geophysics, vol. 47, No.9, p.1315-1324, 1982.

5. B.H. Candy, *Pulse Induction Time Domain Metal Detector*, United States Patent Number 5 576 624 , November 1996.

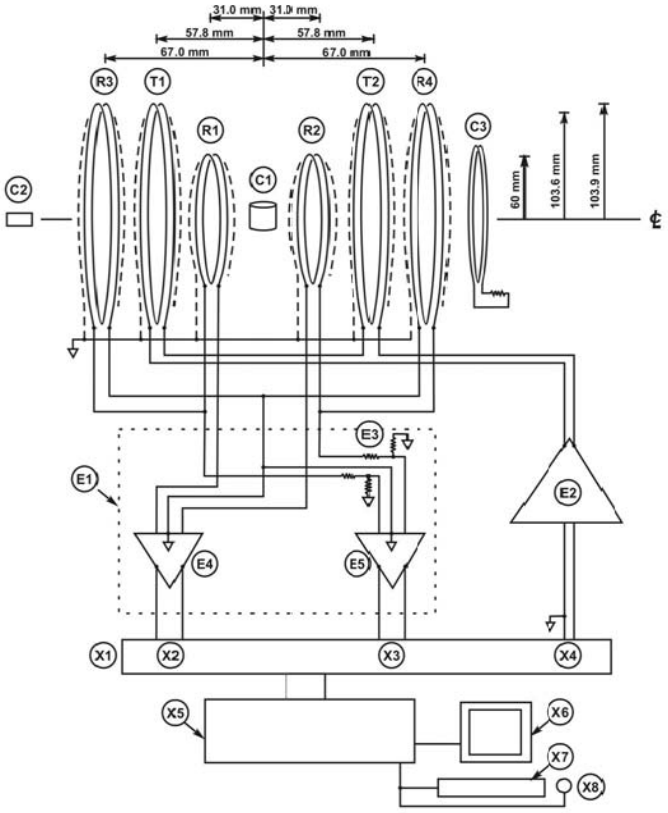

COMPONENTS

R1, R2	Main receiver coils (30T)	E1	Preamplifier unit
R3, R4	Nulling receiver coils (10T)	E2	Audio power amplifier
T1, T2	Transmitter Coils (10T)	E3	Reference signal attn (1:3300)
C1	Specimen	E4	Differential amp (x2500), signal
C2	Ferrite null adjuster	E5	Differential amp (x2500), reference
C3	Damped coil null adjuster		
X1	Hammerfall 9632 sound card	X2	Specimen signal in
X3	Reference signal in	X4	Excitation signal out
X5	Computer (PCI bus, AGP video)	X6	Video display terminal
X7	Keyboard	X8	Mouse

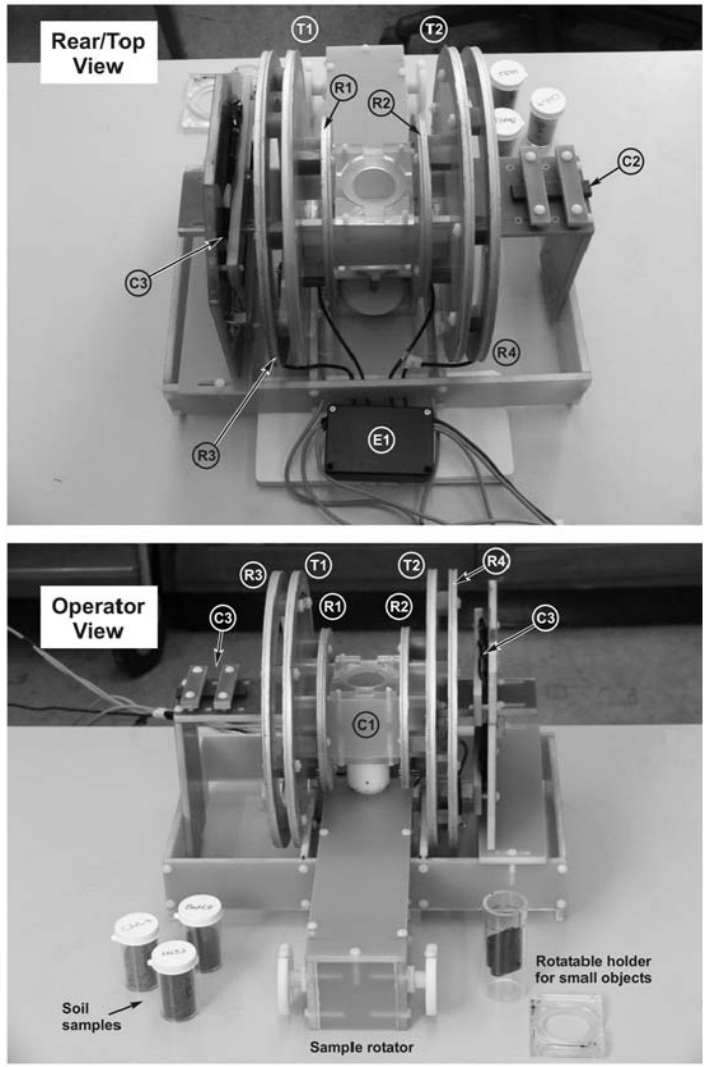

Figure 1 Susceptibility Spectrometer: schematic, left: photos, right

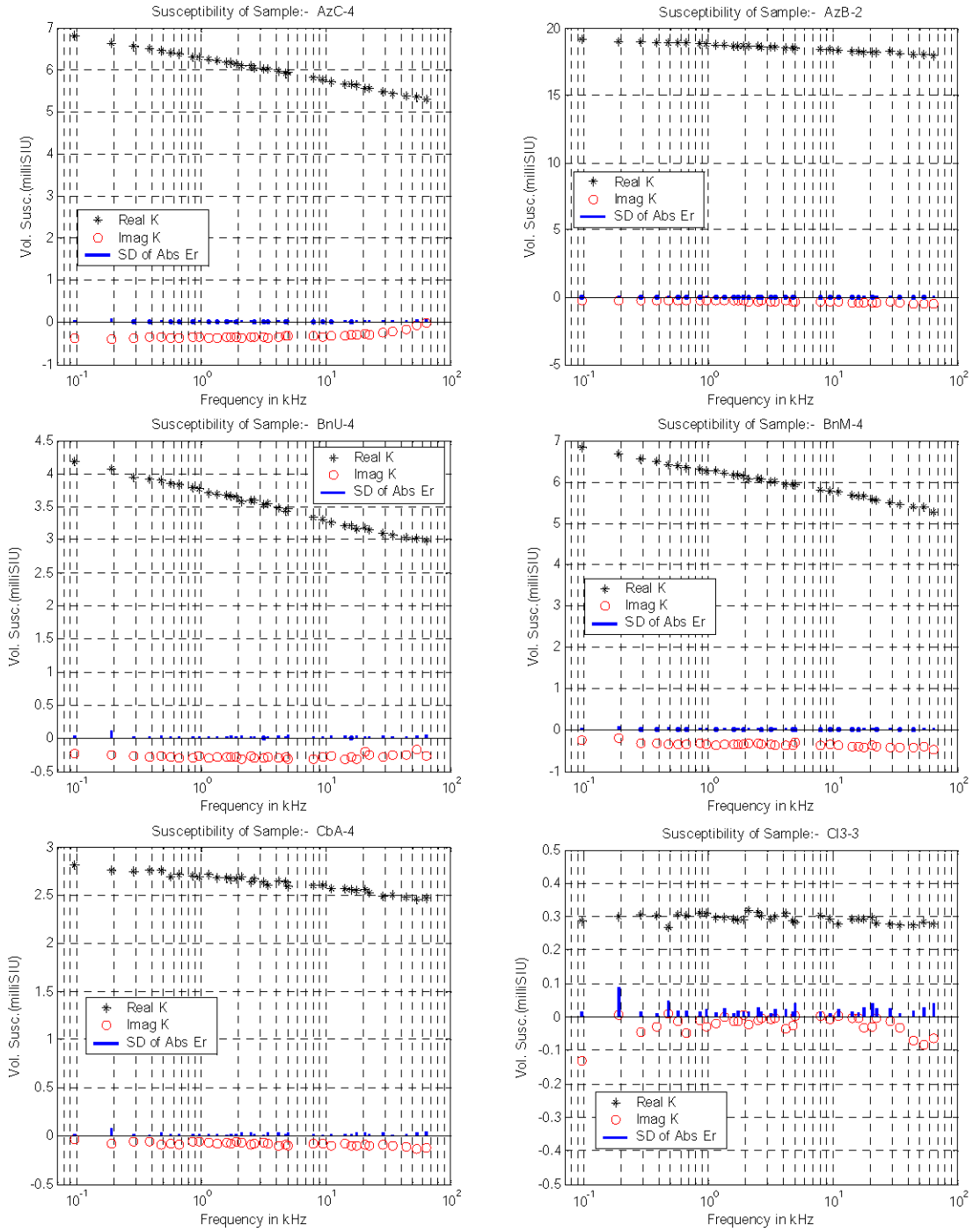

Figure 2 Susceptibility spectra of six soils. Vertical scales vary. Each graph gives the real component (stars, usually positive) and the imaginary component (circles, usually negative) of susceptibility. Vertical bars rising from the zero line show standard deviation estimated from repeated measurements. Row-wise from the upper left are samples AzC-4 and Az-B-2 (Australia), BnU-4 and BnM-4 (Bosnia), and CbA-4 (Cambodia), all significantly ferromagnetic, AzB-2 exceptionally so. All exhibit magnetic viscosity (dispersion) in varying degrees. The final sample, CI3-3 (Columbia) is only weakly magnetic and exhibits very little dispersion. The Bosnian soil, BnM, would likely give a standard EMI metal detector the most difficulty, as it gives the largest negative imaginary response in the important 10-100 kHz range (about -0.5 mSIU).

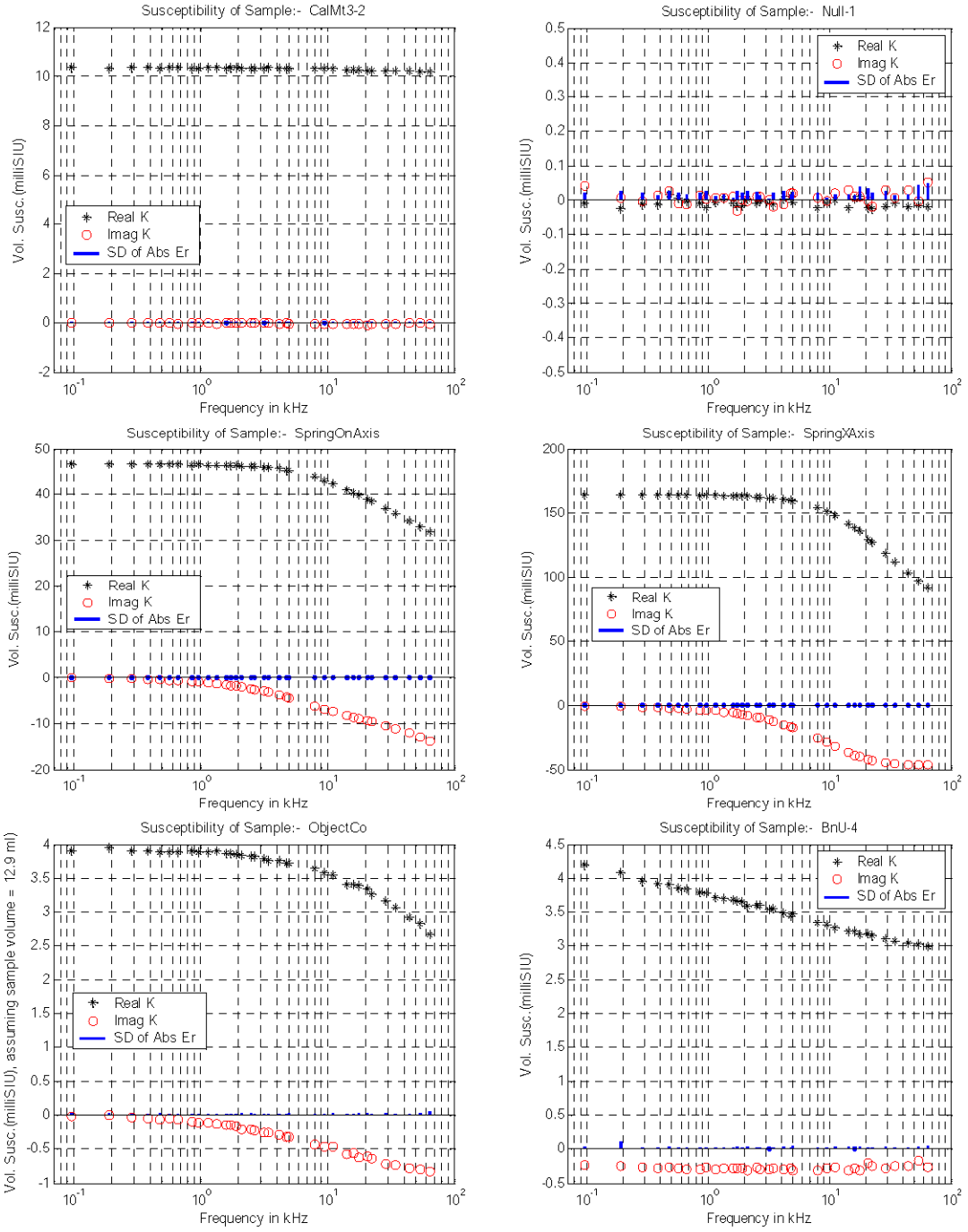

Figure 3 More susceptibility and apparent spectra. Please note the variations in vertical scale. The upper two spectra are instrument tests, the left one a spectrum of crushed, coarse grained magnetite showing almost no dispersion, the right a null measurement (no specimen) showing a noise floor of about 0.03 mSIU. The middle row of spectra show the response of a carbon steel spring (such as might be found in an anti-tank mine) in two principal directions. The lower left is of a very small carbon steel ball employed in hard-to-detect dummy AP mines that are used for detection training purposes. The lower right shows a highly dispersive soil for comparison. Note the very different imaginary component spectra.

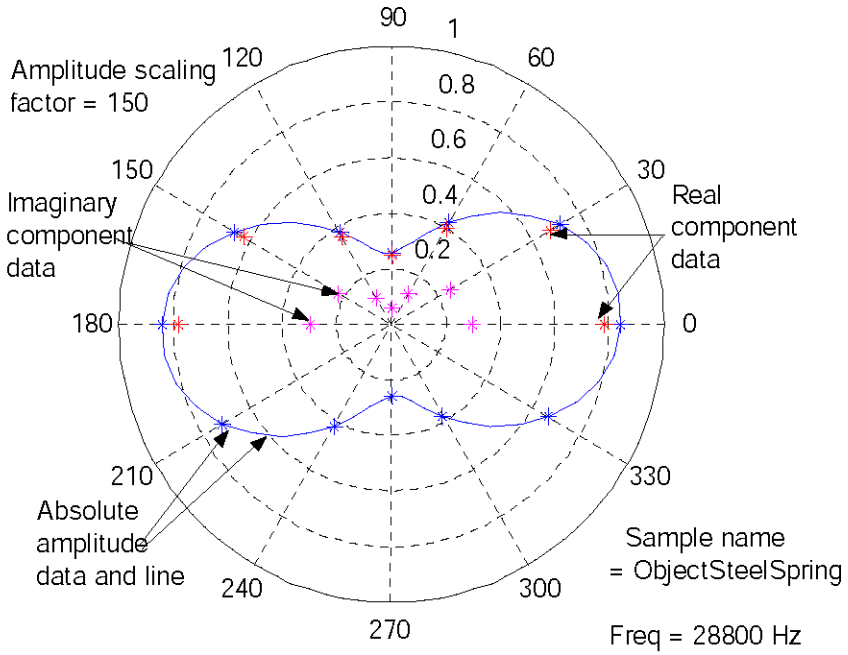

Volume Susceptibility vs Orientation (milliSIU for a 12.9 ml sample)

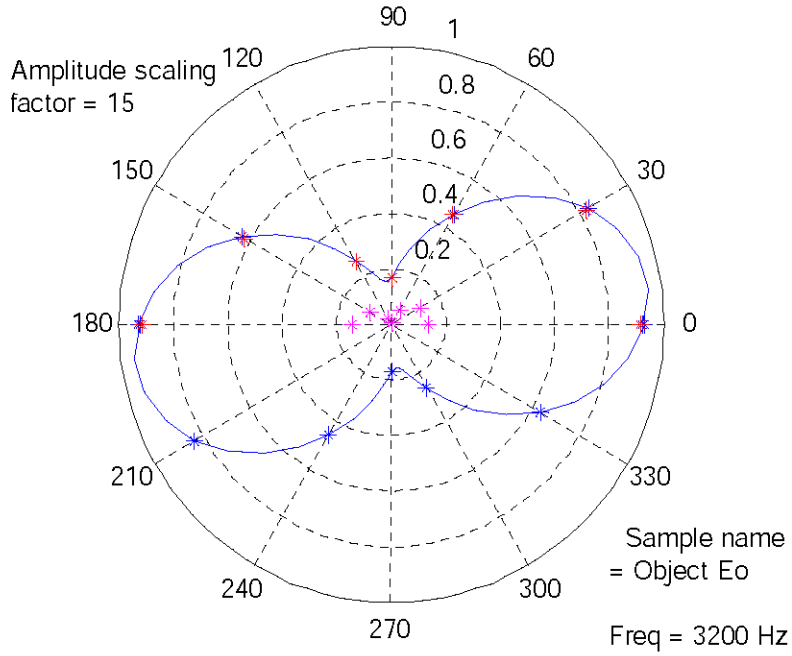

blue line+ blue * = abs(Data), red * = re(Data), magenta * = im(Data)

Figure 4 Polar graphs of apparent susceptibility versus specimen orientation. Absolute amplitude and real and imaginary components are plotted. The top graph is for an object whose principal spectra are shown in Figure 3. The bottom is for a ¼ in. length of carbon steel wire used to simulate a very difficult-to-detect AP mine target.

APPENDIX 2

Spectral representation, a core aspect of modelling the response characteristics of time-domain EMI mine detectors

G.F. West[a] and R. C. Bailey[b]

[a]Physics Department, University of Toronto, Toronto, [b]Physics and Geology Departments, University of Toronto, Toronto, Canada;
Canada

ABSTRACT

Most modern EMI mine detectors can detect the very small conductive and/or ferromagnetic parts of typical mines with relative ease. However, they also respond significantly to certain soils that contain lossy ferromagnetic minerals. In some special environments such as ocean beaches, conductivity of the host soil may also cause a response. Characterizing and modelling both the various target response mechanisms and the EMI detectors quantitatively would be relatively straightforward if it were not for the fact that most modern EMI detectors operate in time domain and use different current waveforms and time gates to observe response. Furthermore, much of the information about targets and interferences and even instrumental spectral limitations is observational rather than analytical data.

In this paper, we put forward a spectral representation method that can be incorporated into both EMI data gathering and instrument modelling and which facilitates efficient quantitative simulation of arbitrary time-domain detection systems. The methodology and examples of its use are presented. Pure induction response from the ground is modelled with a sum-over-N-elements transfer function in which the kernel elements are single pole, pure damping responses which are log-spaced over the spectral range of interest. Instrument transfer functions can be described with a standard sparse pole and zero representation (located anywhere in the damped frequency half plane), if required. Model fitting techniques employing generalized inversion controls are used to go back and forth between frequency and time domain and the set of model parameters.

Keywords: EMI, humanitarian demining, simulation code, magnetic soils, spectral representation

1. INTRODUCTION

EMI metal sensors for mine detection have now (2006) reached a fairly sophisticated level of development. In most cases, the manufacturers' design objectives have been to achieve as high as possible sensitivity to mines of low metal content commensurate with good user characteristics like robustness, reliability, low weight, good battery life, convenience in the field, cost, etc. However, experience in humanitarian demining in many countries is indicating that an additional factor should be considered:- the ability of the sensor to discriminate mine-like conductive objects from the ferromagnetic responses of some soils. Also, in some cases, it appears that small metallic fragments of exploded ordnance (clutter) are frequent generators of false responses, so discrimination against this type of object could also be beneficial.

Most mine detectors are already designed to not respond to a classically magnetically permeable material that is electrically non-conductive. However, it is becoming ever more apparent that many natural soils have non-classical magnetic properties; they contain ferromagnetic minerals that have lossy magnetic properties and behave somewhat like conductors. (?) Figure 1 shows induction spectra for several materials.

Our research program (supported by the Canadian Centre for Mine Action Technologies (CCMAT)) is aimed at investigating how EMI metal detectors for humanitarian demining might be improved. It has two parts:- the first is now well advanced; the second is our current focus.

Further author information: (Send correspondence to G.F.W.)
G.F.W.: E-mail: west@physics.utoronto.ca, Telephone: 1 416 978 3155
R.C.B.: E-mail: bailey@physics.utoronto.ca, Telephone: 1 416 978 3231

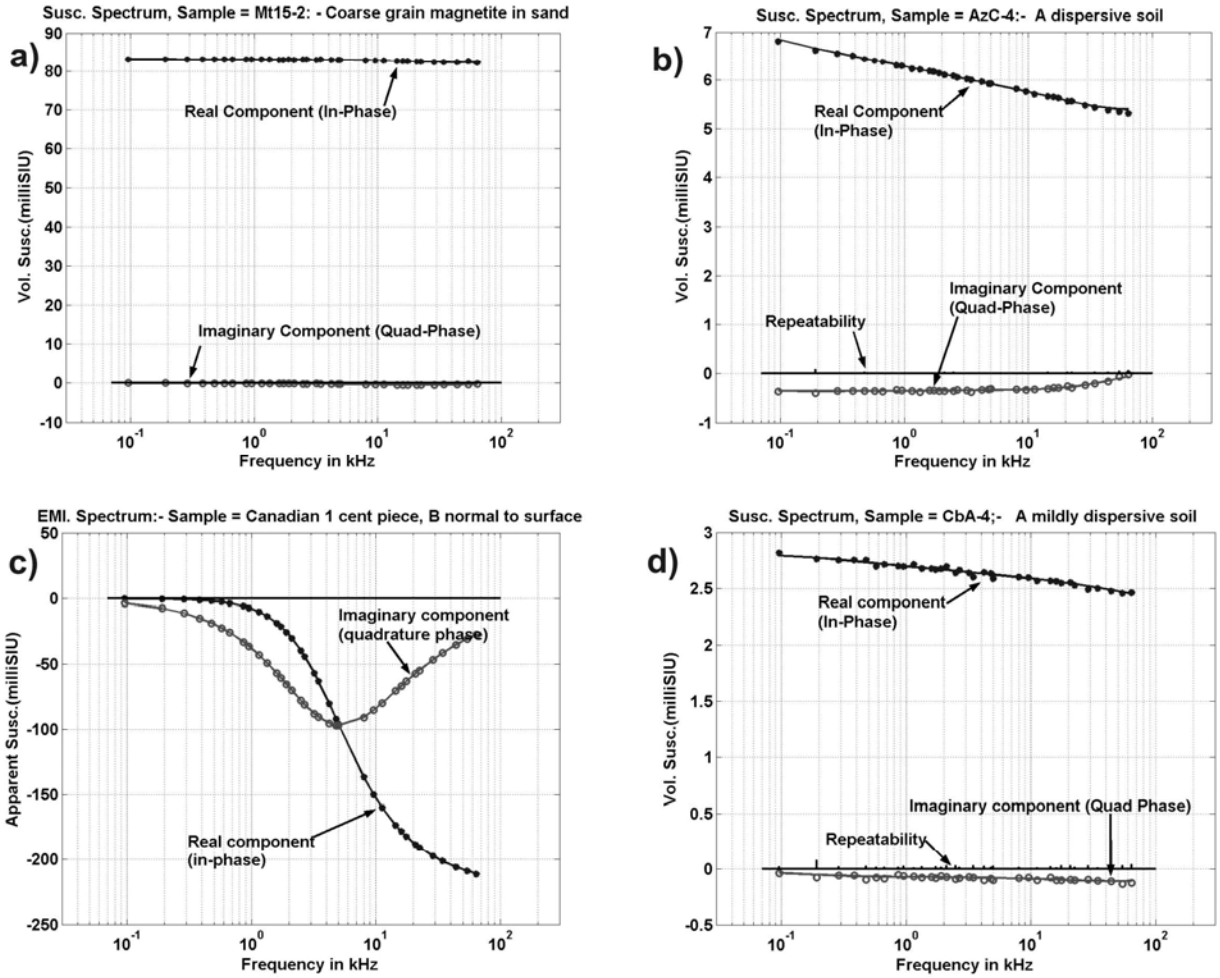

Figure 1. induction spectra for several materials

1. Quantitative, broad spectrum measurement of magnetic susceptibility or EM induction of soil samples from mine fields or metal parts from target objects (mines and clutter). Doing this has required design and construction of a new EMI spectrometer, which was reported upon last year (West and Bailey,[?] 2005). A small suite of measured data has now been obtained, and steps are being taken to extend the measurement program in order to build a more comprehensive data base.

2. Creating a suite of MatLab simulation code modules that can be used to predict quantitatively how a planned EMI sensor will respond to a specified suite of target objects embedded in a realistic host medium. The aim is to enable simulation of hypothetical sensor designs, especially comparison of the responses from possible target objects and from realistic homogeneous and heterogeneous soils. Prediction of the basic (free space detection) noise level of the sensor is not a part of these codes since it is depends greatly on electronic design factors.

This paper focusses on one key aspect of the modelling:- how we handle the spectral responses of the various components in the models.

2. SENSOR RESPONSE TO AN EARTH MODEL

In theoretical-analytical EMI modelling, it is usual and also convenient to formulate the problem in terms of the frequency-domain mutual inductance transfer function $M(\omega)$ between the sensor's receiver and transmitter loops (these may be one and the same physical loop or any combinations of loops) and ω is angular frequency. M is the magnetic flux that cuts the receiver loop per unit current I in the transmitter loop. It has two parts, a primary component $M^{(P)}$ which is the transfer function between the sensor loops in free space, and a secondary part $M^{(S)}$ which is the additional mutual inductance due to target objects and earth materials.

The primary mutual inductance of a pair of sensor loops is real and frequency independent (to the extent that skin-effect and inter-turn capacitances in the coil windings can be neglected). Secondary mutual inductance due to the presence of classically permeable material in the earth is also real and frequency-independent, but it becomes frequency-dependent if any of the permeability is frequency-dependent. However, secondary mutual inductance due to the induction of eddy currents in conductors is a fundamentally frequency-dependent process. And if the parameters of the medium are themselves frequency-dependent, the dependence of $M^{(S)}(\omega)$ just becomes more complicated.

However, most modern EMI sensors do not work in the frequency domain. They repeatedly deliver a time-limited current waveform I(t) into the transmitter loop and observe the secondary voltage induced in the receiver loop, usually after the transmitter current is shut off. In general, the sensor's basic output is the average transient voltage level observed in one or a few predefined time windows after each current pulse. (At a later stage, the sensor output usually is converted to an aural signal. The conversion may involve some sort of thresholding or target recognition concepts, but we do not concerned ourselves with that here.) Thus, the sensor measures one or more window-averaged versions of $\mathcal{R}(t)$ where $\mathcal{R}(t) = -d/dt(M_i(t) * I(t))$ and where $M_i(t)$ is the time domain impulse response corresponding to $M(\omega)$, ie., the inverse Fourier transform of $M(\omega)$. Note that the current waveform usually is repeated periodically, so $I(t)$ has a line spectrum. In some cases, it is alternated in polarity so it has only odd harmonics and no d.c. component.

A more complete discussion of the various the modelling algorithms that can be needed in a simulation package is found in a companion paper (Bailey and West[?] (2006)). To illustrate the utility of our spectral approach, we discuss only two straightforward cases:-

1. Calculating the EMI response of a small inductive object or a voxel of soil.

   In our terminology, a "small inductive object" is a ferromagnetic and/or conductive object that can respond inductively to a time-varying magnetic field by becoming a source of magnetic field. "Small" indicates that the inducing magnetic field can be treated as uniform over the object and the process of generating a magnetic field needs only to involve the induced dipole moment. Then, the induction process can be described as if it were localized at a point.

Mines may contain several inductive objects, and then the total sensor response may be calculated by summing over all relevant objects in the model space. However, such an approach is only useful when the objects are small relative to the size of sensor coils and the distances of closest approach, and when they are separated enough that they do not interact significantly. However, it is also applicable to voxels of a susceptible host medium if, in totality, the medium generates such a weak response that the magnetic fields used by the EMI sensor are not fractionally enhanced or attenuated by it to an important degree. These conditions often are met when modelling the response of a low metal mine in ordinary soils (relative permeabilities usually are less than 1.01 and soil conductivity less than 10 mS/m).

2. Calculating the global response of a host medium by using a layered earth response algorithm. Here the host medium is considered to be a flat-topped half-space in which conductivity and permeability (or susceptibilty) are homogeneous in a set of discrete horizontal layers. The algorithm usually is constructed in the frequency domain, and the layer physical properties may either be real constants of any value or complex functions of frequency. However, they must not be functions of field strength; and to correctly model real passive materials, all frequency dependences must be causal and realizable.

In the first case, the mutual inductance response ($M^{(S)}(\omega)$) of a sensor to a local object or voxel of host medium is calculated using static, free space, vector Green's functions (magnetic induction vector generated at a field point due to current in the loop — or the reciprocal quantity; magnetic flux through the loop due to a local vector magnetic dipole at the field point) and the induction coefficient of the object, which is its induced moment response to a locally uniform exciting field. The induction coefficient may be a 3D spatial tensor (i.e., it describes the vector magnetic moment $\mathbf{m}$ induced in the object by a vector exciting field $\mathbf{B}$) or a scalar quantity (which describes a vector moment $\mathbf{m}$ induced in same direction as the exciting field $\mathbf{B}$). Thus

$$M^{(S)}(\omega) = \overline{\overline{G}}(\mathbf{r}_R, \mathbf{u}_R, \mathbf{r}_0)\ \overline{\overline{R_0}}\ \overline{\overline{T_0(\omega)}}\ \overline{\overline{R_0}}^{\dagger}\ \ \overline{\overline{G}}(\mathbf{r}_T, \mathbf{u}_T, \mathbf{r}_0) \tag{1}$$

where $\mathbf{r}_R$, $\mathbf{r}_T$, $\mathbf{r}_0$, $\mathbf{u}_R$, $\mathbf{u}_T$ are, respectively, the spatial position vectors of the receiver and transmitter loops and the object and unit normal vectors of the receiver and transmitter loops, the $\overline{\overline{G}}$'s are the static real Green's vectors in column format, $\overline{\overline{T_0}}$ is the tensor (or scalar) induction coefficient of the object in its principal axis coordinates and $\overline{\overline{R_0}}$ is a 3 by 3 rotation matrix that describes the object's spatial orientation in the model. The elements of $\overline{\overline{T_0}}$ have dimensions of volume divided by μ_0.

If the inductive element at $\mathbf{r}_0$ exhibits only a classical isotropic permeability/susceptibility, its induction coefficient $\overline{\overline{T_0}}$ will be scalar and static (i.e., real-valued and frequency independent). If it is isotropic but lossy ferromagnetic (like many soils), it will be a complex, frequency-varying, scalar quantity. And if it is a conductive and/or ferromagnetic object that has shape, it will be a second rank 3D tensor whose components are complex-valued functions of frequency. (For an isotropic soil, $T(\omega) = \kappa(\omega)\ dV\ \overline{\overline{I}}$, where dV is the element of volume and $\overline{\overline{I}}$ is the 3D identity matrix.)

If the object has simple symmetry (cubic - orthorhombic), a single a set of principal coordinates can be found in which it can be expressed as only three diagonal elements. Then all nine elements of the matrix are derivable from only three independent frequency-response functions. The three principal elements may all be the same (spherical symmetry), or two the same and one different (spheroidal symmetry), or all different (ellipsoidal symmetry). However, the physics of induction requires their functional forms to be similar. If an object has low order symmetry, the principal axes of its response tensor may rotate with frequency. However, we do not separately consider this case here since, in practise, most such objects can be treated as the sum of two (or more) objects with different sets of principal axes (and thus static rotation matrices $\overline{\overline{R}}$).

In summary, for an earth model consisting of N small, non-interacting objects, we can calculate total sensor response as a function of position, attitude and frequency ($M^{(S)}(\omega, \mathbf{r}_s, \mathbf{u}_s)$) by summing evaluations of (1) over all objects.

This has the form

$$M^{(S)}(\omega, \mathbf{r}_s, \mathbf{u}_s) = \sum_{n=1}^{N} \overline{\overline{K(\mathbf{r}_s, \mathbf{u}_s)}}\ \overline{\overline{T(\omega)}} \tag{2}$$

where $\overline{\overline{K}}$ operates on the diagonal object tensor of the n'th object and incorporates the positional information about the objects' position and orientation, as well as the sensor loop configuration. It involves only the Green's function and rotation matrices from (2) and is real and frequency-independent. All spectral information is carried by the $\overline{\overline{T_n}}$ tensor induction coefficients.

The situation is different for a general stratified earth model,

$$M^{(S)}(\omega, h_s, \mathbf{u}_s) = \mathcal{F}(\overline{\kappa_l(\omega)}, \overline{\sigma_l(\omega)}, \overline{h_l}, h_s, \omega) \tag{3}$$

where $\overline{\kappa_l(\omega)}$ is the vector of layer susceptibilities, $\overline{\sigma_l(\omega)}$ the vector of layer conductivities, $\overline{h_l}$ the vector of layer thicknesses, h_s is the sensor height over the half-space, and ω is angular frequency used by the sensor. In this case sensor response is frequency-dependent, even if the layer variables are real and frequency-independent:

It takes only a few seconds for a modern desktop computer to evaluate $\mathcal{F}$ at one frequency for a number of sensor heights, so it is not too time consuming to tabulate it for different frequencies using different complex values of $\overline{\kappa_l(\omega)}$ (and possibly $\overline{\sigma_l(\omega)}$) for each. Thus, it is straightforward to evaluate $M^{(S)}(\omega)$ in frequency-domain for any desired list of real frequencies; but to do so, we need the model's layer parameters in frequency-domain spectral form.

In summary, we see that simulating an EMI sensor's response to complicated sets of target objects and lossy ferromagnetic soils requires manipulation of many spectral response functions. Some of these will be spectra of soil susceptibilty, some the principal spectra of the tensor induction coefficients of small target objects, some will arise from modelling EM induction in conductive regions of the ground. Some of these spectra may be calculated from analytical formulae; others may be derived from tabulated observations. Since we want to model time-domain EMI sensors, we will need a complete frequency-domain spectrum $M^{(S)}(\omega)$ in order to do the necessary fourier transformation. It is therefore easy to foresee how a simulation code could become bogged down doing repetitive calculations for many frequencies unless one organizes spectral aspects of the calculations effectively.

3. DIFFUSIVE TRANSFER FUNCTIONS: REPRESENTATION PROBLEMS

In principle, it is always possible to transform theoretical or observational EMI system responses between their frequency-domain and time-domain representations if the data are complete. However, complications can hide in the completeness caveat.

Most EMI sensors for mine detection function in the frequency range 1-100 kHz, with interest occasionlly extending out to 0.1 - 1000 kHz, a fractional spectral coverage of 2-4 decades (6 - 12 octaves). Consequently, for negligible loss of information in forward and inverse transformation, a standard numerical DFT or FFT needs to have between 2^8 and 2^{15} sampling points. The lower limit is not onerous, but the upper one may be.

However, in the above-mentioned frequency range and on a distance scale of 1 meter, EM fields are quasi-static. (Even at 1 MHz, the free space wavelength is 300 m.) Therefore, the physics an earth model under the influence of an EMI sensor is diffusive, and the natural scale for plotting the EMI sensor's $M^{(S)}(\omega)$ transfer function is log(frequency). (A hypothetical exception is if a target device in the earth were to contain substantial capacitors, permitting substantial electrical field energy storage and possible high Q resonances.) In time domain, the equivalent is plotting step or impulse responses versus log(delay time).

A sampling of 3-10 points per decade of frequency (or time) should allow a very complete and accurate graphing of any diffusive EMI transfer function. Thus, it should be possible to characterize it accurately with fewer than 50 sampling points, many fewer than the 256 - 32768 presaged above for a numerical fourier transformation.

But, irrespective of the sampling, representing a transfer function by its complex frequency spectrum can lead to problems for numerical calculation. This is because there are constraints on the kinds of frequency spectra that a real physical processes can possess. Transfer functions for passive systems must be causal and realizable (damped) and possess real impulse responses. This means that the real and imaginary components of the spectrum are not independent. However, error in the spectral data may not obey these physical constraints and may not transform sensibly. This is one reason why electrical engineering generally uses parameterized models for describing transfer functions.

With the above in mind, a compact linear basis for representation of a purely diffusive transfer function M is the following:-

$$M^{(S)}(\omega) = \sum_{k=0}^{K-1} A_k F_k(\omega) \tag{4}$$

where

$$\begin{aligned} F_k(\omega) &= \frac{i(\omega/\omega_k)}{1+i(\omega/\omega_k)} \qquad \text{for } k = 1, K \\ &= 1 \qquad\qquad\qquad\qquad \text{for } k = 0 \end{aligned} \tag{5}$$

The terms $F_k(\omega)$ are pole and zero product pairs in complex frequency space. The poles of the pair are logarithmically spaced along the damping (imaginary frequency) axis in the complex ω plane over a range encompassing all the frequencies of interest, with the addition of a constant first term with zero or effectively zero time constant. All the zeros are at the origin. Each term in the expansion is multiplied by an arbitrary real amplitude factor A_k, and it is the vector $\overline{A}$ of A_k's that defines the spectrum. Here we call $\overline{A}$ the Damped Pole Amplitude or DPA vector. A common set of ω_k's is predefined for all the spectra that are to be modelled.

The time domain discontinuity responses $M(t)$ corresponding to $M(\omega)$ are equally simple. The step-off system response function is

$$M_s^{(S)}(t) = \sum_{k=0}^{K-1} A_k T_{sk}(t) \tag{6}$$

where

$$\begin{aligned} T_{ik}(t) &= \exp(-\omega_k t) \qquad \text{for } t > 0 \\ &= 0 \qquad\qquad\quad \text{for } t < 0 \end{aligned} \tag{7}$$

The impulse response is

$$M_i^{(S)}(t) = \sum_{k=0}^{K-1} A_k T_{ik}(t) \tag{8}$$

where

$$\begin{aligned} T_{sk}(t) &= \delta(t) - \omega_k \exp(-\omega_k t) \qquad \text{for } t \geq 0 \\ &= 0 \qquad\qquad\qquad\qquad\quad \text{for } t < 0 \end{aligned} \tag{9}$$

Thus, when we know the DPA vector for a transfer function, we can immediately express the function as a frequency-domain spectral response or a discontinuity delay time response.

4. COMPUTING THE RESPONSE OF A TIME-DOMAIN SENSOR

Usually, we want to compute the time domain flux waveform $\Phi(t)$ or the voltage waveform $V(t)$ of an EMI system that uses a specific current waveform $I(t)$, or compute a set $\overline{V_c}$ of "channel averaged" measurements of $V(t)$ (where V_{cj} is the average of the voltage waveform $V(t)$ integrated with the normalized weight function $W_j(t)$). (See Figure (4).) These quantities are

$$\Phi^{(S)}(t) = M_i^{(S)}(t) * I(t) \tag{10}$$

$$= \sum_{k=0}^{K-1} A_k \left(T_{ik}(t) * I(t)\right) \tag{11}$$

$$V^{(S)}(t) = \frac{d}{dt}\,\Phi^{(S)}(t) = M_i^{(S)}(t) * \frac{d}{dt}\,I(t) = \sum_{k=0}^{K-1} A_k \left(T_{ik}(t) * \frac{dI(t)}{dt} \right) \tag{12}$$

$$V_{cj}^{(S)} = \sum_{k=0}^{K-1} A_k\, C_{jk} \tag{13}$$

where

$$C_{jk} = \int \left[W_j(t) \left(T_{ik}(t) * \frac{dI(t)}{dt} \right) \right] dt \tag{14}$$

in which the integration is over a single period of the transmitter waveform.

Once the distribution of poles has been decided (ω_k^{-1} gives their time constants), and the current waveform $I(t)$ and set of weight functions $W_j(t)$ has been specified, the terms $T_k(t)$ and C_{jk} that multiply A_k in these expressions are very easy to compute. Likewise, transformation from a K element DPA column vector $\overline{A}$ to a J element column vector of channel voltage responses $\overline{V_c}$ is performed simply by multiplying $\overline{A}$ with a precomputed J by K matrix $\overline{\overline{C}}$ which has elements C_{jk}. In matrix notation

$$\overline{V_c} = \left(\overline{\overline{C}}\;\overline{A} \right)^{\dagger} \tag{15}$$

In our code, one period of the current waveform $I(t)$ can be input as a (linearly) sampled time series along with a set of weights in the same format that define the averaging windows. The sample interval must be chosen small enough that all sampling windows can be adequately defined. The extent of sampling is defined by the period of $I(t)$. Usually, 4094 points is more than sufficient. The windowing weights are input as time series with the same sampling times as the current waveform. Note that $I(t)$ is not required to have a diffusive spectrum. Figure (4) shows, for an example half-sine $I(t)$, the form of the $(T_{ik}(t) * (dI(t)/dt))$ elements in equation (14); also, a graphical representation of the rows of $\overline{\overline{C}}$.

5. FINDING THE DPA FROM A DIFFUSIVE FREQUENCY DOMAIN SPECTRUM

If we know a complex diffusive transfer function $M(\omega)$ at a set of real frequencies ω_j and we want the DPA vector A_k for a differently specified set of pole frequencies ω_k (on the imaginary axis), we can define a matrix of complex elements

$$F_{jk} = \frac{i(\omega_j/\omega_k)}{1 + i(\omega_j/\omega_k)} \tag{16}$$

Then, in principle,

$$\overline{M} = \left(\overline{\overline{F}}\,\overline{A} \right)^{\dagger} \tag{17}$$

or

$$M_s = \sum_{k=0}^{K-1} A_k F_{sk} \tag{18}$$

In principle, this can be inverted to give

$$\overline{A} = \overline{\overline{F}}^{-1}\,\overline{M}^{\dagger} \tag{19}$$

or

$$A_k = \sum_{j=1}^{J} (\overline{\overline{F}}^{-1})_{jk}\, M_j \tag{20}$$

However, the matrix relationship will not be straightforward unless the two sets of frequencies are of the same size, cover the same band at similar densities, and the transfer function $M(\omega)$ is error-free. In general, F_{jk} will not be square and, even if square, it may be somewhat poorly-conditioned. But, as long as ω_k and ω_j cover

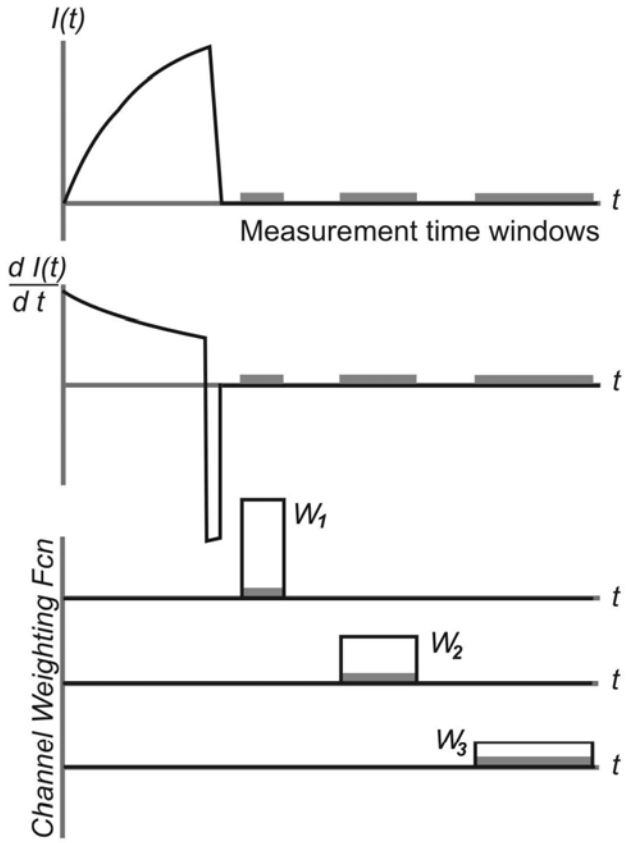

Figure 2. Schematic of how time-domain sensor measures a window averaged response.

the same frequency range with similar densities the problem can easily be dealt with by using a damped least squares solution to find A_k from M_j.

The magnitude of the damping parameter λ controls the required accuracy of fit to M_j. Because, except for the damping parameter λ, the matrix of fitting equations depends only on ω_j and ω_k, it can be calculated in advance of knowing M_j. However, λ ought to be selected appropriately for each M_j, and this may be difficult to do *a priori* with an algorithm. However, by solving the least squares equations for a wide ranging but sparse set of λ's and then finding the vector of M_j misfit for each λ and comparing its norm with the norm of M_j and with an estimate of the error in it, a good solution can be selected automatically.

Figure (5) shows some examples of fitting a discrete pole model to observational spectra. Shown are the observational data (real and imaginary components), the fitted complex spectrum and the DPA vector. Also included is a cumulative version of the DPA vector where terms A_k are progressively summed from the static term. We show several cases with optimal damping and one case where the damping parameter has been varied. One sees immediately that the cumulative DPA vector is quite similar in functional form to the real component of the complex spectrum, except that it varies more sharply in frequency than does the spectrum. The DPA itself is similar in form to a sharpened version of the imaginary component of the spectrum and to the proportional derivative $d\ln(A(\omega))/d\ln(\omega)$ of the real component. These observations accord with the necessary Hilbert transform relationship between the real and imaginary components of a realizable, causal spectrum.

6. COORDINATION OF THE SPECTRAL CALCULATIONS

To be practical, making comparative studies of sensor designs by simulation requires that a database giving the properties of typical soils and prospective target objects (mines or clutter) be already set up. The information

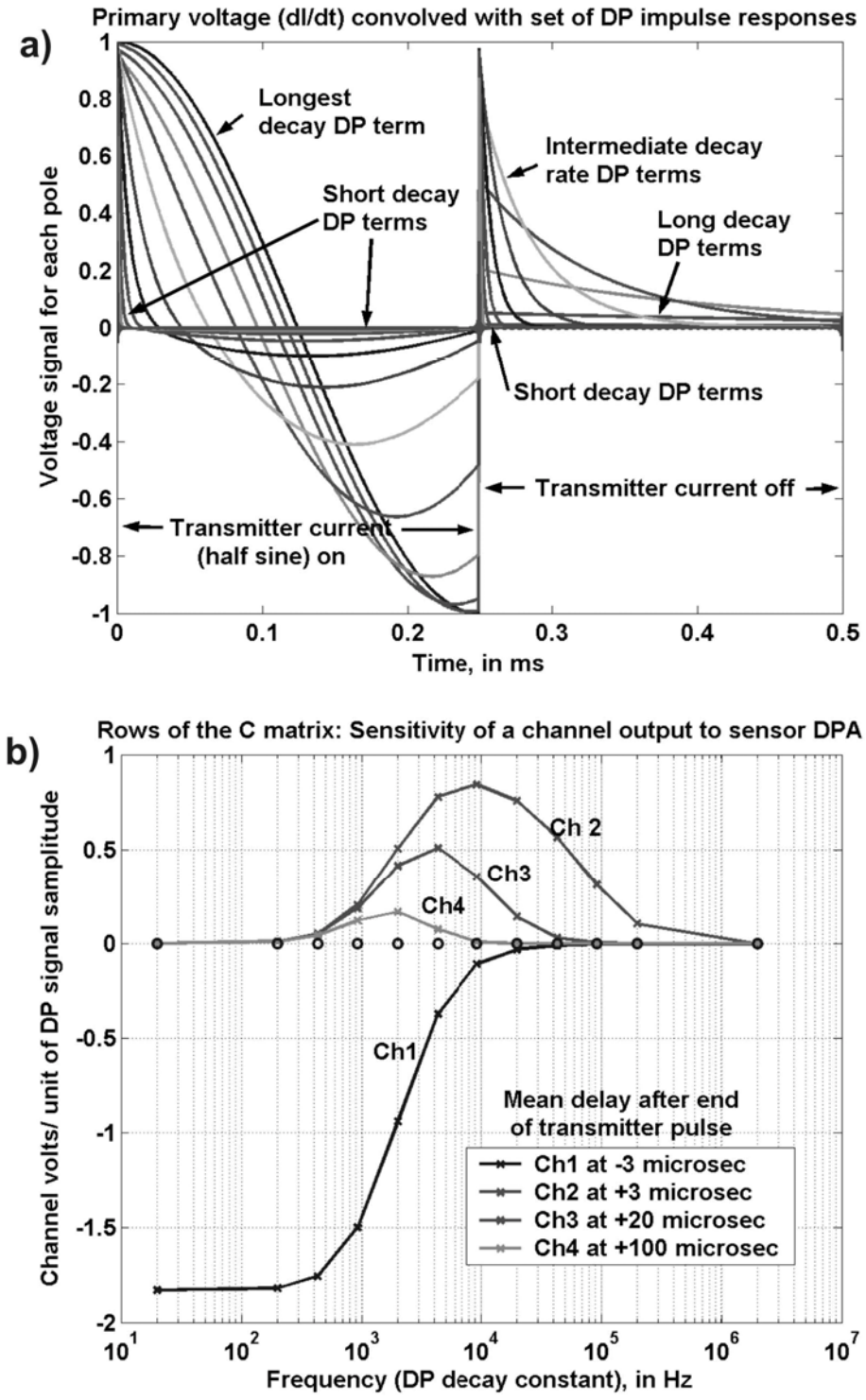

Figure 3. Contributions to receiver voltage by each term in the DP model. a) Voltage waveforms for each term, b) Contributions to channel output from each term. ($I(t)$ is a half-sine pulse .

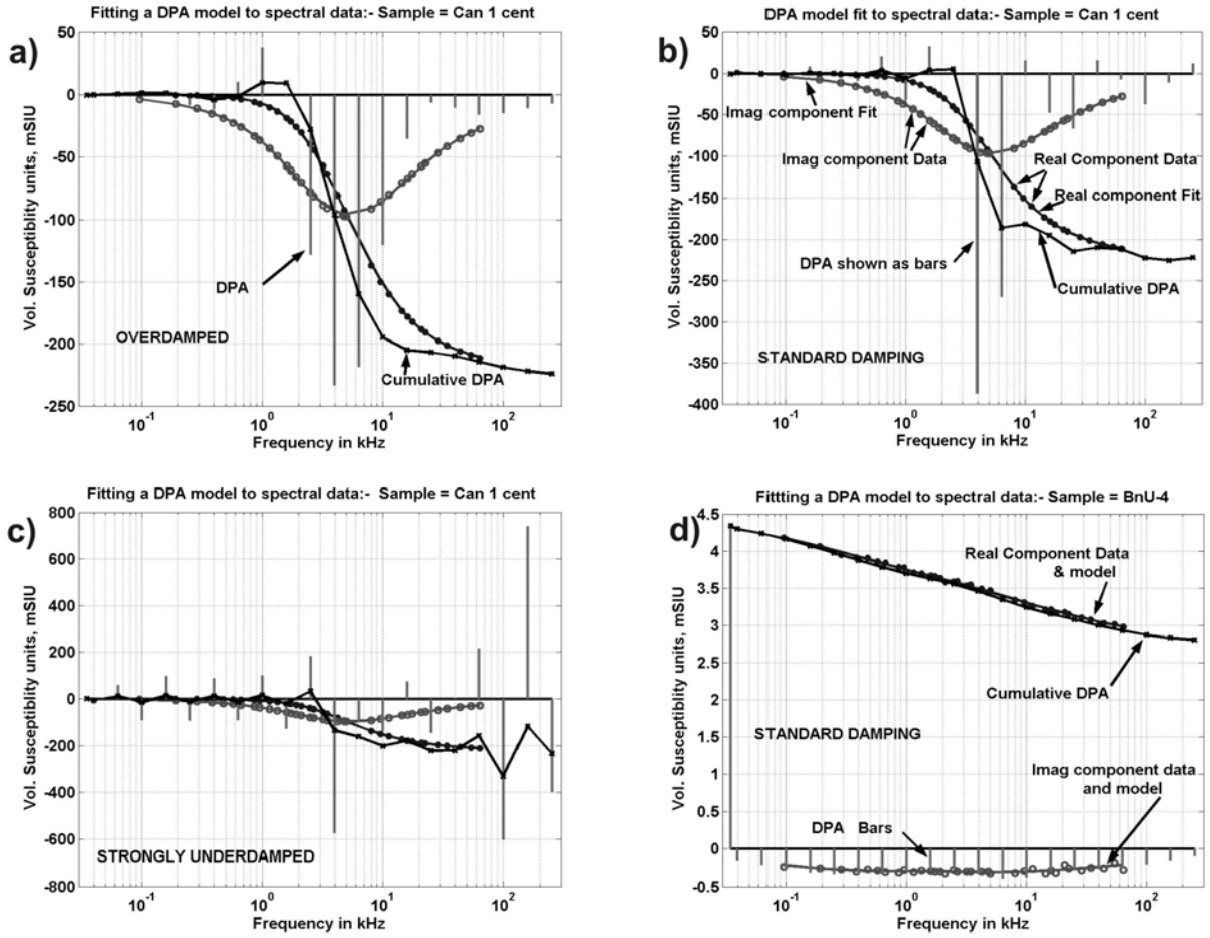

Figure 4. Examples of fitting a DP model to observational spectra using damped least squares. Spectra are from a conductive non-magnetic object and a dispersive soil: a) An overdamped fit to the object spectrum; some misfit is just visible; b) Optimum fit to the object spectrum.; c) a highly underdamped fit to the object spectrum; the DPA is unnecessarily oscillatory; d) an optimum fit to a soil spectrum. Note the resemblance between the DPA and the imaginary component, and the cumulative DPA and the real component.

in the data base will control the spectral characteristics of any simulated response. The data may be in a variety of forms; for example, as parameter values that characterize certain target objects or materials in the host environment (and from which the simulation code will calculate sensor response), or in tabulated data describing the complex susceptibility spectra of typical soils or small target objects. The data could also be theoretical response spectra computed on demand from parameter values in the data base that are input to physical or mathematical spectral modelling routines.

Then, to conduct a simulation, one must provide an input data file that defines an earth model by selecting specific target objects and earth materials from the data base, positioning the targets in space and specifying the characteristics of the host medium that surrounds them. Similarly, additional files must be supplied that specify both the geometrical configuration of the sensor system and also its signal processing aspects (loop geometry and turns, current waveform, sampling windows, etc). Also to be specified is how the virtual sensor system will be moved over the earth model (survey profiles or grids, sensor heights and attitudes, etc.).

The simulation code contains a variety of modules, in order to be able to treat different cases. However, all will work either like the small object code described in equation (1) or the layered space algorithm of equation (3). In the former case, the simulation code first calculates arrays of geometrical coupling data (sensor response versus sensor position) that are not frequency-dependent and then applies them to combine the spectral responses of the various components in the earth model. In the latter case, the simulation code must calculate new arrays of geometrical coupling for each frequency in a list, supplying frequency domain values for relevant model parameters like susceptibility from their respective spectral data files.

To facilitate the calculations, it is very helpful if all spectral response data in the database have already been converted to DPA vectors based on a single common ω vector. In the simulation calcualtions, spectral data are communicated either as vectors of complex spectral amplitude $\overline{M}$ or as real DPA vectors, $\overline{A}$; with both representations using the same ω vector. Conversion back and forth between $\overline{M}$ and $\overline{A}$ then involves only a square matrix $\overline{\overline{F}}$ from equation (16) ($\overline{M} = \overline{\overline{F}}\,\overline{A}$), and its inverse can be used directly (without least squares) provided the $\overline{M}$ data are nearly error free.

Usually, as final output we want a time-domain voltage channel response $\overline{V_c}$ at each sensor location in the survey. $\overline{V_c}$ can be calculated from a DPA vector representation of the sensor's secondary mutual inductance by multiplying $\overline{A}$ by the rectangular matrix $\overline{\overline{C}}$ defined in equation (14). ($\overline{V_c} = \overline{\overline{C}}\,\overline{A}$). In simulations of first type, we could evaluate the sensor DPA response by first combining the DPA responses of all the various components at all survey points according to their geometrical coupling at each point in the survey. Then we could convert the results to channel response $\overline{V_c}$ by $\overline{\overline{C}}$ multiplication. However, if the $\overline{\overline{C}}$ matrix is calculated as soon as the sensor's spectral characteristics have been defined and it is applied immediately to the DPA vectors $\overline{A}_n$ of all relevant inductive components $\overline{T}_{on}$in the model, much calculation can be saved because $\overline{\overline{C}}$ is rectangular and $\overline{V_c}$ usually has many fewer elements than $\overline{A}$. The steps are summarized as follows:-

Standard implementation: Channel response vector $\overline{V_c(\mathbf{r}_s)} = \overline{\overline{C}} \sum_{n=1}^{N} K_n(\mathbf{r}_s)\,\overline{A}_n$ where the geometrical coupling factor $K_n(r)$ implements equation (1) for each element of $\overline{T_0}$ in each object.

Faster implementation: Channel response vector $\overline{V_c\mathbf{r}_s)} = \overline{\overline{C}}\;\overline{A}(\mathbf{r}_s) = \sum_{n=1}^{N} K_n(\mathbf{r}_s)\,\overline{\overline{C}}\;\overline{A}_n$

In the second case, sensor response must be evaluated as a frequency-domain, secondary mutual inductance transfer functions ($M^{(S)}(\omega, \mathbf{r}_s)$). If any input arguments to this calculation are frequency-dependent (e.g., $\kappa(\omega)$), their complex values will have to be obtained from information in the database. Thus, in a preliminary step, the DPA vectors for all the relevant variables are multiplied by the square $\overline{\overline{F}}$ matrix (equation (16)) to put them in complex spectral form. Then, after $M^{(S)}(\omega)$ has been evaluated for all frequencies, it can be converted to the time-domain channel voltage response vector $\overline{V_c(\mathbf{r}_s)}$ by multiplying it by the combination $(\overline{\overline{CF}}^{-1})^{\dagger}$. This matrix converts complex spectral data to DPA and then DPA to channel response. Although this route may be substantially slower than the direct route used in the case above, it is still quite efficient. No large FFT's are needed.

7. CONCLUSIONS

By carefully organizing the spectral calculations, it clearly is possible to make EMI simulation efficient enough that it can be used in engineering design of EMI mine detectors. We have not yet completed our simulation package, so it is impossible to say yet whether significant improvements in discrimination are possible. However, we are hopeful that they will be.

ACKNOWLEDGMENTS

This work was supported by the Canadian Centre for Mine Action Technologies (CCMAT) of Defense Research and Development Canada (DRDC) as part of contract No. W7702-03R942/001/EDM. We gratefully acknowledge the assistance and guidance provided by DRDC personnel in at Suffield, Alberta, and especially the help from Dr.Yoga Das, technical authority for the contract.

APPENDIX 3

Characterizing mine detector performance over difficult soils

R. C. Bailey[a] and G.F. West[b]

[a]Physics and Geology Departments, University of Toronto, Toronto, Canada;
[b]Physics Department, University of Toronto, Toronto, Canada

ABSTRACT

A variety of metal detectors are available for the detection of buried metallic targets in general and for humanitarian demining in particular. No one detector is optimal in all environments: variations in soil conductivity, and more importantly, frequency dependent soil magnetic susceptibility can favor one design over another. The use of computer modeling for assessing different designs is straightforward in principle, at least to first order, but still difficult in practice. No widely available general purpose public-domain code exists for handling the wide range of detector configurations in existence for a variety of targets and difficult soil environments.

The Geophysics Lab of the University of Toronto is attempting to address this problem in two ways. The first is by assembling the required computational algorithms to do this into a single simulation code with a straightforward GUI, intended to be public domain as a MATLAB code. The second, the subject of a companion paper in this conference, is by making measurements of the electromagnetic properties of difficult soils, and finding semi-analytic representations of these responses suitable for modeling purposes. The final version of the code, when completed, is to handle single or multiple transmitter and receiver coils of circular or polygonal shape, general transmitter current waveforms, arbitrary transmitter orientations and survey paths, small targets with frequency-dependent anisotropic responses (permitting both magnetic and inductive responses to be calculated), embedded in multi-layered half spaces with both conductivity and frequency-dependent susceptibility (so-called "difficult soils"). The current state of the simulation code and examples of its use will be described in this paper.

Keywords: EMI, humanitarian demining, simulation code, magnetic soils

1. INTRODUCTION

The need for electromagnetic induction (EMI) detection of buried metallic targets in general and for humanitarian demining in particular, has led to a variety of electromagnetic induction (EMI) metal detectors. It is difficult to design a detector to be optimal in all environments: variations in soil conductivity, and more importantly from the point of view of this paper, frequency dependent soil magnetic susceptibility can favor one design over another. The comparison of projected detector performances in such situations can be assisted by the use of computer modeling. Such modeling capability is pointless without measurements of the frequency dependence of magnetic susceptibility of actual soil samples, and that has been the initial focus of this project. Even with such measurements, modeling is still not trivial in practice: although there are many codes, public domain and otherwise, for computing EMI responses of various targets in various environments, most are adapted to specific instruments, and making comparisons would require collecting disparate codes, trying to make them run equivalent models, and then reconciling disparate outputs. This task is further complicated by the fact that frequency dependent soil susceptibility is not always incorporated in EMI modelling, although straightforward in principle.

One of the goals of this project is to produce such code. No new theory is involved; all of the theoretical material on which this code is based is available in the scientific literature, and in fact common knowledge in such fields as exploration geophysical EMI. Such code, to be useful, is required to be relatively flexible with respect to instrument configuration and operation, since one cannot predict in advance the evolution of instrument design. On the other hand, the range of targets and operating environments is more constrained because it is

Further author information: (Send correspondence to R.C.B.)
R.C.B.: E-mail: bailey@physics.utoronto.ca, Telephone: 1 416 978 3231
G.F.W.: E-mail: west@physics.utoronto.ca, Telephone: 1 416 978 3155

already defined by existing circumstances. However, realistic characterization of these targets and environments is, in the end, necessarily experimental; soils are not designed to prior specifications, and one cannot rely on mine manufacturers to provide reliable specifications of the relevant material properties and shapes of the metal components of their mines. (Even if they did, such specifications might be useless much of the time, for two reasons: first, material properties such as steel permeability are irrelevant to mine operation, and unlikely to be well controlled during manufacture; secondly, there are many shapes (helical springs, L-shapes, *etc.*) for which theoretical calculations of the responses are not at all straightforward.)

Accordingly, the mine detection simulation described here is part of an integrated project. The first part of the project, essentially completed and previously described (West and Bailey, 2005; West and Bailey, 2006), was the design and construction of a broadband susceptibility meter suitable for measuring the frequency-dependent susceptibility of both soils and small metal pieces. Based on an initial working prototype, two further improved spectrometers are now being completed.

To simply provide this experimental information as spectra or equivalent data does not make it readily usable by the demining community. Accordingly, the development of user-friendly code to integrate this information and instrument specifications into a simulation is, as noted above, the necessary second part of the project. The type of instrument modelled here is of the usual type where a signal generator generates a transmitter current, which in turn generates a magnetic field using a transmitter coil. This transmitter coil is inductively and magnetically coupled by the environment (which includes the earth and any targets of interest) to a receiver coil. The receiver coil voltage is then amplified and processed with various detection algorithms. These detection algorithms may extend all the way from recognition of a modulated audio signal by a listening operator, through to computer processing of the signal by various logic algorithms. (This code is *not* intended to model those very simple single-coil devices where the target influences the Q or resonant frequency of an oscillator by interaction with its single transmitter coil.)

Coil arrangements in existing and future detectors have a variety of configurations, so that the finished product should be able to handle any such arrangement, including multiple coils with arbitrary relative orientations and shapes. Transmitter current waveforms are also highly variable, particularly if one includes the variety of EMI waveforms that might be inherited from EMI applications in exploration geophysics. To rely on manufacturers' design intentions for such waveforms, even if publicly available, would be imprudent, since design specifications do not always reflect final realities. It is more useful to be able to work with an arbitrary digitized waveform as measured with an external sensor.

The classic humanitarian demining problem involves a very small metallic target, embedded in the Earth which is usually relatively resistive (in the sense that the transmitter field at the target location is not very different from the value it would have in free space). This permits the transmitter-receiver couplings induced by soil conductivities and susceptibilities, even if frequency dependent, to be regarded as independent of the transmitter-receiver couplings induced by the target, so that they may be summed.

The code is written in MATLAB. This platform enables two important run-time features, whose role is described in the last section of this paper. The first is dynamic creation of structures at run time (to permit new instrument configurations and properties to be easily added without rewriting the core code). The second is the ability to read and execute user-entered formulae as MATLAB code, enabling new instrument signal processing algorithms to be easily added, also without rewriting the core code).

2. SPECIFIC GOALS

It is tempting to design code to cover all possibilities, *i.e* to make sure every cell of Table 1 is filled in. However, this usually requires that the most general algorithms (i.e. the slowest) be adopted, in order to be able to simultaneously handle all complications. This application of a sledgehammer to every peanut guarantees that code will almost always run much slower than it needs to.

	HCC	HPC	TPD	TPC
FS	U,S	U	U,S	U
LHS	U,S		U,S	
FD3DS	U	U	U	

Table 1. A table showing localized target types (S: host shielding calculated; U: host shielding ignored) possible in this code with combinations of different instrument coil configurations (across) and host combinations (down). Instrument acronyms are as follows: HCC - horizontal circular coils; HPC - horizontal polygonal coils; TPD - tilted point dipoles; TPC - tilted polygonal coils. Target and host acronyms are: UFDPT - unshielded frequency-dependent point target; SFDPT - shielded frequency-dependent point target; FS - free space; LHS - conductive layered half-space with conductivity and frequency-dependent susceptibility specified in each layer; FD3DS - 1, 2, or 3D weak susceptibility distribution with single frequency-dependence;

2.1. Targets and hosts

Since the primary purpose of this code is to enable the simulation of the effects detecting small conducting and possibly magnetic targets in "problem soils", the range of targets and host environments need not be larger than required to address this problem. In particular, since the metal parts such as strikers in modern anti-personnel mines are typically very small, and the distance to target, coil diameters and separations of multiple targets typically significantly exceed these target dimensions, non-interacting point target responses are probably suitable for assessing most detection problems associated with problem soils. These are of course endowed with realistic frequency dependent responses, as equivalent magnetic susceptance moments, for comparison with the frequency dependent responses of host media made of magnetic soils. Since the only reliable characterizations of such responses are experimental, the target descriptions must include compatibility with such characterizations.

It is the frequency dependence of such host media, rather than the geometry, which is of primary importance in assessing soil-target detection interference, so that uniform half-spaces provide some of what is required. Spatial variations in the frequency-dependent susceptibility of problem soils, however, can mimic the spatial localization and the frequency dependence of both response amplitude and phase of the desired mine targets. It is therefore important to be able to model an arbitrary three-dimensional spatial distribution of at least weak (non-self-demagnetizing) susceptibility, and this is therefore included. Electrical conducting soils can also provide an interfering response; since computing the responses of general horizontally layered conductive half spaces is straightforward and described in the literature, at least for horizontal planar coils, this feature is implemented also.

Electrical conducting soils also influence the response in another way: they electromagnetically shield the targets of interest from the instrument, particularly in a very conductive soil. The target excitation is modified by soil attenuation, in accordance with the general theory summarized by Das.[?] Accordingly, the code is intended to permit high-conductivity soils to be modeled, but with a significant speed penalty.This will be available in the code, but potentially slows the execution; the default is therefore to neglect such shielding and use the free space coupling of instrument to target. In resistive soils, this effect of the host shielding on the instrument response via the target is second order relative to the direct response of the host, and can often be neglected.

2.2. Instrument configurations

Since a wide range of instruments exist now or may in the future, it is important that such code be able to handle as many transmitter waveforms and coil configurations as possible. Accordingly, the code is set up to handle any transmitter waveform, and an arbitrary number of transmit/receive coils. Instrument orientations are more problematic. For the case of targets in a soil with frequency-dependent weak magnetic susceptibility and negligible conductivity, any instrument orientation is handled. This permits assessment of the interaction of instrument orientation with the problematic magnetic soils. However, the general layered earth host medium is only easily done, and implemented here, for planar coils with parallel axes, which except for one case described below, also have to be horizontal. Fortunately, this is the most common instrument configuration.

2.3. Survey configurations

Survey locations can be specified as single points, profiles, grids, or arbitrary sequences. As noted above, instrument orientations other than horizontal restrict the cases that can be handled to non-conductive uniform half-spaces. Variable instrument heights are enabled straightforwardly, but slower in calculation than constant height measurements.

3. RESPONSE REPRESENTATIONS

Since the code must handle arbitrary transmitter waveforms and arbitrary measured frequency dependent soil susceptibilities and target responses, it is worth detailing the way in which this is done efficiently. Consider a transmitter current in a single turn coil with angular frequency ω and amplitude I. This produces a receiver voltage V (a complex phasor) in the presence of a conductive-susceptible earth defined by $V = C(\omega)I$, where C is a coupling or transfer function. The computation of the transfer function is the numerical core of the computation; many algorithms are available in the literature for different types of targets or host media, most often for circular coaxial coils; a number of these are incorporated into the code, but will not be reviewed in detail here. Because of the separability of the relevant differential equations, these algorithms normally work in the frequency domain, and time domain responses, if required, are synthesized by computing the transfer functions at many frequencies so that a Fourier transform can be applied.

If, as in a frequency domain instrument, the number of different transmitter frequencies is small, it is computationally feasible to simply repeat the above calculation for each frequency. However, a wide-band transmit signal such as a square wave or other arbitrary function of time may require hundreds or thousands of frequencies for an accurate (high dynamic range in both time and amplitude) representation via Fourier series. A survey map of response versus location will also require repeating this entire computation at many locations as well. It then becomes worthwhile to avoid repeating any parts of the above calculation, and also to take advantage of parsimonious representations of various properties. Here, because it is central to the code, we paraphrase the description of the parsimonious representation of time-domain responses given by West and Bailey (2006).

3.1. Parsimonious representation of time-domain responses

If a transmitter coil is energized by a unit impulse current of strength I ($I\delta(t)$ where), the magnetic flux through a receiver coil can be written in the form

$$\phi_\delta(t) = \left(K_0\delta(t) + \sum_{m=1}^{\infty} K_m\, H(t)\, e^{-\lambda_m t} \right) \tag{1}$$

where $\delta(t)$ is the Dirac delta function, and $H(t)$ is its integral, the Heaviside function.

$\phi_\delta(t)$ is actually the Fourier transform of the frequency-dependent mutual inductance of a single turn of each of the transmitter and receiver coils, *including* the effects of the environment. That mutual inductance can be therefore written as

$$M(\omega) = K_0 + \sum_{m=1}^{M} \frac{K_m}{j\omega + \lambda_m} \tag{2}$$

where ω is angular frequency and $j = \sqrt{-1}$. The term K_0 describes the instantaneous coupling of the two coils, and the sum describes the fluxes generated by decaying eddy currents or magnetizations in targets and host media. For purely electromagnetic behavior of finite targets, this representation is exact: the sum is over the actual physical decay modes of the eddy currents. For other situations, the representation can be made as accurate as desired by taking enough decay modes; in the limit of a continuum of modes over all possible λ, this is simply the inverse Laplace transform representation of a time domain transfer function.

Although an infinite number of decay rates λ can in principle required, a satisfactory representation over all important times in (??) can often be obtained with a few dozen, spaced about 5 or 6 per decade. As an extreme example, a simple conducting ring target of fine wire has only a single decay mode with $\lambda = R/L$ where R and L are the resistance and inductance of the loop respectively. Obtaining such parsimonious representations

of transfer functions for targets and soils is the subject of a companion paper in this conference by West and Bailey[?]; we will assume in what follows that they are available, and replace (??) with

$$\phi_\delta(t) \cong \left(A_0\delta(t) + \sum_{m=1}^{M} A_m\, H(t)\, e^{-p_m t} \right) \tag{3}$$

where the rates p_m are prescribed in advance and A_m are the amplitudes of the parsimonious representation. These rates must be chosen at the beginning of a simulation run to encompass the range of all rates which are important in the result, since all subsequent response calculations will be only for these rates. The corresponding approximation to the mutual inductance (??) becomes

$$M_P(\omega) = K_0 + \sum_{m=1}^{M} \frac{A_m}{j\omega + p_m} \tag{4}$$

The receiver flux $\Phi(t)$ response to an arbitrary transmitter current waveform $i(t)$ can therefore be written as the convolution of $i(t)$ with the impulse response ϕ_δ:

$$\Phi(t) \cong \int_{-\infty}^{\infty} i(t-\tau) \left(A_0\delta(\tau) + \sum_{m=1}^{M} A_m\, H(\tau)\, e^{-p_m \tau} \right) d\tau \tag{5}$$

(In West and Bailey,[?] the same symbol ω is used to describe distances along both real and imaginary frequency axes; here we have used p_k to denote pole positions on the imaginary axis rather than ω_k.)

3.2. Representing the instrument

The above equations are too general for convenient use. If, as is usually the case, the transmitter current has an arbitrary repetitive waveform $I(t)$ with period T, (??) can be split into integrals over each period, giving

$$\Phi(t) \cong \int_{0}^{T} i(t-\tau) \left(A_0\delta(\tau) + \sum_{k=1}^{\infty} \sum_{m=1}^{M} A_m\, H(\tau)\, e^{-p_m(\tau+kT)} \right) d\tau \tag{6}$$

or

$$\Phi(t) \cong \int_{0}^{T} i(t-\tau) \left(A_0\delta(\tau) + \sum_{m=1}^{M} A_m\, H(\tau) \frac{e^{-p_m \tau}}{1-e^{-p_m T}} \right) d\tau \tag{7}$$

If one restricts its evaluation to the time range 0 to T, equation (??) effectively regards the transmitter current waveform as existing only for a single cycle, and builds the response to all previous cycles into a response modified by the terms $1/(1-e^{-p_m T})$.

The receiver voltage is product of the number N_R of receiver coil turns, the number N_T of transmitter coil, and the time derivative of the flux, or

$$V_R(t) \cong N_R N_T \int_{0}^{T} \left(\frac{d}{dt}\, i(t-\tau) \right) \left(A_0\delta(\tau) + \sum_{m=1}^{M} A_m\, H(\tau) \frac{e^{-p_m \tau}}{1-e^{-p_m T}} \right) d\tau \tag{8}$$

Typically, it is not the entire receiver voltage waveform that is analysed, but a number of filtered or integrated sections of it as detected "channel voltages" s_n (V_C in West and Bailey,[?] 2006), weighted integrals of the form

$$\begin{aligned} s_n &= \int_{0}^{T} w_n(t) V_R(t)\, dt \\ &\cong N_R N_T \int_{t1}^{t2} \int_{0}^{T} w_n(t) \left(\frac{d}{dt}\, i(t-\tau) \right) \left(A_0\delta(\tau) + \sum_{m=1}^{M} A_m\, H(\tau) \frac{e^{-p_m \tau}}{1-e^{-p_m T}} \right) d\tau\, dt \end{aligned} \tag{9}$$

The weighting functions $w_n(t)$ are simple rectangular functions if the integrated voltage over a time window is desired. In a real instrument, the s_n are the results of sampling the filtered channel voltages.

Equation (??) can be rewritten as

$$s_n = \sum_{m=0}^{M} C_{nm} A_m \tag{10}$$

where the "instrument transfer coefficients" C_{nm} are properties of the instrument alone, and can be evaluated just once prior to iterating over instrument positions to produce a map. Specifically

$$C_{n0} = N_R N_T \int_0^T \int_0^T \delta(\tau)\, w_n(t) \frac{d}{dt} i(t-\tau)\, d\tau\, dt = N_R N_T \int_0^T w_n(t) \frac{d}{dt} i(t)\, dt \tag{11}$$

and

$$C_{nm} = N_R N_T \int_0^T \int_0^T w_n(t) \left(\frac{d}{dt} i(t-\tau) \right) \frac{e^{-p_m \tau}}{1 - e^{-p_m T}}\, d\tau\, dt \tag{12}$$

If the weighting function is a simple time window from t_1 to t_2, these reduce to

$$C_{n0} = N_R N_T \left(i(t_2) - i(t_1) \right) \tag{13}$$

and

$$C_{nm} = N_R N_T \int_0^T \left(i(t_2 - \tau) - i(t_1 - \tau) \right) \frac{e^{-p_m \tau}}{1 - e^{-p_m T}}\, d\tau \tag{14}$$

Given these pre-computed instrument transfer coefficients C_{nm}, the desired instrument channel signals can be computed quickly for each survey location using the matrix multiplication (??) as soon as the amplitudes A_m of the coupling from transmitter to receiver for that survey location are known.

4. COUPLING COEFFICIENT CALCULATIONS

The transmitter to receiver coupling amplitudes A_m are considered to arise in from two ways: by the direct response of the host medium alone (the earth in which targets of interest are embedded) and by the response of localized targets (which are themselves coupled through the host medium to transmitter and receiver). If there are multiple localized targets, they are assumed to have negligible interaction with each other. For purposes of calculating the host response, the general host medium in the present code is a plane horizontally layered earth with conductivity and frequency dependent magnetic susceptibility specified for each layer. To permit quick calculation of the host response, the instrument arrangement is currently limited to horizontal coplanar circular coils, not necessarily coaxial. In what follows, we do not discuss the theory of EMI responses in general, as these are widely described in the literature. Rather we concentrate in this section on those non-standard aspects of the computation of responses which have been used to make the code faster in execution.

4.1. The host medium response

A number of different host media are provided. Host media are involved in two ways: they provide a direct response, and they shield localized targets. It is possible, if the shielding is not strong, to need the host in the first role but to not require it it in the second, and still achieve reasonable accuracy. The simplest host is free space, which is the effective host for instrument-target coupling when shielding is neglected.

4.1.1. Free space

For this host, arbitrary polygonal coil shapes and orientations are possible for the instrument-target coupling, since the magnetic induction B and vector potential A can be computed straightforwardly using the Biot-Savart law (described in any undergraduate textbook on electromagnetics), for a sum of straight line coil segments. For the direct transmitter-receiver coupling, a circular coil approximation is used, to avoid the integrals required to exactly compute the mutual induction. Getting the coil shape right is more important for instrument-target coupling, since all of a target can be very close to an irregular section or corner of a coil and thus very dependent on the coil shape for certain instrument locations; it is impossible for the host medium as a whole to be close to a corner, and for all of its response to be thus affected.

Rather than a finite loop, point dipoles are used when the effects of tilt have to be modeled (see Table (??)). The free space fields of a magnetic dipole are available in any undergraduate text on electromagnetics.

4.1.2. Layered conductive and permeable host

Since this is the most general conductive Earth presented, we discuss the equations in some detail. The notation is based on that presented by Ward and Hohmann[?] (1987), but many earlier treatments of the same theory are available (*e.g.* Wait,[?] 1982). A horizontal planar coil of arbitrary shape carrying a current I can be regarded as a sheet of adjacent infinitesmal square loops of area dA and vertical magnetic moments $dm = IdA$, each of which will produce flux through the receiver coil. The vertical field of each infinitesmal vertical magnetic dipole moment m is, in cylindrical coordinates,

$$H_z(\rho, z) = \frac{IdA}{4\pi} \int_0^\infty \left[e^{-u_0(z+h)} + R_{TE}\, e^{u_0(z-h)} \right] \frac{\lambda^2}{u_0} J_0(\lambda\rho)\, \lambda d\lambda \tag{15}$$

where ρ is horizontal distance from the dipole, and z vertical distance. The reflection coefficient R_{TE} is

$$R_{TE} = \frac{Y_0 - \hat{Y}_1}{Y_0 + \hat{Y}_1} \tag{16}$$

The admittances $\hat{Y}_n$ are calculated recursively using

$$\begin{aligned} \hat{Y}_n &= Y_n \frac{\hat{Y}_n + 1 + Y_n \tanh(u_n h_n)}{Y_n + \hat{Y}_{n+1} \tanh(u_n h_n)} \\ \hat{Y}_N &= Y_N \\ Y_n &= \frac{u_n}{j\omega\mu_n} \\ u_n &= \sqrt{\lambda^2 + k_n^2} \\ k_n^2 &= \omega^2 \mu_n \epsilon_n - j\omega\mu_n\sigma_n \end{aligned} \tag{17}$$

Here, σ_n, μ_n, ϵ_n and h_n are the conductivity, permeability, permittivity, and thickness of the n'th layer, counting down down from the surface. For demining cases, the dielectric behavior controlled by the permittivity is likely to be negligible. However, magnetic problem soils will require that the permeability be allowed to be frequency dependent. The recursion proceeds upwards from a basal interface at the bottom of the N'th layer, above an assumed uniform half-space.

The Hankel transform in (??) in this code uses the convolution method of Guptasarma and Singh[?] (1997). If the resulting $B_z = \mu_0 H_z$ is numerically doubly integrated over the area of the transmitter and receiver coils, and divided by the area of the transmitter loop, the result is the flux penetrating one turn of receiver coil generated by one turn of transmitter coil, or I times mutual inductance $M(\omega)$ described in (??). For a frequency-domain instrument, it is necessary to repeat this calculation once for each of the operating frequencies of the instrument, usually a small number.

As for the free space host, point dipoles sources and receivers are used when the effects of tilt have to be modeled (see Table (??)). The calculations are similar but simpler; the results for an arbitrarily oriented dipole are summarized in Wait[?] (1982).

4.1.3. Three dimensional irregular magnetic soil

Although a host rather than a localized target, this is computed in the same way as the sum of a volume distribution of localized targets. Here an irregular distribution is synthesized in a 3-D grid of voxels in the survey region. For normal small (relative to unity) soil susceptibilities, where demagnetizing effects and interactions are unimportant, the free-space fields of the transmitter coils can be used to compute the magnetization density of the field. Reciprocity permits the same calculation using the receiver coils, and integrating over the soil volume, to extract the induction response of the receiver.

4.2. Localized target responses

Localized targets are assumed to be negligible in size, and either described by the user in general terms as a parsimonious frequency-dependent magnetic susceptance (typically from actual measurements in our wideband susceptibility spectrometer), or converted to such a representation within the program for some standard types (wire loop, conducting permeable sphere, *etc.*). This mutual inductance can be in tensor form $X_{ij}(\omega)$. It is most easily specified from theory and measurements with three principal axes and three corresponding parsimonious frequency-amplitude series, as in

$$X_{ij}(\omega) = \sum_{k}^{3} n_{ik} n_{jk} X_k(\omega) \tag{18}$$

where n_{ik} is the i'th component of the k'th principal axis of the target, and $X_k(\omega)$ is the associated frequency response for inducing fields directed along that axis. Although this representation is exact only for ellipsoids, it is likely to be a reasonable approximation for other shapes; experimental measurements will be the final arbiter of this.

The contribution of such a target to the single turn mutual inductance $M(\omega)$ of the instrument is calculated as the product of the three principal axis couplings in the standard way as described by Das[?] (2005) in the EMI demining context and by many others.

$$M(\omega)^{TARGET} = \sum_{i=1}^{3} \sum_{j=1}^{3} B_i^T(\omega, \mathbf{r}_t) X_{ij}(\omega) \Phi_j^R(\omega, \mathbf{r}_t) \tag{19}$$

where $B_i^T(\omega, \mathbf{r}_t)$ is the magnetic induction produced at the target location $\mathbf{r}_t$ in the i direction by a unit current flowing in a single turn of the transmitter coil, $\Phi_i^R(\omega, \mathbf{r}_t)$ is the magnetic flux in a single turn of the receiver coil produced by a unit magnetic moment at the target location $\mathbf{r}_t$ in the j direction. Because of reciprocity, the flux Φ_j^R is actually be computed as $B_i^R(\omega, \mathbf{r}_t)$, using identical code for both $B_i^R(\omega, \mathbf{r}_t)$ and $B_i^T(\omega, \mathbf{r}_t)$.

If the earth is relatively resistive, the free space fields of the coils can be used without significant error for $B_i^R(\omega, \mathbf{r}_t)$ and $B_i^T(\omega, \mathbf{r}_t)$, making them frequency independent. Since they need be computed only once for each instrument location for a given target, this makes the computation much faster as described by West and Bailey[?] (2006).

If the earth is very conductive, and shields the target from the full transmitter field, the calculation is much slower, since the recursive frequency-dependent method described for the host medium calculation above is required to obtain $B_i^R(\omega, \mathbf{r}_t)$ and $B_i^T(\omega, \mathbf{r}_t)$. However, that can still be converted to the parsimonious representation described above, and shielding results computed at the parsimonious imaginary frequencies p_m only.

5. THE CODE

By and large, the code is organized to take advantage of the fast factorization of the problem described in the companion paper by West and Bailey[?] (2006), and that will not be repeated here. However, the material above says nothing about how the primary goal of flexibility is attained. The description format whereby users can specify configurations of instruments, targets and surveys is an important special feature of the code, however; we describe it here.

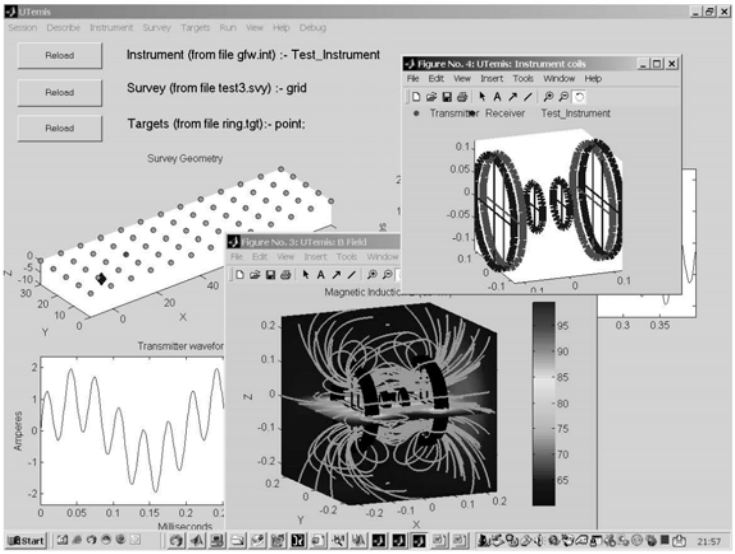

Figure 1. Screenshot of recent GUI version. The program is designed to export figures as regular MATLAB figure windows, thus making accessible all the figure editing tools of MATLAB. (The instrument displayed, with field lines, is actually the coil and field configuration of the wideband EMI spectrometer designed and built as part of this project).

5.1. Describing instruments, targets, and surveys

The need to model a variety of instruments, targets and survey configurations suggested that details of particular instruments, targets and survey geometries should not be built into the code, but rather described in user-editable configuration files which would be read by the GUI at run time.

These configuration files are all text files, and editable by any text editor. There are currently three types, survey files (*.svy), target files (*.tgt) and instrument files (*.int). The format is the same in all: each line names some entity of interest, and follows that name with property name - property value pairs. Generically,

```
"name   propertyName1=valueString1 propertyName2=valueString2 . "
```

No blanks are permitted within the propertyName/valueString groups. ValueString can be any valid MATLAB expression (numeric, array, string or a combination) but with no embedded blanks (underscores can be used to replace blanks). Embedded blanks are forbidden, since they are used by the GUI to separate one property name-value pair from another.

The internal model of the code for an instrument consists of (1) a waveform generator, (2) one or more transmitter coils, (3) one or more receiver coils, (4) a (possibly frequency dependent) amplifier, (5) a set of linear filters or integrators to characterize the waveform in different ways, (6) a multiplexing analog to digital converter (ADC), (7) a logic unit which computes an output signal or signals from the ADC outputs. Simulating all this requires the user to specify a number of properties: a transmitter waveform (either a standard form such as cosine, square, triangular, *etc.*); geometries of the transmitter and receiver coils (shape, dimensions, spacings and orientations) and their share of the transmitter current or receiver voltage (usually just the number of turns in the coil); a receiver amplifier gain, either as a number of a MATLAB formula which can be a function of frequency; a set of receiver voltage integrator specifications (either as sample times, weighted time integration intervals, or a user specified MATLAB function for arbitrary processing) for each of the analog-to-digital converter (ADC) channels; a final set of processing options on the ADC outputs specified again as a MATLAB formula (which can be non-linear) in terms if the ADC outputs v(k).

Since it is not the purpose of this preliminary report to act as the user's manual for the code, an exhaustive description of the possible properties will not be given here. Some examples will make the file style clear. A

sample instrument configuration file for a two-frequency horizontal coil device with a single transmit coil, primary signal nulling by two receiver coils, and two outputs is given by

```
information name=Test_Instrument    date='15/03/06'
txcoil shape=circle  location=[0,0,0]  radius=0.10 axis=[0,0,1] currentshare=100.0
rxcoil  shape=circle  location=[0,0,.10] radius=0.10 axis=[0,0,1] currentshare=50.0
rxcoil  shape=circle  location=[0,0,-.10] radius=0.10 axis=[0,0,1] currentshare=-50.0
waveform shape=sine frequencies=[5000,30000] current=[.5,.02]
acquisition method=frequency  gain='1.0e7*f/(1+f^2)' noise=0.01
output algorithm='abs(imag(v(1))),abs(real(v(2))'
```

This configuration method is extremely flexible. It utilizes MATLAB's ability to construct structure fieldnames dynamically at run time, so that one can add properties to the configuration structures long after the GUI code is finalized with no updates to that code. All that is required is that any added code pluck the new properties out the configuration structure.

A second important reason for coding in MATLAB is evident in the example above, MATLAB expressions are permitted for property values, and for computing the output signal: the frequencies and currents in the above expression for the waveform are given as 2-element arrays; the amplifier gain is given as a valid MATLAB expression utilizing an internally defined variable f (frequency) maintained by the code for just this purpose.

Similarly, a target configuration file might look like

```
target  name=targetA type=pointsphere location=[10,10,-10] radius=0.002 conductivity=1e6
target  type=conducting_halfspace rho=100
```

and a survey configuration file like

```
survey  type=profile first=[0,0,0] last=[0.75,0,0] sites=26
```

6. DISCUSSION

Although the code development and validation is not finalized, the essential features are as described above. When complete, the code and documentation will be made publicly available. Although we plan to release a compiled version for users without MATLAB licenses, the full power of graphical output processing will only be available in a MATLAB environment.

The purpose of the documentation is twofold: to allow users to actually use the code, and also to warn them when they are misusing it. Code which makes approximations, as this code does, is potentially subject to misuse. We have tried to flag such misuse with warnings where possible, but not to prevent it: solutions which violate assumptions in one respect may still usefully reflect reality in other respects.

ACKNOWLEDGMENTS

This work was supported by the Canadian Centre for Mine Action Technologies (CCMAT) of Defense Research and Development Canada (DRDC) as part of contract No. W7702-03R942/001/EDM. We gratefully acknowledge the assistance and guidance provided by DRDC personnel in at Suffield, Alberta, and especially the help from Dr.Yoga Das, technical authority for the contract. We also acknowledge assistance provided by Dr. Rob Moucha, undergraduate student assistant Xiaoyu Ouyang, and graphic artist Raul Cunha.

APPENDIX 4

Improving electromagnetic induction detector technology in humanitarian demining

R.C. Bailey, University of Toronto, Departments of Geology and Physics, Toronto, Canada
G.F. West, University of Toronto, Department of Physics, Toronto, Canada

SUMMARY

A variety of metal detectors using electromagnetic induction (EMI) are available for the detection of buried metallic targets in general and for humanitarian demining in particular. Detector designs suitable for humanitarian demining must be simple, robust and cheap. No one detector is optimal in all environments: variations in soil conductivity, and more importantly, frequency dependent soil magnetic susceptibility can favor one design over another. In particular, soils containing magnetic minerals can have as a result, a frequency dependent magnetic susceptibility which overlaps or coincides with the frequency range used for mine detection. Such soils are common enough that appropriate technology to understand and deal with these effects can make the dangerous job of humanitarian demining somewhat safer.

The Geophysics Lab of the University of Toronto is attempting to improve the technology in two ways. (supported by the Canadian Centre for Mine Action Technologies (CCMAT)) is aimed at investigating how EMI field instruments for humanitarian demining might be improved. The first is by constructing a better laboratory instrument to make measurements of the electromagnetic properties of difficult soils, in particular of frequency dependent magnetic susceptibility, and by finding semi-analytic representations of these responses suitable for modeling purposes. Based on experiments with a prototype, two production versions of this EMI spectrometer instrument are being built, with noise levels of the order of a few times 10^{-5} S.I. units, over a frequency range of 100 Hz to about 70 kHz. The second approach is by coding the software to allow such data to be used effectively in the simulation of detector performance. This involves assembling a number of induction algorithms into a single simulation code with a straightforward GUI, intended to be public domain as a MATLAB code. The final version of the code, when completed, is to handle single or multiple transmitter and receiver coils of circular or polygonal shape, general transmitter current waveforms, arbitrary transmitter orientations and survey paths, small targets with frequency-dependent anisotropic responses (permitting both magnetic and inductive responses to be calculated), embedded in multi-layered half spaces with both conductivity and frequency-dependent susceptibility (so-called ``difficult soils'').

Keywords: Electomagnetic induction, Humanitarian Demining, Frequency-dependent susceptibility

INTRODUCTION

With support from Defense Research and Development Canada's program on humanitarian demining, we are developing software tools to help simulate the performance of electromagnetic induction (EMI) metal detectors of arbitrary design. In order to make valid simulations, we need quantitative descriptions of the induction response of mine-like target objects and of the electromagnetic properties of the soils in which the mines may be hidden. The information must be valid in the spectral range employed in typical mine detectors, 1 to 100 kHz, and should preferably cover from 0.1 kHz to 1 MHz. Unfortunately, with the exception of a few susceptibility amplitude measurement at two frequencies (465 and 4650 Hz) using the Bartlington susceptibility meter (ref), few spectral data are available in the scientific literature.

Modern anti-personnel mines typically contain only a few grams or less of electrically conductive metal; often only ~ 1 mm to ~ 1 cm in extent. Thus, it has become necessary to increase the basic sensitivity of mine detectors to a level where discrimination between the desired EMI response from a significant target object and the unwanted responses from magnetic minerals naturally present in the soil is often

the key issue --- not just simple target detectability. Furthermore, in wet locales such as marine beaches, the bulk electrical conductivity of the environment may possibly generate significant interference. Therefore, most modern detectors are designed to be unresponsive to ideally permeable, non conductive materials and they use a spectral window below about ~100 kHz to minimize possible response from the bulk conductivity of the soil.

Figure 1. EMI detector for humanitarian demining use.

Although experience with the best modern EMI metal detectors has been relatively favourable, it has also revealed that many naturally magnetic soils do not behave as ideally permeable materials. Some may exhibit a frequency dependent, complex, magnetic susceptibility capable of confusing most detectors (sometimes termed *viscous magnetization* or VM, (Dunlop, D.J. and O. Ozdemir, 1997)). In the few cases where the effect has been investigated seriously, it usually is attributed to the presence of very fine grained ferromagnetic material close to the Nèel superparamagnetic transition (Mullins and Tite, 1973). The problem was first noticed in Australia where EMI metal detectors are widely used in prospecting for gold nuggets in weathered soil, and at least one manufacturer there (MineLab) offers an instrument that can be trained to reject a VM background signal (Candy, 1996).

It is, of course, possible to estimate by theoretical methods (*e.g.* Das, 2005) the EMI response characteristics of conductive and permeable objects like those present in mines. However, the metal objects in actual mines may have poorly known compositions and odd shapes, so direct experimental confirmations seem necessary. Likewise, the volume magnetic susceptibility of typical soils (real or complex) can be estimated from the limited available studies, and electrical conductivity can be estimated from porosity and water salinity data. However, because reality often differs from prior expectations, we believe that direct observation would be better.

THE EMI SPECTROMETER

The spectrometer (West and Bailey, 2005) uses a pair of transmitter coils in a Helmholtz configuration and a pair of receiver coils also in a Helmholtz configuration, to achieve uniform sensitivity over as large a volume as possible. Samples of standard paleomagnetic size (12.9 ml) are easily accommodated, and even over twice this sample volume, the sensitivity does not vary by more than about 5%. An additional pair of reference coils is used to null the directly coupled signal. A small number of turns in the coils keeps self-resonances above about 0.5 MHz. The signal is locally preamplified before sending to a PC computer for processing.

Signal acquisition is done with a high-end commercial sound card in a PC, driven by MATLAB. A wide-band signal generated with this card is used to drive the transmitter. current input to the transmitter coils is used The received signal is sampled at 192 kHz; a frequency-dependent susceptibility is computed by correlation and spectral division. A null (sample-free) measurement run is incorporated to reduce the effects of instrument drift. Measurement of a sample can take as little as 30 seconds, including loading and unloading. Tensor measurements for anisotropic samples are also possible, utilizing a rotating sample holder and a more complex measurement protocol.

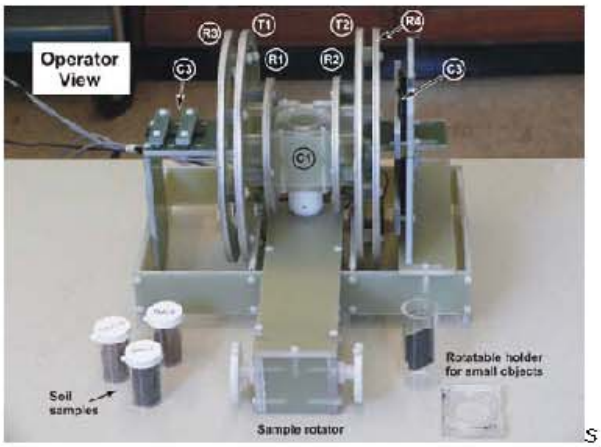

Figure 2. Prototype of wideband EMI spectrometer. The prototype does not have a case. Not shown are the s

preamplifier, the transmitter unit or the computer used for signal acquisition.

Magnetic soils that present a serious problem for mine detection usually have susceptibilities of 1 mSIU or greater. Thus the sensitivity objective for the instrument was an ability to delineate accurately the susceptibility spectrum of a standard 12.9 ml specimen with a susceptibility of about 1 mSIU. Therefore, base level drifts and noise should not much exceed 0.01 mSIU over the measurement bandwidth of 100 Hz to about 70 kHz.

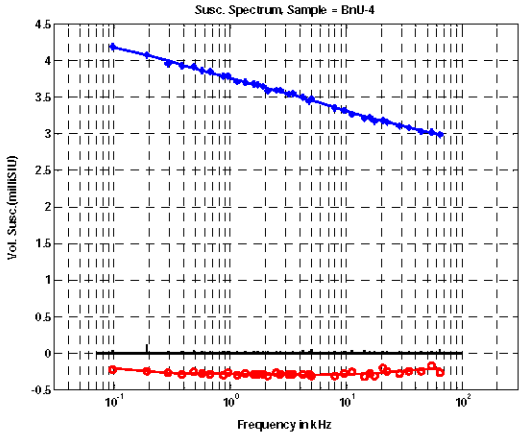

Figure 3. Wide-band susceptibility response of a "problem soil" from Bosnia, in milliSI units. In-phase as blue crosses; quadrature response (emulating an induction response) of about $-3{\cdot}10^{-4}$ SI as red circles.

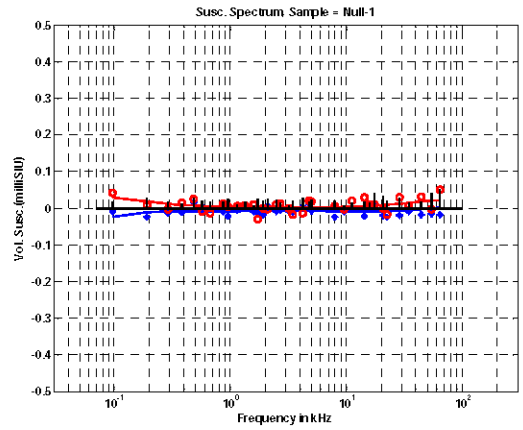

Figure 4. Wideband noise floor of the instrument a measurement, from an empty sample holder, close to 10^{-5} SI units. Colors and symbols as in Figure 3.

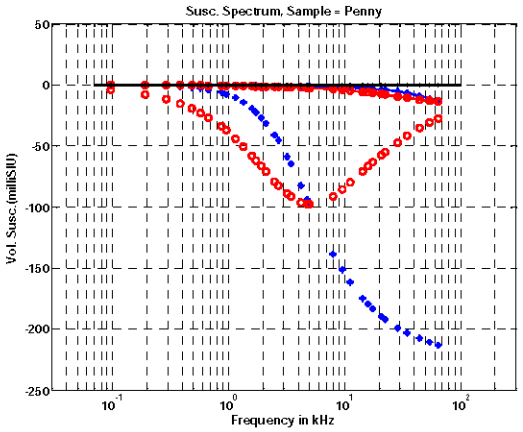

Figure 5. Induction response of a small metal object (Canadian penny) in two orthogonal directions, expressed as a equivalent susceptibility of a sample volume of 12.9 ml. Colors and symbols as in Figure 3.

SIMULATION CODE

The main challenge in preparing the simulation code is not the computation of electromagnetic responses of soils and targets. In general, targets are small, so point target responses are appropriate (that is, the inducing field can be assumed uniform over the region of the target, and the fields of the target at the receiver can be assumed to be those of a point dipole). With targets typically buried less than 10 cm, shielding by overlying soil is typically small and often negligible. Standard algorithms for calculating fields in a layered environment have been available in the literature for some time (*e.g.* Grant and West, 1965; Wait, 1982; Ward, S and Hohmann, 1987; Guptasarma and Singh, 1997). The primary goal in coding was to achieve usability by instrument designers on a wide range of instrument designs, with arbitrary coil arrangements, transmitter waveforms, and signal acquisition and processing, as well as the ability to use target and soil response data based on both theoretical models and experimental data such as produced by the spectrometer above.

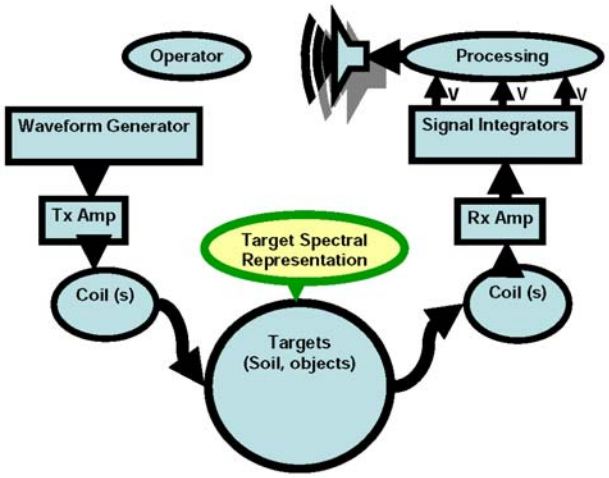

Figure 6. Components of the detection simulation model used by the code.

Accordingly, effort has been directed towards an effective GUI and flexible methods of describing instrument configuration and target characteristics (Bailey and West, 2006). Target responses are characterized in terms of a pole-zero description (West and Bailey, 2006) in the complex frequency plane, a separate response for each principal axis of the target if required.. The exponential decays associated with each pole can be pre-processed with the instrument signal processing algorithms. This permits a simple sum over these decay modes to be performed at each instrument location in a simulated survey, in which only the instrument-target coupling amplitudes need be recomputed at each location, not the full frequency or waveform dependence.

The final suite of models which the code is planned to handle are summarized in Table 1. The code is written in MATLAB. This facilitated several important features: users can enter theoretical responses as MATLAB formulae, which the code will understand; all of MATLAB's edittable plotting facilities are available, and the GUI permits exporting numerical results to the MATLAB workspace, where users can do any further analysis of them with their own code.

	HCC	HPC	TPD	TPC
FS	U,S	U	U,S	U
LHS	U,S		U,S	
FD3DS	U	U	U	

Table 1. Design goals of the code. Sensor abbreviations are HCC - horizontal circular coils; HPC - horizontal polygonal coils; TPD - tilted point dipoles; TPC - tilted polygonal coils. Target and host abbreviations are: UFDPT - unshielded frequency-dependent point target; SFDPT - shielded frequency-dependent point target; FS - free space; LHS - conductive layered half-space with conductivity and frequency-dependent susceptibility specified in each layer; FD3DS - 1, 2, or 3D weak susceptibility distribution with global frequency-dependence.

CONCLUSIONS

We have developed an instrument for wideband measurements of magnetic susceptibility over the frequency range 100 Hz to 70 kHz. We have developed code for utilizing this data in the calculation of the induction response of small metal targets embedded in soils with frequency dependent magnetic permeability. These two tools should be useful in producing better designs for field instruments for humanitarian demining, which can distinguish between the quadrature response of the desired metal targets and the quadrature response caused by the frequency-dependent magnetic susceptibility of problem soils.

ACKNOWLEDGEMENTS

This work was supported by the Canadian Centre for Mine Action Technologies (CCMAT) of Defense Research and Development Canada (DRDC) as part of contract No. W7702-03R942/001/EDM. We gratefully acknowledge the assistance and guidance provided by DRDC personnel in at Suffield, Alberta, and especially the help from Dr.Yoga Das, technical authority for the contract. We also acknowledge the assistance provided by Dr Rob Moucha.

REFERENCES

Bailey, R.C. and West, G.F., 2006, Characterizing mine detector performance over difficult soils, in Proc. SPIE 6217, Detection and Remediation Technologies for Mines and Minelike Targets XI, J.T. Broach, R.S. Harmon, and J. Holloway, eds., 62170P_1-621702_10.

Candy, B. H., "Pulse Induction Time Domain Metal Detector", United States Patent Number 5 576 624, November 1996.

Das, Y. 2005, Electromagnetic induction response of a target buried in conductive and magnetic soil, in Proc. SPIE 5794, Detection and Remediation Technologies for Mines and Minelike Targets X, R.S. Harmon, J.T. Broach, and J. Holloway, eds., 263--274,.

Dunlop, D.J. and O. Ozdemir, 1997, Rock Magnetism, Cambridge University Press.

Grant, F.S. and West, G.F., 1966, Interpretation theory in applied geophysics, McGraw-Hill, New York.

Guptasarma, D. and Singh, B., 1997, New digital linear filters for hankel j0 and j1 transforms, Geophysical Prospecting 45, 745--762.

Mullins, C.E. and M.S. Tite, 1973, Magnetic viscosity, quadrature susceptibility, and frequency dependence of susceptibility in single-domain assemblies of magnetite and maghemite, Journal of Geophysical Research 78,
804--809.

Wait, J.R., 1982 Geo-electromagnetism, Academic Press.

Ward, S.H. and Hohmann, G.,1987, Electromagnetic Methods in Applied Geophysics vol. 1, ch. Electromagnetic Theory for Geophysical Applications, Society of Exploration Geophysicists.

West, G.F. and Bailey., R.C., 2005, An instrument for measuring complex magnetic susceptibility of soils, in Proc. SPIE 5794, Detection and Remediation Technologies for Mines and Minelike Targets X, R.S. Harmon, J.T. Broach, and J. Holloway, eds., 124-135.

West, G.F. and Bailey, R.C., 2006, Spectral representation, a core aspect of modelling the response characteristics of time-domain emi mine detectors, in Proc. SPIE 6217, Detection and Remediation Technologies for Mines and Minelike Targets XI, J.T. Broach, R.S. Harmon, and J. Holloway, eds., pp. 621702_1-621702_12

APPENDIX 5

UTEMI Spectrometer

Quick Start Manual (V.2)

G.F. West
2007

Quick Start Instructions:- Utemi Spectrometer

These instructions are to help a new operator take a functioning UTEMIS instrument out of its packing case and put it into service quickly.

The Utemis 1.1 instrument consists of a Penguin 1630 ABS foam-lined packing case containing the following items:-

1. Spectrometer coil-set, with connecting cables to preamp and power amplifier (Coil Set).
2. Sample holder rotation actuator (Sample Rotator)
3. Power Supply and Power Amplifier (PS-PA) module.
4. Preamplifier module (PreAmp).
5. Shuttle AMD64 WinXP computer (Computer) containing one RME Hammerfall sound card.
6. A 17" liquid crystal TFT Video Dispay Terminal (VDT)
7. A short format ASCII Keyboard
8. USB Mouse
9. Interconnecting and power cables for the above.
10. Box holding samples, sample containers and ancillary components
11. 2 Folders containing instructions, software CD's, component documents
12. Power bar extension cord

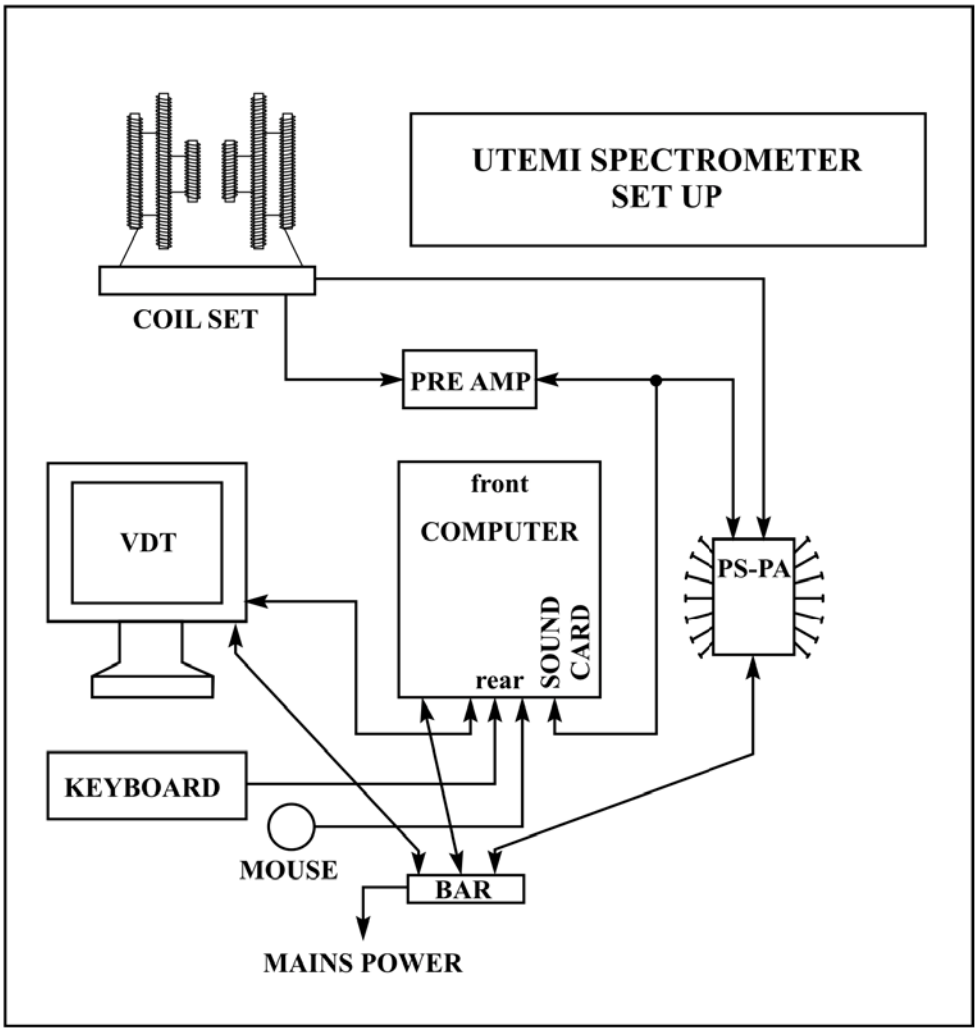

Fig. 1 Schematic diagram showing interconnection of the UTEMIS components.

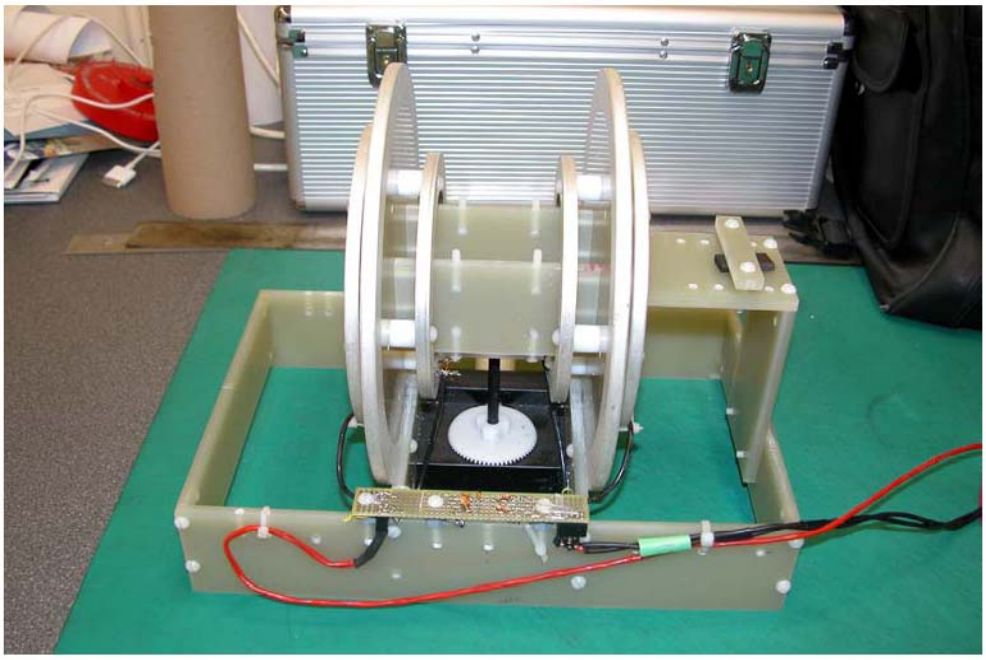

Fig. 2: UTEMI Spectrometer Coil Set; view from rear.

Windows XP OS software and a basic set of utility programs has been installed on the C hard disk. The specialized software necessary to operate the UTEMIS system has been installed on the D hard disk.

INSTRUCTIONS (Step by step)

1. Open the keyless padlocks on the shipping case using the codes provided to you. Open the case and store the locks and their codes in a safe place in the case.

2. Find a suitable pair of tables (packing cases or whatever); one for the computer and VDT, etc., and the other for the Coil Set, Preamp and Sample box. The PS-PA Module is better located on the computer table, but it may be placed on the Coil-Set table. . The Coil Set table MUST be non-metallic, without any screws or metallic fasteners within about a foot (30 cm) of the base of the coil set. The PS-PA module should be > 2 feet from the coil set; the preamp about one foot.

3. Using the power and interconnecting cables (9), set up the apparatus according to the schematic diagram of Figure 1. Note that as delivered, the instrument is set for 110-125 VAC, 50-60 Hz mains power. If the system must be run on 220-250 VAC, it will be necessary to change the power cords and some settings on the power entry modules of the PA -PS, the computer and the VDT. (See component manuals).

4. When all is ready, connect the mains power to the VDT and the PS-PA and turn them on. A green pilot light should light up on the left side of the PA-PS and a yellow one below the screen of the VDT. Next, momentarily press the power on-off button of the computer (centre left of front panel) and listen for the computer's fan to start up. The computer screen should then momentarily display start-up data of the computer's Bios and then begin booting Window XP. XP should open in single user mode without any password (administrator level). Confirm that the mouse is working by clicking on the icon "Shortcuts". A list of software should then be displayed.

5. OPTIONAL Connect the system to the internet by plugging an ethernet cable into the rear of the computer. This will enable you to use Firefox and Internet Explorer. HOWEVER; please note that high activity on the internet can compromise use of the computer as a real-time instrument,

because the activity of firewall, virus checking and system upgrading software may interfere with the real-time instrument software. Thus, it is safer to operate the UTEMIS instrument system with the internet disconnected. If you do connect to the internet, you will need to setup the type of internet connection in XP. (Control panel -> Network connection -> Local Area Connection Status -> Properties)

6. The UTEMIS computer software has been written using the MatLab high level programming language from Math Works. The instrument is shipped with a licensed copy of MatLab 7.2 (R14, service pack 2) installed on Drive C in Program Files. THIS INSTALLATION IS ONLY FOR SYSTEM VERIFICATION PURPOSES. The new user MUST install his own licensed copy ASAP. (It may be possible only to install a new licence product key).

Although the original prototype software was developed on MatLab 6.5 (R13), it has been finalized in R14. Backward compatibility is not to be expected without a considerable effort, because of changes to MatLab audio recording functionality and to GUI handling between R13 and 14. Contact GFW if there is a need to operate on MatLab R13.

7. Once the computer's XP desktop is available, check that the soundcard is set up and active. This can be done by starting hdsp32.exe and hdspmix.exe from the Shortcuts menu or from the small icons on the lower right of the screen. The correct parameter setup is shown in Fig. 2 (Buffer Size (Latency) set to 1024). The second item (the mixer panel) is more complicated than is needed for UTEMIS. Only the two left hand indicator columns are relevant. The upper pair of level indicators shows the utilized pair of audio inputs, and the lowermost pair shows the pair of outputs. The Inputs should display a barely visible level of noise. This comes steadily from the preamp at a level of -60 -70 dbu as long as the preamp is on but not in operation. No output or larger input should be visible until the spectrometer is being operated.

If, on the setup panel, the Input Level is changed from its normal +4db setting to hi gain, the levels of noise displayed by the mixer indicator bars should become more visible. Remember to set the Input gain back to +4db when you finish. You may close or hide either or both of the hdsp screens, or leave them open.

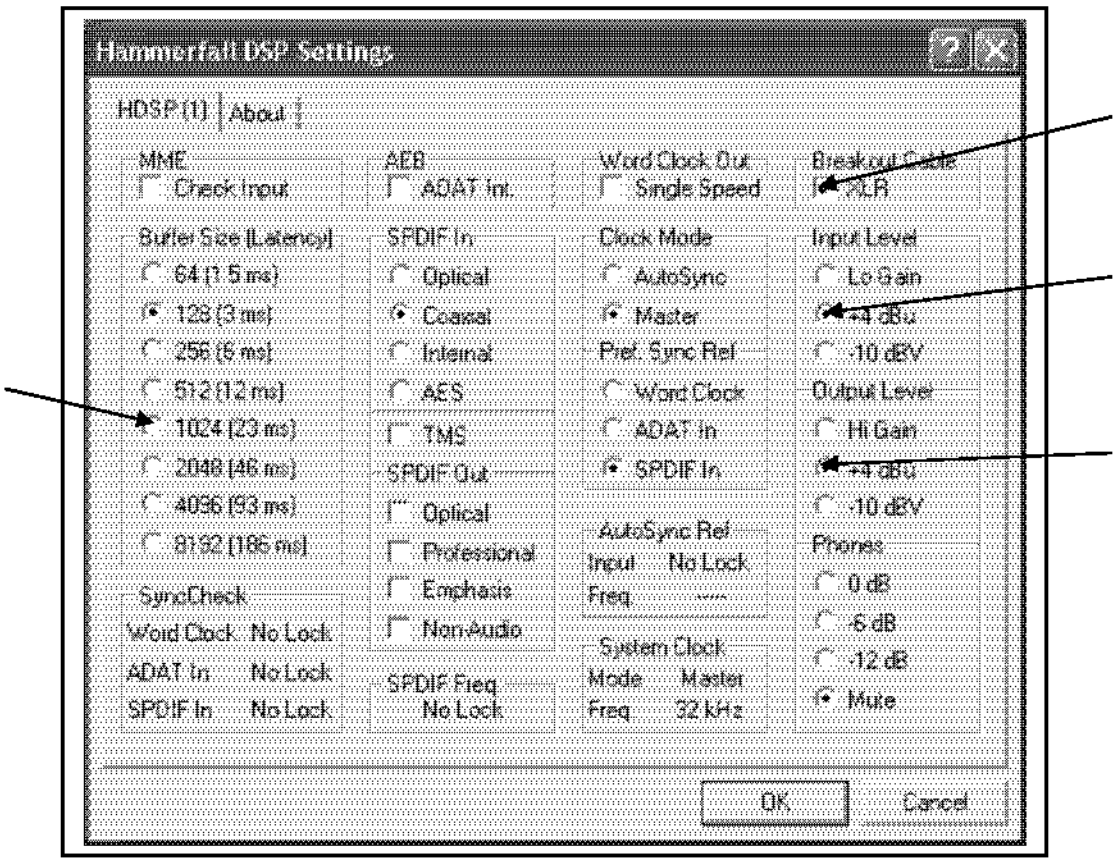

Fig.3. Essential settings on the sound card setup screen

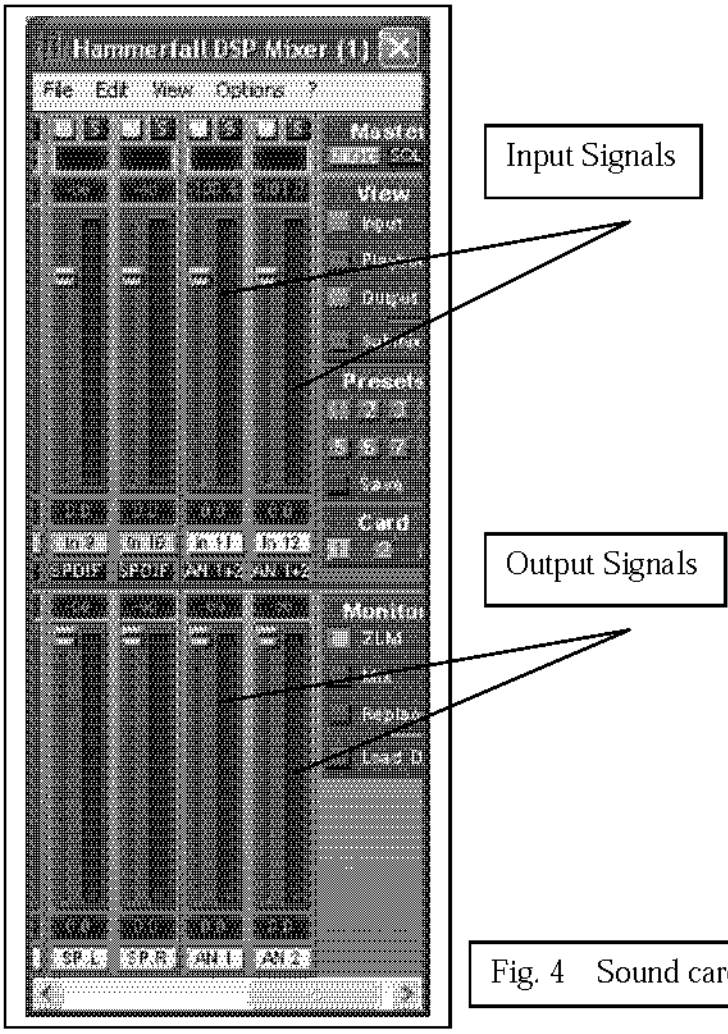

Fig. 4 Sound card signal level indicators.

8. Familiarize yourself with the structure of the File Systems on disk drives C: and D:. As delivered, UTEMIS 1.1 computer systems have a pair of identical 70 GB SATA hard drives. Originally, these were setup as a Raid 1 (mirror) system using the Uli SATA RAID drivers supplied with the Shuttle computer system. The operating system and utilities then were installed. However, after MatLab and the UTEMIS system software had been installed, some erratic behaviour of the audio data transfer commands was experienced, and there was a possibility that the RAID system was a source of interference. To avoid this, the file system was reverted to two independent drives, C and D. Drive C is now used for the operating system, peripheral drivers and MatLab system software. Drive D is used for MatLab user files in the UTEMIS directory. (It also contains an image of the operating system and other software, but note that it is not being updated. However, if drive C should fail, D can be used for an emergency reboot by going to the bios and setting D drive into the boot sequence).

9. Examine the D:\UTEMIS\ file tree. The MatLab programs used by the Spectrometer are in UtemisCode and its folders. There are two main programs:- UtemisMeasure and UtemisTest. The former is used to run the spectrometer in normal use; the latter is used to check out and maintain the instrument if there is a need. UtemisTest can also be useful for familiarization and training purposes. Folders have been set up for automatic storing of Utemis data files.

CAVEATS:- 1) UTEMIS 1.1 is a prototype instrument still undergoing development. The original prototype (1.0) was built as a single copy. Model 1.1 currently exists in only two copies. The

electronics and coil set can be considered a stable version for desktop operation in a lab or field camp environment. The instrument software will likely undergo a few upgrades as experience is gained. It is hoped that a final version (for the 1.1 hardware) will be completed before Sept 2007.

2) We have taken advantage of MatLab's powerful development environment to design and upgrade the software easily. MatLab has some excellent tools for connecting to external devices and for passing data back and forth quickly and flexibly in the computer memory allocated to Matlab. However, it is not necessarily very robust in real time control applications. The problem is not in the speed of the sdftware or the computational engine. Modern computers are many times fast enough. However, they divide tasks into small chunks and do many kinds of automatic caching, prioritizing and time ordering of the chunks in order to use their amazing speed effectively. This internal decision-making can prevent a high level application program from ensuring execution of its requested tasks on any precisely specified timing schedule. Compiled software that has been closely integrated with computer's device drivers can do a lot better in this regard. This level of software control is expected to be available in UTEMIS 2. In the meantime, we believe that very satisfactory performance will be obtained with UTEMIS1.X as long as recommended device and computing environment settings are employed. Please note that MatLab and Windows upgrades may possibly cause performance changes. Also note that MATLAB R14 operating in the Shuttle AMD Athlon 64 requires that the soundcard NOT be operated at the lower latency (small buffer size) settings. (A buffer size of 1024 has given excellent results in development work).

10. Operation of UTEMIS requires that MatLab be started first. A convenient way to do this is by clicking MatLab in the Shortcuts Window. You should note that there are two MatLab shortcuts, the usual Matlab 7.02 icon and another labeled UtemisMatLab. Both open MatLab 7.02. The first gives MatLab programs normal execution priority, the second gives them the highest possible priority (real-time). If you are experiencing any problems with erratic behaviour, use UtemisMatlab.

If you are new to MatLab, you should spend some time familiarizing yourself with MatLab's mult-paned control window (especially with the Command Window part of it) and learn how to open, edit and run MatLab " .m" files, in either function or script form. You should also learn how to set a "path' for MatLab to find and store the files it needs in appropriate directories. A correct path has been set up in the instruments as initially delivered. However, if the user alters or elaborates the UTEMIS directory system, the MatLab path will need to be reconfigured (look for path under file in the main MatLab window).

11. To start the UTEMI Spectrometer, ensure first that the equipment is properly connected and that the PS-PA is turned on. Then, in the MatLab "Command Window", enter either "UtemisTest" or "UtemisMeasure" and "return" (no quotes). A GUI should display itself. Use of the UtemisTest GUI is fairly straight forward. The UtemisMeasure GUI is more complicated. Instructions for both are given in the following pages.

UtemisTest

The GUI is started by typing " UtemisTest" (no quotes) and "enter" in the Matlab Command Window. This should raise a graphical display like Figure 1 on the VDT screen. Three test programs are available, started by clicking the relevant button on the GUI.

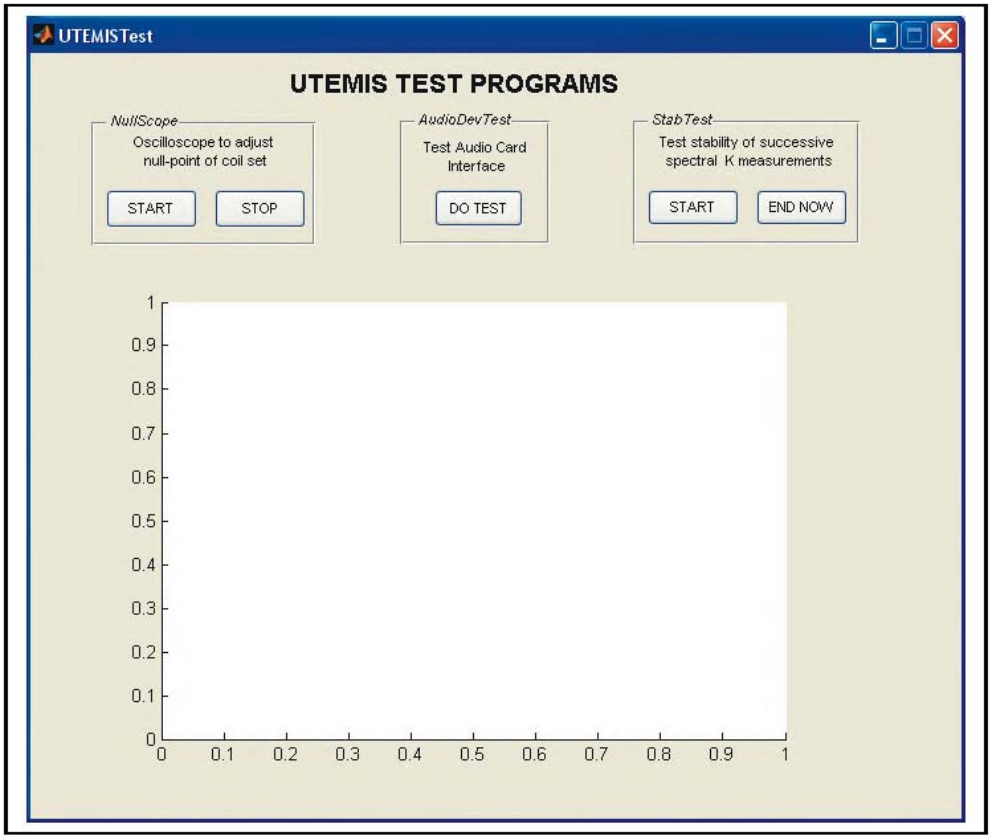

Figure 5. GUI for the UtemisTest program.

Audio Device Test. (Centre)
This tests the connection between the Utemis MatLab software and the RME Hammerfall 9632 sound card. It also checks that the coil set, preamplifier and PS-PA unit are properly attached and operating.

The results of the software connection test are printed in the MatLab Command window. Sets of print lines will appear that document the audio input and output device settings that Matlab and Windows XP have agreed upon. (See Figure 6.) If the soundcard is in the PCI slot you should see it listed for devices 1 to 5. If the starred lines do not appear as shown, you should open the Windows control panel "Sounds and Audio Devices" and go to the Audio panel. There you should check that the sound playback and sound recording selectors are set to channel 5, the analog inputs and outputs of the Hammerfall card.

Figure 6. Printout from the AudioTest program..

```
Output Devices
Device 0 = HDSP ADAT Out (1+2)(1)
Device 1 = HDSP ADAT Out (3+4)(1)
Device 2 = HDSP ADAT Out (5+6)(1)
Device 3 = HDSP ADAT Out (7+8)(1)
Device 4 = HDSP SPDIF Out (1)
Device 5 = HDSP Analog Out (1+2)(1)
Device 6 = Realtek HD Audio rear output
Input Devices
Device 0 = HDSP ADAT In (1+2)(1)
Device 1 = HDSP ADAT In (3+4)(1)
Device 2 = HDSP ADAT In (5+6)(1)
Device 3 = HDSP ADAT In (7+8)(1)
Device 4 = HDSP SPDIF In (1)
Device 5 = HDSP Analog In (1+2)(1)
Device 6 = Realtek HD Digital input
Device 7 = Realtek HD Audio rear input
Output Device accepts 192kHz,24 bit stereo sound data on device address 5    ********
Input Device will record 192kHz,24 bit stereo sound via device address 5   **********
playing 1 second of Handel
Play time for handel in seconds is next
Elapsed time is 1.508868 seconds.
recording stopped
```

In the second part of the test, a short excerpt of a sound file stored in Matlab is played to the soundcard, and an oscillogram is plotted on the screen of the data received back on the sound card's stereo inputs (sample signal and reference channels from preamp). If nothing appears in the plot area, it is likely that the PS-PA is turned off, or the coil set is not correctly coupled to its electronics and to the sound card.

NullScope (Left hand side)
This program is used to check that the coil set and its ferrite adjustor are correctly set up. The sample holder of the coil set must be empty for this test. Bursts of a special 2 kHz waveform are sent repeatedly to the C2 primary field coils, and the signals received from the sample signal and reference preamplifiers are displayed on the screen.

The reference signal should be a slightly rounded square wave with a peak amplitude of about 75 mV. A small amount of high frequency noise is likely to be visible on it. The sample signal should be substantially weaker. Note, however, that this signal is the difference of two much larger signals and is subject to 3300 x more amplification than reference signal. It will probably show some transients near the transition instants of the reference square wave due to slight differences in the high frequency properties of the C1 and C3 coil pairs. Also, more high frequency noise may be visible.

When the instrument is correctly balanced, the sample signal from the coils should be about 1/3 - 1/4 of the reference signal and in-phase with it. Then, if a strongly susceptible sample (i.e, the 3%

magnetite calibration sample) is inserted in the sample holder, the sample signal will change to a 180 degree out-of phase signal of similar magnitude.
(The sign convention of the coil set makes the signal from a susceptible sample opposite in polarity to the reference signal; but this is accounted for in the spectrometer's data processing.)

Once started, NullScope continues indefinitely. You must stop it with the "stop" button.
Shortly afterwards, the program will display the Fourier amplitude spectrum of the signals from the last burst. This display is used to check that the sample and reference signals recorded by the sound card have not been seriously contaminated by internally generated, periodic, switching signals related to the digitizing process.

Stability Test (Right hand side)
This program is used to check the stability of the Utemi spectrometer. In normal operation, Utemi induction measurements are made nearly simultaneously over a wide range of frequencies. Each full sample measurement is the difference between a measurement with the sample not present (called a "background measurement") and one made several seconds later with the sample present in the coil set (called a "sample measurement"). In dealing with anisotropic samples, twelve sample measurements are made as the sample is successively rotated by 15 or 30 degree increments, and from these is subtracted the average of background measurements made just before and just after the set of sample measurements. For this to give a true and accurate measure of induction in the sample, it is essential that a background measurement by the spectrometer be adequately repeatable and stable over times from a few seconds to a few minutes.

The StabTest program makes a series of background measurements at intervals of ~ 6 seconds, and repeatedly plots the whole set on the screen, as measurement proceeds. Each individual background measurement consists of a set of real and imaginary amplitudes at a fixed set of frequencies. To make small differences visible in the plots, the Re and Im means (for each frequency) over the whole set are subtracted from each individual pair. The level of scatter and systematic drift revealed by this test gives a good indication of the error level likely to be present when determining the induction in any sample. The program stops by itself after 10 measurements, but may be requested to stop earlier.

A few seconds after the final suite of null measurements has been plotted, the display will plot the real and imaginary components of the last individual background measurement. Note the change in y amplitude scales. Comparison of this measurement with the difference ranges for a set of measurements indicates the fractional repeatability level that is achieved in an individual measurement.

While operating, StabTest prints information about the strengths of the so-called "segment" signals that Utemis sends and receives during a measurement. An example is given below.
The list gives the maximum amplitude of the periodic signal received in the reference and sample signal channels of the sound card. 1 Volt is the absolute maximum signal that can be recorded, and neither signal should exceed about 0.5 V in any segment. (See main manual for description of segment signals.)

NSInSigOut = 763304 NSInSigIn = 802816
NSigStart = 3019
Max Amplitude In Segment (Pri,Sec)
  0.1996 0.1792
  0.3661 0.0287
  0.4563 0.0246
  0.4035 0.0299
  0.2003 0.0160
  0.0570 0.0065

Example Print Out from StabTest

UtemisMeasure

The GUI is started by typing " UtemisMeasure" (no quotes) and "enter" in the Matlab Command Window. This should raise a graphical display like Figure X on the VDT screen. The spectrometer is operated by clicking relevant buttons on the GUI and entering data about the samples to be measured. Figure X shows the GUI with all its sections visible. In operation, those parts of the GUI that are not in current operation will appear grayed out.

Preparation for measurement

The spectrometer coil set should be set upon a metal free table. Small metal objects smaller than the coil system should be kept at least 5- 10 times their maximum dimension away from the coils. Large objects such as metal chairs, boxes or desks should not be closer than about 3-5 feet (~1.5-2 m). The PS-PA unit should be at least 2 feet (~0.65 m) away.

The spectrometer should already have been connected up, as shown in Figure 1. Ensure that the sample holder is clean and, if samples in standard vials are to be measured, that the top guide of the sample region is in place; also that the sample carrier (a clear plastic object resembling a miniature tennis racquet) and the samples to be measured are in a handy location. The names or ID numbers and ancillary information such as sample volume should be available for entry into the computer.

The equipment should be set up so the operator is able to work with the computer and to move samples back and forth from the coil set without significant physical disruption. If anisotropic objects are to be measured, the detachable part of the sample rotator must be attached to the front of the coils set (friction fit plus two plastic retaining screws). Also, make sure that objects to be measured have been oriented in their containing vials so they may be rotated about the vial's axis and that reference axes for the samples have been clearly marked.

Re current version of UtemisMeasurement (April 2007)
This version is just a reworking in MatLab R14 of the R13 software used with Utemis 1.0 (soilk2b). Several features remain to be added, probably before September 2007. Planned enhancements are

1) Additional categories in measurement type, with new letters identifiers for objects.
2) An entry point for sample volume.
3) Implementation of attenuation for measuring very strong samples and an nsns…n measurement sequence for very weak ones
4) Remembering entries for previous sample.
5) Optional auto saving of graphic displays in UtemisDataFigs and UtemisDataEmf folders.

Re File Names for measurements.
The spectrometer logs measurement data in a standard format, a MatLab "struct" or "structure" called MDat (short for Utemis Measurement Data). Structures are easily saved and recalled by Matlab as … .mat files, each identified by file name. To prevent accidental overwriting of any MDat data, all are uniquely during acquisition by including the date/time of the measurment in the filename. An MDat Filename consists of a capital letter identifying the type of sample, an ID supplied by the operator, followed by the numerical datetime.

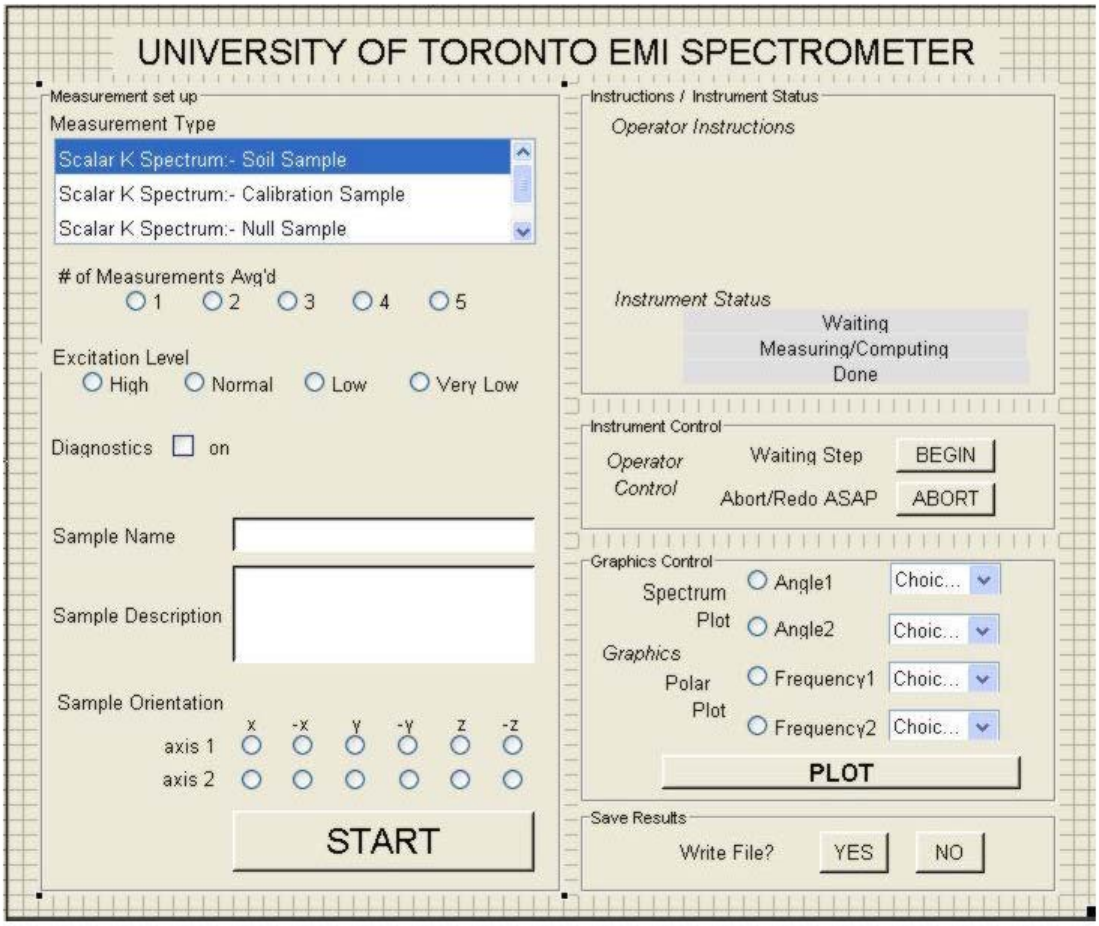

Figure 4. The UtemisMeasure GUI, shown with all panels active.

Using the GUI

When the GUI first starts, the left hand (measurement setup) panel will be activated and the right hand panels will be grayed out. Begin at the top and work towards the bottom. When all necessary data have been entered, press "START" to begin the measurement process.

Measurement Setup

1. *Measurement type* Select the appropriate sample or measurement type from the list.:-
   S:- a soil sample (or other homogeneous material) for susceptibility measurement.
   N:- No sample:- a measurement for checking null errors.
   C:- A homogeneous calibration sample.
   A:- An anisotropic sample needing tensor measurement.
   In the above list, all measurements are treated as susceptibility determinations on a standard volume of sample (12.5 ml).

2. *Number of repeated individual measurements averaged.* Select 1-5.
   As currently set up, the instrument takes about 3-5 seconds to take an individual measurement (background or sample). However, this provides no data on error and noise level. You can request multiple measurements, in which case standard deviations will be calculated. Usually, 2 or 3 measurements are sufficient.

3. *Excitation level.*
   This feature is incomplete. Its intention was to increase the dynamic range of the

instrument by optimizing the measurement parameters for samples of very different inductivity (very weak to very strong). Currently, only the Normal and High buttons have meaning. Low and Very Low are the same as Normal. The original idea was to vary the level of the primary field signal according to the order of magnitude susceptibility of the sample. However, this has been difficult to implement because the characteristics of the new coils and power amplifier were not accurately known until recently. Furthermore, experience with the 1.1 instrument shows that it is only necessary to change signal strength if samples with extremely strong inductivity (like a milliliter or more of pure ferrite or conductive metal) are to be measured. At the moment, the selection does not change excitation level. However, when high sensitivity is requested, the measurement cycle is changed from the normal 'background – then sample" to 'background – sample – background to reduce error due to drift.

Diagnostics.
This is only needed if the measurement process stops for some reason, perhaps due to too strong signals from the sample. It provides a print out of the peak signal strengths (sample and reference) for each of the six segments of the excitation signal. These data enable adjustment of the signal parameters to correct the problem. At the moment, the easiest way to handle samples of extreme inductivity is to go to the hdsp32exe window and temporarily reduce the sound card output level by setting it to -10db (and possibly also to reduce the input signal by setting the input level to lo gain).

Sample Name. This will become part of the filename for the measurement results.
It is a simple identifier (ID) for the sample.

Sample Information. This will archived in the MDat structure of measurement results.
If the sample volume is not standard, the correct volume should be entered here.

Sample orientation. This is only used when anisotropy is to be determined.
Two buttons corresponding to two different sample axes must be checked; one in each row, to record the initial orientation of the sample in the sample holder. Axis 1 and axis 2 are marked on the top plate of the coil set's sample holder (respectively parallel and normal to the axis of the coil set). The X, Y, Z axes are those marked on the sample itself. Note that a separate anisotropy measurement must be made and recorded for each axis about which the sample is rotated. The minimum data neeeded to define an arbitrary 3D space tensor is rotation about two orthogonal axes.

START Press START when all the above information has been entered.
If essential data have been missed, the program will prompt for additional input.

Measurement
Once START has been successfully activated, the *Set Up* panel will gray out and the *Instructions/Instrument status* and the *Instrument Control* panels will activate. The two are used together, the upper one to give information and instructions to the operator, the lower one for the operator to control the measurement process by clicking. The upper lines of the upper panel are instructions, the lower lines show whether the instrument is busy or waiting for operator input. The instructions depend on the information provided in Measurement Setup. The procedure should be self explanatory. If the operator makes a mistake, so the results will be incorrect, the measurement sequence can be aborted. This really is only useful when making anisotropy measurements (where the measurement sequence may contain more than nine individual measurement.

Plots
When the final step of the measurement sequence has been completed by the spectrometer, the *Instructions/Status* and *Control* panels will gray out and the *Graphics Control* panel will activate. If the measurement was scalar, there are no choices to be made and pressing PLOT brings up a

graph of the observed real and imaginary spectral response of the sample. However, if a single axis tensor measurement has been made, one can choose either a spectral plot for 1 or 2 angles or a polar plot of response at 1 or 2 frequencies. The Plot command can be issued more than once, changing the selected frequency or angle as desired.

Save Results
This final step completes the current measurement cycle and readies the GUI for a new cycle. The operator must chose whether to save the measured data or flush it from the instrument. (respond YES or NO to Write File?). Currently, only the Mdat file may be saved in this way. The plotted results may be saved manually using the Matlab built in save and export routines accessible from the figure's 'file' pull-down menu. There, you can store any plot as an editable MatLab .fig file or export it as an .emf or other kind of graphic.

New measurement
After a decision has been made to save or flush the current results, or after an 'abort' command, UtemisMeasure will return to its initial state with the *Measurement Set Up* panel activated, ready to begin a new measurement.

Program failure
It is possible for UtemisMeasure to crash. At this stage of the instrument development, we have not been able to design the programs so they can clear all error conditions and automatically restart. Possible reasons are mostly associated with the sound card, for instance:-

Starting a measurement cycle with the PS-PA turned off;
Introducing a sample with extremely large inductivity without reducing the output signal level;
Upsetting Matlab by running and crashing a program simultaneously with UtemisMeasure;
Having more than 1 instance of MatLab and UtemisMeasure going.

If a serious error arises in the program, it will probably be necessary to close and reopen both MatLab and UtemisMeasure. If a persistent java error arises, it may be necessary to reboot Windows to clear it. If inexplicable crashes occur, check the hdsp setup panel. It may be that the Buffer Size (Latency) has somehow been reduced from the recommended 1024 to a small value.

MDat Fields in an example MDat structure.

```
MDat =
          sample: 'test'
       sampleDes: ' '
          volume: 12.5
            axis: [0 0]
            type: 'S'
          option: 1
        DateTime: '2007-04-11 17:15:30'
           nmeas: 3
            sens: 2
           nfreq: 35
           freqs: [35x1 double]
         nangles: 1
          angles: {7x1 cell}
               K: [1x1 struct]
MDat.K =
              Re: [35x1 double]
              Im: [35x1 double]
            Ampl: [35x1 double]
           Phase: [35x1 double]
   StdDevAbsErr: [35x1 double]
```

APPENDIX 6

University of Toronto Electromagnetic Induction Spectrometer (Utemis), Model 1.1

G.F. West

October 5, 2007

1 What does the UTEMI Spectrometer measure?

Utemis (University of Toronto EM induction spectrometer) is a transportable tabletop instrument for measuring the time-varying magnetic moment induced in small, laboratory-scale samples by a time-varying, spatially uniform, magnetic field. The linear dimensions of the specimens should not much exceed 3 cm and vials of $\sim$1 inch diameter filled to $\sim$1 inch (vol 12.5 ml) are typically used to handle soil samples. The spectral range of measurements is 80 Hz to 70 kHz.

Broadly speaking, there are two principal mechanisms by which EM induction may occur in materials; magnetic induction (involving partial alignment of atomic magnetic moments and often referred to as magnetic permeability), and foucault induction (involving circulating electrical conduction currents created by a time-varying magnetic field). Magnetic induction increases the strength of the magnetic field in the inducing body, whereas foucault induction tends to reduce it

In the sub MHz range, magnetic induction usually is such a fast process that the induced magnetic moment is completely synchronous with its causative magnetic field. Thus, it is a frequency independent phenomenon. In contrast, foucault induction is fundamentally a dynamic process involving electric current flow in a finite sized circuit. It is characterized by a time constant; thus, it varies in phase and amplitude with frequency.

The Utemis instrument is designed to observe either kinds of induction or the two in combination, and especially those cases which are intermediate between the two paradigms. It is sensitive enough to observe diamagnetic induction in water, but it can also determine the induction response of a few millilitres of ferromagnetic or metallic conductive material. When using standard 12.5 ml samples, the measurement range of volume magnetic susceptibility is from about 2e-5 to 2 in System Internationale units (SIU).

The excitation employed in Utemis is a time-varying magnetic field, of similar magnitude to the Earth's weak static field (50 microTeslas (B) or 4 Amperes/m (H)). At this low level, the induction response of most ordinary materials usually is linear with field strength. Linear superposition can then be assumed valid. A sinusoidally alternating magnetic field therefore generates a sinusoidally varying induced magnetization, and Fourier methods can relate time- and frequency- domain response data.

Because of the linear relationship induction can be expressed as the ratio of induced magnetic moment m (Am^2) per unit of exciting magnetic field H (magnetic field intensity, Am^{-1}). We call the ratio m/H the magnetance ($\mathcal{M}$) of the sample, although there is no official name for this quantity. It has the dimension volume, and its SI unit is m^3. Practical units for samples of small volume samples are millilitres or microlitres (mL or μL).

For soils and other granular or fluid materials, magnetance per unit volume of sample is a more appropriate measure. This has a well established unit name – volume magnetic susceptibility – and is dimensionless (a pure ratio).

Unfortunately, in earlier unrationalized systems of units, magnetization and magnetic susceptibility differ from their current SI definition by 4π. Thus, the cgs and SI volume susceptibilities (respectively k and κ) are related by $\kappa = 4\pi k$. In physics experiments, it is usually the specific magnetic susceptibility (magnetance per unit of sample mass (χ) that is recorded, and in chemistry the molar susceptibility (χ_m)). All measurements with the Utemis instrument are in SIU of volume susceptibility or magnetance.

When considering the magnitude of a magnetance measurement, it may be useful to know that a perfectly conductive sphere exhibits a negative foucault magnetance of 3/2 its volume at all finite frequencies (this level of magnetance annuls B inside the sphere), whilst a sphere of infinitely permeable material exhibits a positive magnetance of 3 times its volume (limited by self-demagnetization.) Thus, the magnetance of a sample can be thought of as describing the "effective" or "equivalent" volume of ideally permeable or conductive material in the sample. Note, however, that the magnetance of any conductive or strongly ferromagnetic object or grain will be shape- and direction- dependent unless the object is geometrically isotropic.

The Utemis 1.1 instrument reports its measurements of magnetance or susceptibility as a complex frequency domain transfer function ($\mathcal{M}(f)$ or $\kappa(f)$), with the measurements given directly as real and imaginary components at a standard list of frequencies. The susceptibility option requires entry of sample volume by the instrument operator.

The sample space in the UTEMIS 1.1 instrument can accommodate specimens of up to about about 50 mm in size ($\sim$ 2 inch or 100ml). However, the instrument has been designed for routine use of smaller samples in order that the measurements are completely insensitive to sample heterogeneity. Powdered or granular solid materials or liquids are usually inserted into the instrument in cylindrical, polystyrene vials, inside diameter 25.0 mm ($\sim$ 1

inch) filled to a height of 25 mm (1 inch) (sample volume $\sim$ 12.5 ml).

In many kinds of sample, the induced magnetic moment is likely to be very weak. The magnetic field generated by the induced moment will therefore be a very small fraction of the exciting field. To detect such a small perturbation, the instrument must work in a differencing mode, i.e., comparing measurement made when a sample is present with measurements when no sample is present.

Magnetic moment **m** and magnetic field intensity **H** are spatial vectors. Thus, if the sample is aelotropic (anisotropic), its magnetance (at any specific frequency) will be a second rank tensor rather than a scalar. To accommodate this possibility, the instrument includes a device for rotating the sample between successive measurements about a (vertical) axis perpendicularly to the exciting magnetic field. If sets of measurements are made as the sample is rotated 180 degrees about 2 or 3 different axes, the sample's full tensor magnetance can be determined.

2 Instrument configuration

The sensing apparatus consists of three pairs of coils symmetrically disposed about the sample. The configuration is shown schematically in Figure 1. One pair (C2-1 and C2-2) produces the primary exciting magnetic field. The other two measure the fields created by the C2 pair and the sample (primary and secondary). The inner pair (C1-1 and C1-2) is sensitive to both the sample and the primary magnetic field, the outer pair (C3-1 and C3-2) is sensitive mainly to the primary magnetic field. The difference signal from the C1 and C3 pairs is then strongly sensitive to the sample's induced moment, and only mildly sensitive to the primary magnetic field.

The C2 coils are driven by an audio power amplifier (low output impedance) via a series current limiting resistor. The signal from the C1 -C3 set of four coils and an attenuated version of the signal from the C3 set of two coils (respectively, the Sample and Reference signals) are sent via identical wide band differential amplifiers to a stereo input 24 bit 192 kHz sound card in a computer running MatLab in MS Windows The power amplifier is driven from one of the stereo outputs from the sound card. Data acquisition and processing is via a set of MatLab programs.

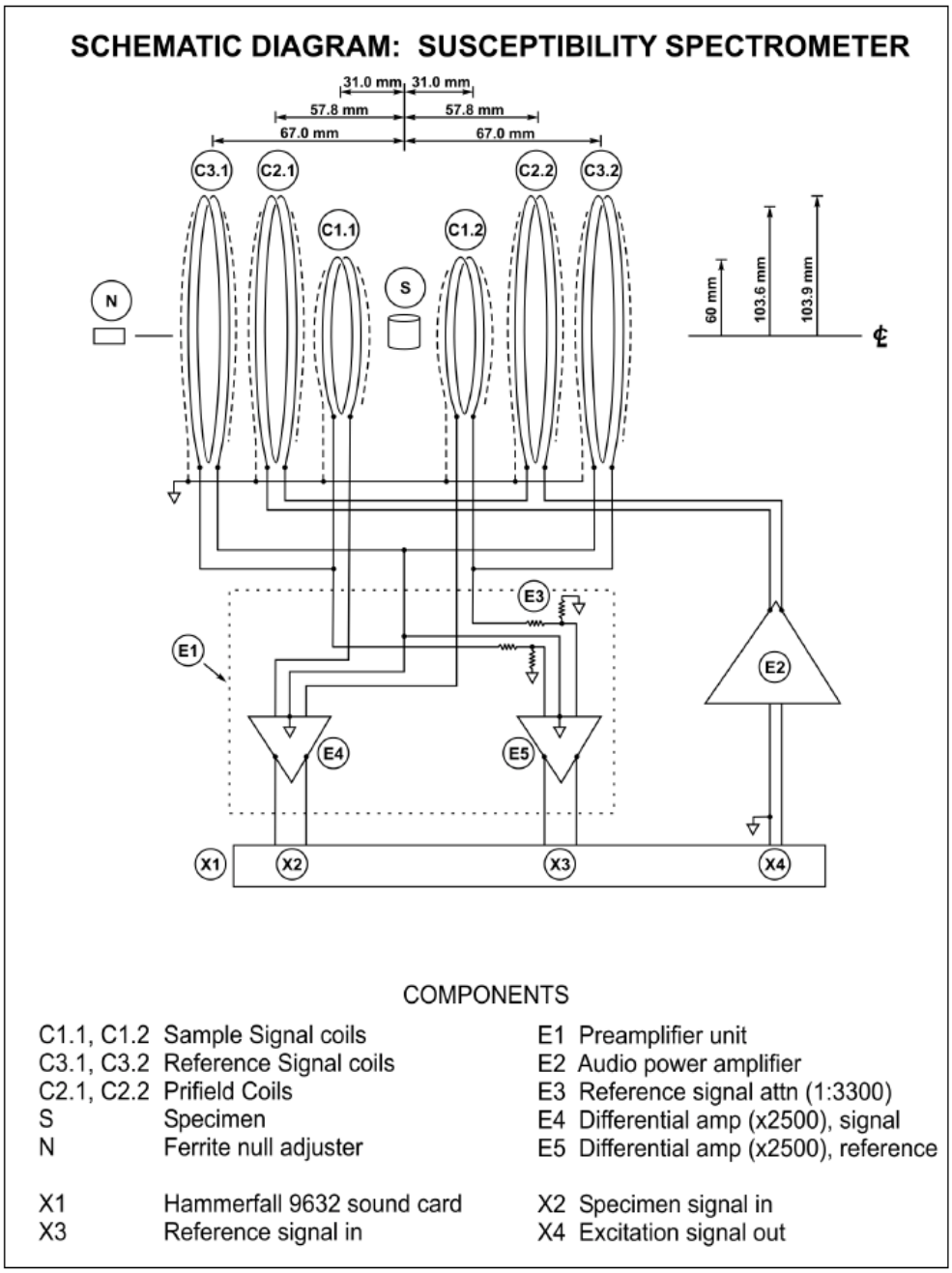

Figure 1: Susceptibility spectrometer schematic.

3 Principles of Operation

The measurement of magnetance is made by comparing the difference signal between the C1 and C3 pairs (called the sample signal) with the signals induced in the C3 coil pair (called the reference signal). More specifically, it is the ratio of the complex amplitudes of the sample and reference signals at each of several measurement frequencies which is measured.

Because of imperfections in nulling, the sample signal is certain to contain some primary (reference signal) in addition to the signal due to induced moment . Thus, two measurements are always made, one with the sample present and a second with it absent. The magnetance of a specimen (at each frequency) is computed from the difference between the "sample present" and "sample not present" ratios. This is summarized in the following:

- $M_m(f)$, $M_k(f)$ are *measurements* of sample magnetance or susceptibility at frequency f,
- $S_s(f)$ is the complex amplitude of the *sample signal* from the differenced coil pairs C1-C3
- $S_r(f)$ is the complex amplitude of the *reference signal* from the single coil pair C3.
- C_m , C_k are *calibration constants* for object or susceptibility measurement respectively.
- $R_1(f) = S_s(f)/S_r(f)$, sample present; $R_0(f) = S_s(f)/S_r(f)$, sample absent;
- $M_m(f) = C_m(R_1(f) - R_0(f))$; Magnetance measurement
- $M_k(f) = C_k(R_1(f) - R_0(f))$; Susceptibility measurement, where $V_k =$ *sample volume* and $C_k = C_m/V_k$;

Dimensions of the calibration constants C_m, C_k and thence of the magnetance or volume susceptibility are:

- *volume* for magnetance of discrete sample objects
- *dimensionless* for susceptibility of samples of known volume.

The calibration constant C_m is calculated theoretically directly from the known geometry and numbers of turns of the C1 and C3 coils using the Biot Savart law.

The signal and reference voltages from the coils ($S_s(f)$ and $S_r(f)$) are passed to the instrument's computer via a pair of identical preamplifiers and a high quality sound card digitizer working at a 192 kHz sampling rate. There, the complex amplitudes of the signals are measured using MatLab digital computation techniques. The reference signal is always very much stronger than the sample signal. Thus, in order that signals of similar magnitude are passed through the preamplifiers and to sound card, the reference signal is attenuated by a known frequency-independent factor $A = 1/3300$ before it goes to the preamplifier input This means that if $R(f)$ is the ratio of sample and reference signal amplitudes as computed by MatLab, the required sample measurements are given by

$$M_m(f) = AC_m(R_1(f) - R_0(f)); \tag{1}$$

and

$$M_k(f) = AC_k(R_1(f) - R_0(f)); \tag{2}$$

The primary magnetic field is created by passing a current through coil pair C2. It will be uniform throughout the sample region (to within a very few percent) because the C2 coils are in a Helmholtz configuration. Up to about an ampere of current can be supplied to the C2 coils by an audio amplifier module which receives its input signal from one of the the sound card's twin digital-to-analogue outputs. The digital signals are created by Matlab programs and sent to the sound card through a necessary antialiasing filter.

The sampling rate of the sound card is 192 kHz, giving a Nyquist (maximum usable) frequency of 96 kHz. Necessary practical anti-aliasing filters in the sound card limit the practical maximum usable frequency to about 70 kHz.

There are many ways of covering the spectral range of interest (0.1 - 70 kHz). For instance, the primary signal could be a sequence of sinusoidal signals at a chosen suit of frequencies. Or it could be a long broad band signal like a pseudorandom binary sequence (pseudo random noise) or a swept frequency. However, in order to maximize the dynamic range capabilities of the instrumentation, we have found it best to work with signals contain only a few harmonically related signals (odd harmonics) that may spread

over a 1 -1.5 decades of frequency. Currently, the sound card is made to generate a continuous signal which is about 2-3 seconds long and which is a sequence of six different periodic segments together with a starting signal. The duration, base frequency, harmonic content, harmonic amplitude in each segment may be adjusted by editing variables in the script program named UtemisSigMaker.m. More details on the MatLab data acquisition programs are given below.

Immediately after the transmission and recording of a multi-segment primary signal, the recorded segments are separated from one another and stacked at each segment's base frequency. The stacked sample and reference signals are then Fourier analyzed to obtain the complex amplitude of each of the signal harmonics, and to reject all noise that is not at one of the transmitted frequencies. The ratios described above are then formed to give the required measurement. Since the sample and reference signals are recorded simultaneously, it is not essential that the primary signal be highly stable from one measurement to the next.

4 Software

The MatLab software for the Utemi Spectrometer is listed in Table 1. Use of the programs is described in UtemisQuickStart.doc. The programs are reasonably well documented line by line in the MatLab code. The general measurement concepts that are implemented by the programs have been described above. If further details are necessary, it would be best to expand the internal documentation of the code. The only program that is somewhat difficult to follow is the UtemisMeasure GUI. Anyone planning to alter it must first read and understand the MatLab documentation on their GUI making function GUIDE. The original version of UtemisMeasure.m and UtemisMeasure.fig was made with MatLab 6.0 (R12). It has been successively updated to versions R13 and R14 to take advantages of some updates to GUIDE. It is not easily reverted to the earlier releases.

UtemisMeasure.m is a moderately large and somewhat complex program. Because it implements a GUI (graphical user interface), it is directly linked with a MatLab graphic "UtemisMeasure.fig" that opens as soon as the function is called. Once activated by user actions on the GUI, UtemisMeasure.m loads a Matlab data file (.mat) that contains (the digital representation of) the primary signal used to excite the Utemis apparatus. It then calls several

additional .m file subroutines. Names and interrelationships of these functions are given in Table 1. Also listed there are three ancillary programs:- UtemisTest.m, which is a GUI type program which provides access to three instrument test procedures; UtemisSigPrep.m which is a Matlab script that generates the signal file UtemisSig.mat; and UtemisDataAnal.m which opens MatLab Utemis data files created by the instrument and allows fitting of spectral models to the instrument observations.

The Utemi Spectrometer code makes use of two large MatLab structures denoted as S and MDat.

S is used to control the signal generation and signal processing operations.

MDat is a structure for holding sample data that has been either entered on the UtemisMeasure GUI (sample name, size, type, etc.), or are the GUI-selected measurement parameters or the measurement results.

Utemi Spectrometer Computer Programs (MatLab):

```
>>>>>>>>>>>>>>>>>>>>>>>>>>>>>>>>>>>>>>>>>>>>>>>>>>>>>>>>>>>>>>
UtemisMeasure.m   +  UtemisMeasure.fig      GUI program
    Normal location:-  \UTEMIS\
    Purpose:-   Overall operation of  the Utemis Spectrometer
        when measuring sample magnetance or susceptibility.
>>>>>>>>>>>>>>>>>>>>>>>>>>>>>>>>>>>>>>>>>>>>>>
    Subroutines called:-
        GetAvgdSegdKData2.m    m-file function
            Normal location:-  \UTEMIS\UtemisCode\UtemisCalledFncns
            Purpose:-   In conjunction with the subroutine below,
            sends to the apparatus, receives from it, and
            analyses a repeated set of signals which together
            constitute a single magnetance measurement
            (with or without the sample present).

            The above routine calls:-
                GetBasicSegdKData2.m   m-file function
                Normal location: \UTEMIS\UtemisCode\UtemisCalledFncns
                Purpose:- Sends, receives and analyses one
                multisegmented signal waveform.
```

```
        UtemisPlot.m   m-file function
            Normal location:-  \UTEMIS\UtemisCode\UtemisCalledFncns
            Purpose:-  Plots measured data, in either spectral
                or polar form as required by GUI input

            The above routine calls:-
                PolarKPlot.m **     m-file function
                    Normal location:-  \UTEMIS\UtemisCode\UtemisCalledFncns
                    Purpose:- Plots, in polar form, a
                    suite of inductivity measurements
                    acquired as specimen is rotated.

                    The above routine calls:-
                    ScaleData.m **   m-file function
                    Normal location:-  \UTEMIS\UtemisCode\UtemisCalledFncns
                    Purpose:- chooses a scaling factor so polar
                        plot will be readable

                **  May be included as a subfunction in its calling m-file.

Data file required:-
    UtemisSig.mat    A MatLab  .mat data file
        Normal location:-  \UTEMIS\UtemisCode\UtemisSigFiles
        Purpose:-  Contains the several MByte long Utemis multisegment
            signal.  It is reread each time a measurement sequence is
            begun by GUI action.


>>>>>>>>>>>>>>>>>>>>>>>>>>>>>>>>>>>>>>>>>>>>>>>>>>>>>>>>>>>>>>>>>>>>>>>>>>>>>>>
UtemisSig.mat   is generated by the MatLab script m-file UtemisSigMaker.m.

>>>>>>>>>>>>>>>>>>>>>>>>>>>>>>>>>>>>>>>>>>>>>>>>>>>>>>>>>>>>>>>>>>>>>>>>>>>>>>>
UtemisSigMaker.m.     m-file function
    Normal location:-  \UTEMIS\UtemisCode\UtemisSigFiles
        This script is run whenever a new version of UtemisSig.mat
        is needed, for instance when alterations are to be made
        to the Utemis multisegment spectrometer signal. (The
        user may wish to have a variety of signals on hand, for
```

```
        instance signals tailored to 50 Hz and 60 Hz noise
        environments; but only the currently used file can have
        the name UtemisSig.mat.  It is up to the user to give
        appropriate temporary names to any currently unused signal files.)

    The above routine calls:-
       kaiserwin.m     m-file function
                Normal location:-  \UTEMIS\UtemisCode\UtemisCalledFncns
            Purpose:-  A substitute for the MatLab function
                    kaiser.m supplied in the "Signal Processing"
                    MatLabTool Box. It is provided so this toolbox
                    need not be licensed.
>>>>>>>>>>>>>>>>>>>>>>>>>>>>>>>>>>>>>>>>>>>>>>>>>>>>>>>>>>>>>>>>>

>>>>>>>>>>>>>>>>>>>>>>>>>>>>>>>>>>>>>>>>>>>>>>>>>>>>>>>>>>>>>>>>>>>>>>>>>>>>
UtemisTest.m + UtemisTest.fig    GUI program
    Normal location:-  \UTEMIS\UtemisCode
    Purpose:- Runs the Utemi spectrometer in one of  three
    different test modes.
>>>>>>>>>>>>>>>>>>>>>>>>>>>>>>>>>>>>>>>>>>>>>>>>>>>>>>>>>>>>>>>>>
```

MDat Data Structure:

```
MDat =
     DateTime: '2007-10-02 15:29:47'
               %Year, Month, Day, Hour, Minute, Second for 'Start'
            K: [1x1 struct]
               % see below
       KUnits: 'milliSIU'
               % string of K units
         KorM: 'M'
               % Susceptibility or Magnetance plotting
            M: [1x1 struct]
               % See below
       MUnits: 'microlitres'
```

```
                % String of M units
        angles: {7x1 cell}
                % Rotation angles in degrees for tensor measurement:
                % cell array of strings
          axis: [0 0]
                % Codes for sample orientation
         freqs: [35x1 double]
                % list of frequencies in Hz
       nangles: 1
                % Number of rotation angles at which measurements have
                % been taken (1 or 7)
         nfreq: 35
                % Number of column elements in freqs, K and M
         nmeas: 1
                % Number of individual measurements average in each
                % full measurement
        option: 1
                % Sample option choice (Sets index letter in name,
                % see 'type' below)
        sample: 'Test'
                % Sample Name entry; String
     sampleDes: '  '
                % Sample Description entry text; String
          sens: 2
                % Code for excitation intensity, 2= normal,
                % 3=normal/3.16 4=normal/10
          type: ' '
                % [S = K or M sample, C = Calibration sample,
                % N = Null check (no sample),
                % A = Anisotropy (Tensor)  measurement on one axis]
        volume: 'object'
                % volume in volUnits or the word object: string
      volUnits: 'ml'
                % volume unit: string

MDat.K =
          Ampl: [35x1 double] % Amplitude of susceptibility
            Im: [35x1 double] % Imaginary component of susceptibiity
```

```
        Phase: [35x1 double] % Phase of susceptibility
           Re: [35x1 double] % Real component of susceptibility
 StdDevAbsErr: [35x1 double] % Standard deviation of absolute
                             % repeatablility error of susceptibility

MDat.M =
         Ampl: [35x1 double] % Amplitude of magnetance
           Im: [35x1 double] % Imaginary component of magnetance
        Phase: [35x1 double] % Phase of magnetance
           Re: [35x1 double] % Real component of magnetance
 StdDevAbsErr: [35x1 double] % Standard deviation of absolute
                             % repeatablility error of magnetance
```

5 Instrument set-up

The UTEMI Spectrometer consists of the following components packed in a foam-lined shipping container

1. Computer system consisting of
   (a) Shuttle ST20G5 with AMD processor and two 70 Gb hard-drives
   (b) CDROM drive
   (c) on board ATI graphics
   (d) RME HDSP 9632 sound card
   (e) Monitor: Viewsonic 17" 702b LCD video display terminal (VDT)
   (f) Short keyboard and mouse
2. Instrument modules manufactured by Geosystems consisting of
   (a) Coil Set with detachable sample rotator
   (b) Power Supply and Power Amplifier module (PS-PA)
   (c) Preamplifier module.

They connect together as in Figure 2. See the Quick Start Instructions for explicit help on starting up the instrument. The Utemi Spectrometer is operated by the MatLab program UtemisMeasure.m via a graphical user

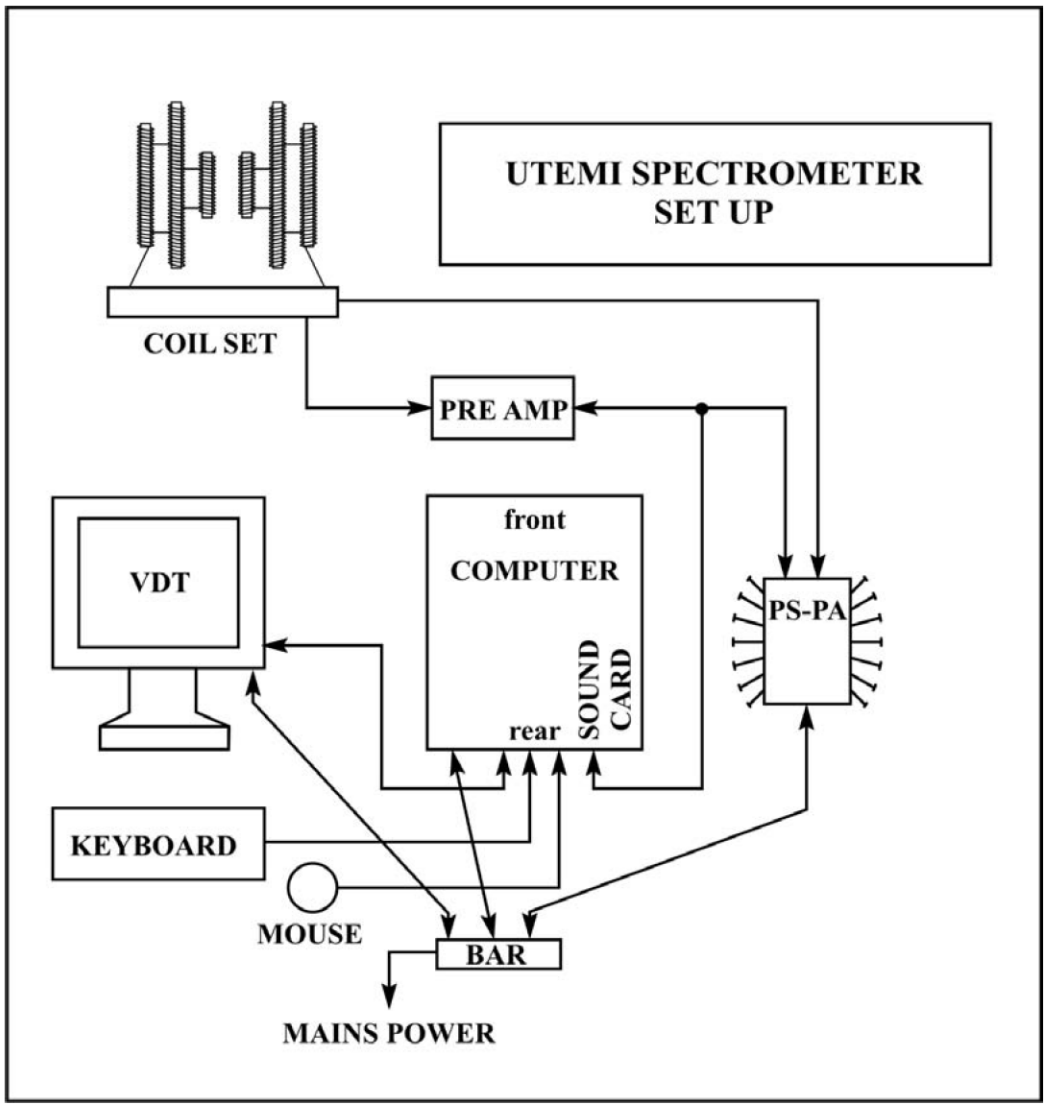

Figure 2: Susceptibility spectrometer schematic.

interface (GUI). The operator controls and monitors the instrument by mouse clicks and keyboard entries. A screen display guides the user. Results are initially plotted to the computer screen. After examination, they can be stored in standard formats in files placed in specific folders of the computer file system.

5.1 Sample Holder

The Utemi spectrometer was designed to have a uniform sensitivity to ~ 1 % throughout a roughly spherical sample region whose origin is the symmetry centre of the coil set and whose radius is approximately 20 mm. This means that a small isotropic element of magnetance such as a ferromagnetic mineral grain or piece of conductive metal will give the same measurement result wherever it is placed in the allowable sample region as long as its orientation remains unchanged. If measurement errors up to a few percent can be tolerated, the acceptable region may be expanded to a radius of ~ 30 mm or even more. The standard cylindrical sample vial (25 mm diameter filled to a depth of 25 mm) confines all parts of the sample to be within a ~ 20 mm radius. Lateral positioning ($\pm$ 3 mm) of a specimen object in the vial is therefore not critical. However, if the sample is anisotropic (aelotropic), the orientation of sample in the sample holder may need to be controlled to ~ 2 $^{\circ}$.

The apparatus may be used in a scalar or tensor mode. In the scalar mode, the sample is inserted into the apparatus in only one orientation, and the sample-present measurement is referenced to one or two sample-absent measurements made before, or before and after the sample-present measurement. Sample orientation is determined by the operator when inserting the sample into the apparatus. For isotropic samples in vials, it is convenient to manipulate the vial in a small acrylic "tennis racquet" and to hang the sample vial and its holder (with its axis vertical) from the thin acrylic top plate pegged to the top the sample space. If sample orientation is significant, the sample must be firmly fixed in the vial with a known orientation with respect to the vial axis and with an an orientation line marked on the vial top. The orientation of the sample axes with respect to the spectrometer X1 and X2 axis needs to be specified on the GUI.

In the tensor measurement mode, a set of 7 magnetance measurements is made as the sample is rotated 0° - 180° in 30° steps about a vertical axis perpendicular to the coil set axis. These sample-present measurements are

referenced to a pair of sample-absent measurements made before and after. A rotating stage located beneath the sample space controls sample orientation. It is driven by a hand operated, geared, crank system that converts one 360° rotation of the crank about a horizontal axis into a 30° rotation of the sample about a vertical axis. If the sample is mounted in a standard vial, it should be inserted into the sample space without using the acrylic mini "tennis racquet". Then the bottom of the vial will rest on the cork-surfaced rotating stage of the sample rotator; and will also be loose enough in the top guide plate that the vial can rotate with the stage. The operator must set the initial orientation of the sample, and is responsible for checking at the end of a set of measurements that a full 180° rotation was achieved.

APPENDIX 7

Manual for UTemis Simulation Software

R.C. Bailey

October 4, 2007

Contents

Chapter 1

About UTEMIS

UTEMIS is MATLAB software to calculate the electromagnetic response of localized targets embedded in a host medium, for a variety of instrument configurations. It was developed as part of a project to provide tools for improving electromagnetic detection technology in humanitarian demining. The sponsor of the project was the Canadian Centre for Mine Action Technologies (CCMAT), the project was administered through Defense Research and Development Canada (DRDC) as part of contract No. W7702-03R942/001/EDM (technical authority Dr. Yoga Das), and the work was done at the University of Toronto.

The need for electromagnetic induction (EMI) detection of buried metallic targets in general and for humanitarian demining in particular, has led to a variety of electromagnetic induction (EMI) metal detectors. It is difficult to design a detector to be optimal in all environments: variations in soil conductivity, and more importantly from the point of view of this paper, frequency dependent soil magnetic susceptibility can favor one design over another. The comparison of projected detector performances in such situations can be assisted by the use of computer modelling. Such modelling capability is pointless without measurements of the frequency dependence of magnetic susceptibility of actual soil samples, and that has been the initial focus of this project. Even with such measurements, modelling is still not trivial in practice: although there are many codes, public domain and otherwise, for computing EMI responses of various targets in various environments, most are adapted to specific instruments, and making comparisons would require collecting disparate codes, trying to make them run equivalent models, and then reconciling disparate outputs. This task is further compli-

cated by the fact that frequency dependent soil susceptibility is not always incorporated in EMI modelling, although straightforward in principle. One of the goals of this project is to produce such code. No new theory is involved; all of the theoretical material on which this code is based is available in the scientific literature, and in fact common knowledge in such fields as exploration geophysical EMI. Such code, to be useful, is required to be relatively flexible with respect to instrument configuration and operation, since one cannot predict in advance the evolution of instrument design. On the other hand, the range of targets and operating environments is more constrained because it is already defined by existing circumstances. However, realistic characterization of these targets and environments is, in the end, necessarily experimental; soils are not designed to prior specifications, and one cannot rely on mine manufacturers to provide reliable specifications of the relevant material properties and shapes of the metal components of their mines. (Even if they did, such specifications might be useless much of the time, for two reasons: first, material properties such as steel permeability are irrelevant to mine operation, and unlikely to be well controlled during manufacture; secondly, there are many shapes (helical springs, L-shapes, etc.) for which theoretical calculations of the responses are not at all straightforward.) Accordingly, the mine detection simulation described here is part of an integrated project. The first part of the project, essentially completed and previously described (West and Bailey, 2005; West and Bailey, 2006), was the design and construction of a broadband susceptibility meter suitable for measuring the frequency-dependent susceptibility of both soils and small metal pieces. Based on an initial working prototype, two further improved spectrometers are now being completed. To simply provide this experimental information as spectra or equivalent data does not make it readily usable by the demining community. Accordingly, the development of user-friendly code to integrate this information and instrument specifications into a simulation is, as noted above, the necessary second part of the project. The type of instrument modelled here is of the usual type where a signal generator generates a transmitter current, which in turn generates a magnetic field using a transmitter coil. This transmitter coil is inductively and magnetically coupled by the environment (which includes the earth and any targets of interest) to a receiver coil. The receiver coil voltage is then amplified and processed with various detection algorithms. These detection algorithms may extend all the way from recognition of a modulated audio signal by a listening operator, through to computer processing of the signal by various logic

algorithms. (This code is not intended to model those very simple single-coil devices where the target influences the Q or resonant frequency of an oscillator by interaction with its single transmitter coil.) Coil arrangements in existing and future detectors have a variety of configurations, so that the finished product should be able to handle any such arrangement, including multiple coils with arbitrary relative orientations and shapes. Transmitter current waveforms are also highly variable, particularly if one includes the variety of EMI waveforms that might be inherited from EMI applications in exploration geophysics. To rely on manufacturers' design intentions for such waveforms, even if publicly available, would be imprudent, since design specifications do not always reflect final realities. It is more useful to be able to work with an arbitrary digitized waveform as measured with an external sensor. The classic humanitarian demining problem involves a very small metallic target, embedded in the Earth which is usually relatively resistive (in the sense that the transmitter field at the target location is not very different from the value it would have in free space). This permits the transmitter-receiver couplings induced by soil conductivities and susceptibilities, even if frequency dependent, to be regarded as independent of the transmitter-receiver couplings induced by the target, so that they may be summed. The code is written in MATLAB. This platform enables two important run-time features, whose role is described in the last section of this paper. The first is dynamic creation of structures at run time (to permit new instrument configurations and properties to be easily added without rewriting the core code). The second is the ability to read and execute user-entered formulae as MATLAB code, enabling new instrument signal processing algorithms to be easily added, also without rewriting the core code).

1.1 Features of UTemis version 1.0

Version 1.0 as delivered offers the following computational simulation capabilities[1] for modelling the response of electromagnetic induction detection of small targets:

1. Complete integration with a MATLAB computing environment, including export of computed results to MATLAB as workspace vari-

[1]Not all capabilities are available simultaneously because of the need for reasonable response times with reasonable accuracies; such limitations are noted where relevant throughout the manual.

ables for further user analysis, to files in MATLAB m-file format, and as MATLAB graphics with all standard MATLAB facilities for graphics editing. Specification of user-defined complex functions (such as frequency-dependent instrument amplifier gains, or detection algorithms, or voltage-to-audio mappings) below can be done using MATLAB syntax.

2. Arbitrary single or multiple transmitter and receiver coils of arbitrary geometries.[2]

3. Frequency domain instrument or time domain instrument simulation, with an arbitrary frequency set or arbitrary waveform specification (some standard waveforms are defined for user convenience).

4. Simulation of arbitrary instrument frequency-dependent signal amplification stages[3].

5. Arbitrary sequencing of measurements in an arbitrary survey configuration.

6. Arbitrary selection of frequency or weighted time windows for generation of subsequent processing signal channels.

7. Arbitrary algorithmic processing of multiple signal channels by user-specified detection algorithms[4].

8. Response simulation of arbitrarily located small localized targets in terms of arbitrary decay amplitudes and times along arbitrary axes, including the ability to describe them on the basis of data collected by the accompanying UT EMI spectrometer.

9. Response simulation of a arbitarily frequency-dispersive magnetic halfspace, described either theoretically or on the basis of data collected by the accompanying UT EMI spectrometer.

---

[2]With the caveat that complex surveys with multiple instrument heights will take longer to compute.

[3]Very complex frequency dependences are most easily incorporated by a user-coded MATLAB function

[4]Again, very complex algorithms are most easily incorporated by a user-coded MATLAB function

10. Extensibility, to other targets such as background soil responses (e.g. a conductive earth) by simply adding "plug-in" routines developed by U of T or users (including the ability to incorporate modifications to the instrument-target couplings from the default free-space coupling), without requiring a new version of the UTemis code.

11. A flexible GUI[5] with

    (a) the ability to easily load, edit, reload and save configuration files describing instruments, surveys, and multiple targets,

    (b) the ability to plot instrument transmitter waveforms/spectra, receiver waveforms/spectra, receiver time-domain averaging-gate channel definitions, receiver amplifier frequency responses,

    (c) single-button recalculation of responses following any change to instrument, survey, or target specifications,

    (d) the ability to plot map or 3-D views of the survey geometry, and mouse-click-select a specific site for followup analysis with response plots,

    (e) the ability to plot, either in profile mode or map mode, (any channel of) the response of the target during a survey,

    (f) the ability to add/subtract gridlines, change plot scales, or switch between log and linear scales on any of the GUI plots, via right-mouse-button context menus,

    (g) the ability to export any GUI plot as a standard MATLAB figure to the desktop, for follow-up analysis or editing for publication,

    (h) the ability to save and reload an entire session, with associated instrument, survey, target and responses, for quick resumption of previous analysis.

12. A batch (non GUI) mode of operation for unattended computationally-intensive simulations.

13. The ability to conduct audio "pseudo-surveys" by moving the mouse over the output channel map, with either a default voltage-to-audio conversion function, or a plug-in supplied by the user.

[5]Graphical User Interface

14. Companion software (*utemispolefit*) to convert user-provided target response spectra (whether theoretically or experimentally obtained, as for example by the accompanying University of Toronto EMI.

15. A number of sample configuration files describing example instruments, targets, and surveys. spectrometer).

16. Instructions for the simple installation process.

1.2 Algorithmic structure

This section provides an overview of what is simulated by UTemis and how the major features described above are implemented. The computation of simulation results is broken down into a number of steps as shown in Fig. 1.1. Each step, from calculation of the transmitter waveform through to the output signal delivered to the instrument operator, requires an algorithm, and a user-provided description of the relevant part of the instrument or target. Here we briefly outline these steps, using Fig. 1.1 as a reference. A more complete description is provided in Chapter 6.

1.2.1 Steps 1 and 2: Waveform generator and TX amp

Although numbered in the Figure as two separate steps (as would be the case with real electronics), the waveform generation and amplification are actually dealt with as a single step in UTemis. The information required by UTemis to calculate the transmitter (current) waveform[6] is provided by the user in the instrument configuration file. An instrument can be either a frequency-domain or time-domain instrument. If frequency-domain, the frequencies, phases, and amplitudes of one or more Fourier components of the waveform are described by the user. If time-domain, the user describes a transmitter waveform either as a standard type by name (square, triangle, protem, input, *etc.*) and properties (amplitude, period, risetime, *etc.*), or as an arbitrary digitized waveform to be extracted from a user-provided file. For a time-domain instrument, the user explicitly or implicitly defines here the digitizing interval to be used in calculating and displaying the receiver responses.

[6]That is, the current in amperes to be provided to the transmitter coil.

1.2.2 Step 3: Transmitter transducer(s)

Again in the instrument configuration file, the user must describe the transmitter transducer(s). All transducers have a location described for the instrument reference origin. Only two types are recognized at present, coils and point magnetic dipoles[7]. Multiple transducers can be specified, with the assumption that these are connected in series so that they all carry the same transmitter current waveform as described in the previous section[8]. Coils are described by a shape (circle or polygon) and a number of turns. If a polygon, a series of vertex positions with respect to the instrument reference origin must be described by the user, either in the instrument configuration file or in a data file referred to by the instrument configuration file.

In the present version of UTemis, some of the response-computing routines have some limitations on what coil properties may be specified, in particular for conducting Earth eddy current responses. For that target, transmitter vertical-axis circular coil transducers are required (with all transmitter and receiver coils coaxial). If polygonal coils are specified, they will be approximated as equivalent circular coils for this response only, but treated as polygonal for magnetically susceptible soils or for localized targets. Since a localized target may be much closer to one part of the coil than another, correct coil shapes are important in computing localized responses; this is not so important for global targets.

1.2.3 Step 4: Survey descriptions

A survey is described as a set of 3D locations of the instrument reference origin. They may be specified as a set of points along a line (a *profile* survey, or a set of points filling a horizontal rectangle (a *grid* survey). (Profiles can subsequently be extracted from grid surveys for plotting.) Instrument responses will be plotted as a function of instrument position in the survey. A current limitation of UTemis is that instrument orientation cannot be varied from that originally specified in the instrument configuration file. For some targets, surveys have to be conducted at constant height.

[7]The magnetic dipole transducer can be regarded as a very small multi-turn coil with an area-turns product (effective area) of one square meter.

[8]This restriction can be bypassed by altering the specified number of turns in the coil from the actual number to a number which correctly describes the net current circulating in the coil.

1.2.4 Step 5: Target descriptions

Multiple targets, from a list of allowed types, are described by the user in the target configuration file. The user must specify the target type (from a list of allowed types). The actual computation of target responses is handled outside the main UTemis program, using outboard functions dedicated to each target type, so that more target types can be added in future versions of UTemis without requiring revisions to existing code. This functional separation requires that all target response calculating functions adhere to a strictly defined standard of describing the response (defined, in the frequency domain as the transimpedance $Z(\omega)$ between the receiver sensor voltage and transmitter source current). The standard adopted by UTemis is to represent this response as the amplitudes and decay rates of a sum of a series of exponential decays (even for frequency-domain response calculations), with a few extra terms to represent the singularities associated with step function source. Chapter 6 gives details. Specifically,

$$Z(\omega) \cong \sum_{k=0}^{K} N_k \, (j\omega)^k + \sum_{m=1}^{M} \frac{j\omega D_m}{j\omega + p_m} \tag{1.1}$$

The time-domain transimpedance representation[9] is therefore

$$z(t) \cong \sum_{k=0}^{K} N_k \, \delta^{(k)}(t) + \sum_{m=1}^{M} D_m \delta(t) + \sum_{m=1}^{M} D_m H(t) \, e^{-p_m t} \tag{1.3}$$

The target responses are therefore summarized in the (relatively few) values of N_k, D_m and p_m ("NDP" format). This is, for most targets, a far more efficient representation than a full list of frequency domain responses at all frequencies. Most localized targets have responses which can be shown to be dominated by one or a few exponential decays. Large targets (such as a conducting half-space, which has a power law decay at late times) can be adequately represented by a few dozen such exponentials[10] over the time and frequency ranges utilized by a real instrument.

[9]This is the response to a delta-function transmitter current waveform. The corresponding step response is

$$s(t) \cong \sum_{k=0}^{K} N_{k+1} \, \delta^{(k)}(t) + N_0 H(t) + \sum_{m=1}^{M} D_m \, H(t) \, e^{-p_m t} \tag{1.2}$$

[10]Typically 3 or 4 poles p_m per decade.

The advantage of this representation is that the (time consuming) calculation of the influence of each exponential decay on the final receiver waveform shape can be done (using Fourier techniques) just once, except for its amplitude. Subsequent calculation of the response for the many different instrument locations during a survey requires only a location-dependent recalculation of the amplitudes N_k and D_m, and adding the correct amount of the precalculated individual decay responses into the receiver waveform.

Two types of target are recognized and specified: global targets and localized targets. For global targets, the outboard response functions compute the transmitter-receiver transimpedance using target properties specified by the user and passed unaltered by the UTemis GUI through to the outboard functions. Currently available global targets are free space (the direct transmitter-receiver coupling), a uniform magnetic half-space with frequency dependent magnetic susceptibility specified by the user in NDP format, or a electrically conductive halfspace with user-described layer thicknesses and conductivities. These global targets can be used simultaneously.

The second target type is the localized target, which is assumed to be small compared to its distance to the instrument. For these, the outboard response functions are expected to calculate an NDP response for the target *magnetance*, the susceptibility-volume product of the target (or rather a susceptance magnetance, if the target is not isotropic). UTemis then calculates the transmitter-target and target-receiver couplings to convert this to an NDP representation of the transimpedance. At present, free-space couplings are used. This is normally a good approximation for simulating land-mine detection. Future editions of UTemis may use coupling fields corrected for magnetic and electric shielding of the simultaneous global targets.

For some simple targets, an NDP representation can be calculated analytically (an example is the ring target described later). For many, however, actual measurement is the only way to reliably get an NDP response. The UTemis simulation code is accompanied by a program (utemispolefit, described later) for using a frequency response (measured or theoretical) and generating an NDP representation in a format suitable for cutting and pasting into a target configuration file.

Complex targets are intended to be described as the sum of several simple ones. An example of this is a small asymmetric conductive object: the response of each principal axis of this can be individually described as a uniaxial tensor NDP target. The target configuration file will include all three as separate subtargets to be added together. Organization of such

target groupings is made easier by the availability of an *include* statement in configuration files, so that a grouped set of subtargets can be stored as a separate file to be included as a group in an overall configuration file.

1.2.5 Step 6: Receiver transducer(s)

The characteristics and description of the receiver transducers are essentially the same as those of the transmitter transducers (the magnetic dipole source is replaced by a point magnetic field sensor with a sensitivity of one volt per Tesla). The coils are assumed to be connected to a receiver amplifier of infinite input impedance to keep current in the coils to negligible amounts.

1.2.6 Step 7: Receiver amplifier

The simulation of the receiver amplifier includes *gain*, specified either as a constant, as a MATLAB formula as a function of frequency, or as a set of gain values as a function of frequency in a file. The output of this stage of processing is twofold: the information needed for the gate signals described below, and an amplified receiver waveform for whichever survey location is selected as "current".

1.2.7 Step 8: Signal integrators

Mine detectors in actual operation do not usefully present actual waveforms, but rather single signals derived from the waveforms. One such example would be the mean voltage level over a certain time interval (known here as a time *gate*) in the waveform[11], often chosen to allow unwanted interference from irrelevant targets to be minimized. More sophisticated designs may utilize several such integrating gate signals in an algorithm for better interference rejection. Finally, the average over a time interval may not most usefully be a simple average; a weighted average may be used in some instrument designs.

Accordingly, the instrument configuration file allows the specification of one or more averaging gates. If unweighted averaging is desired, it is necessary to specify only the start and stop times of the gates. If weighted

[11]Mean values are better than samples at an instant, because of the noise rejection thereby achieved.

averaging over the waveform is desired, these weight functions are specified in a file referred to by the instrument configuration file.

1.2.8 Step 9: Processing of the gate signals

The final stage of processing in most instrument designs may be simply the conversion of a single gate signal to an audio signal for the operator. However, better detection performance (in particular, false alarm reduction) can be achieved by using several gate signals in some algorithm which may involve both logical and arithmetic calculations to determine if a target is present. The instrument configuration file permits the specification of such an algorithm, as a MATLAB formula (which may in turn use external functions provided by the user) to convert gate voltages to final instrument outputs, which UTemis can then plot or export.

1.2.9 Step 10: Audio output

Because so many instruments use an audio signal to communicate detection results to the operator, UTemis allows the user to draw a path across a map plot of a computed survey, and listen to the result. Although a default conversion function exists, users can specify their own with a MATLAB formula, which again may refer to an external function provided by the user.

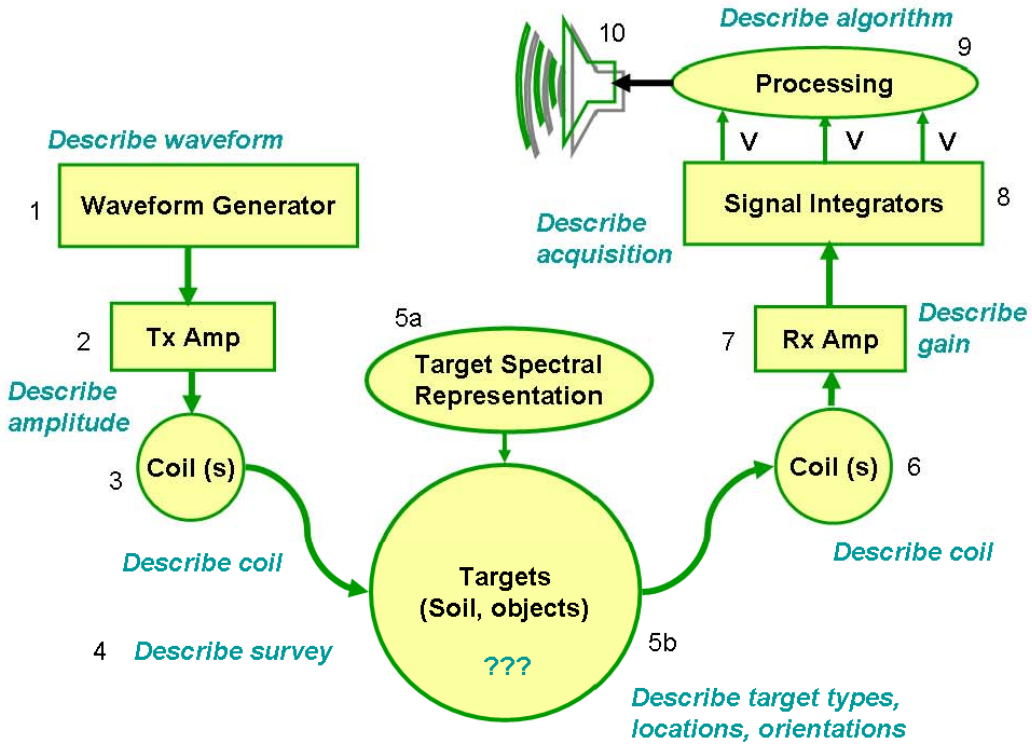

Figure 1.1: Structure of the representation used by UTemis for simulation. A sequence of steps (numbered) is involved in computation of a simulated response, from calculation of the transmitter waveform through to the output signal delivered to the instrument operator. The corresponding information at each step that has to be described to UTemis by the user-created configuration files is noted.

Chapter 2

Using UTEMIS

2.1 Installation

UTEMIS can be used either as a compiled executable file *utemis.exe* or a MATLAB m-file *utemis.m*. UTEMIS was developed for, and has only been tested with MATLAB 6.5 under 32 bit Windows operating systems. Although MATLAB code is supposed to be platform independent, there is no guarantee that it will work with any particular operating system. UTEMIS comes as a zipfile archive.

2.1.1 MATLAB version

For the m-file version, make a subfolder of your MATLAB toolbox folder (itself a subfolder of your main MATLAB folder) and call it *utemisim*. Unzip the archive file utemis.zip into this folder.) Add this folder permanently to your MATLAB path using "Set Path" under the MATLAB File menu. All the documentation files (*e.g.* .doc, .txt and .pdf files) will be included here; you may prefer to move these to some more accessible location.

Note that some graphics cards do not handle MATLAB graphics correctly under all circumstances, particularly when using OpenGL (for example, see http://www.mathworks.com/support/tech-notes/1200/1201.html). Some of these problems can be resolved by preventing MATLAB from using OpenGL rendering by entering the command *opengl neverselect* into the MATLAB command window.

2.2 Invoking and running UTEMIS

2.2.1 Configuration files

UTEMIS requires configuration files to be present that describe the instrument, the target(s), and the survey geometry. These are not input into UTEMIS by the user while running UTEMIS, but rather prepared beforehand (or during) as "configuration files". The configuration files are all text files, and editable by any text editor. Configuration edit sessions can be invoked from within UTEMIS. There are three types, survey files (*.svy), target files (*.tgt) and instrument files (*.int). Their preparation and formatting is described later; several sample configuration files are provided with the software.

2.2.2 Starting UTEMIS

If you are using a compiled version of UTEMIS, you can invoke it directly by double-clicking on its icon, or entering *utemis* at the command line in a DOS window. When UTEMIS starts, it will display only blank plots. At this point, one loads the configuration information, either directly from the desired configuration files, or in the form of a previously saved session, saved as a "session file" (of type *.ses). If configuration files are loaded manually rather than through a session file, no response information will be displayed until the survey is "performed" by selecting Run under the Survey menu item. Be aware that you may at some point have session files that are older than the current versions of the configuration files they reference. The response data initially displayed will therefore not reflect the current configuration files on disk. In such circumstances, any attempt to recompute the responses will produce a warning that the loaded information is older than the configuration files, along with an opportunity to reload.

Be also aware that session files created with older versions of UTEMIS are not guaranteed to work with newer versions.

2.3 GUI layout

The graphical user interface (GUI) displays a main plot window, which can display up to four plots, has three quick-load buttons for reloading configuration files, and a menu system. Separate windows are or can be opened

for some aspects of the computation. Detailed descriptions of the available menu items are given in the next Chapter. The fastest way to get started is to follow the tutorial session described in a later chapter.

Chapter 3

Guide to UTEMIS menus

3.1 The Session menu

A "session" consists of the current state of your analysis, including computed responses if any. It can be saved and reloaded to resume analysis without setup or reloading configuration files (beware: session save files do not travel well between different computers or folders, since they save full pathnames for configuration files. Other options here are clearing existing sessions, and exist with and without closure of exported ("detached") graphics. Note that Utemis always makes a "stub" cleared session in whatever folder you are working in. These session files are meant for immediate convenience, not archiving; there is no guarantee that updated versions of UTemis will be able to load session files saved by previous versions.

3.2 The Describe menu

This permits printing or plotting descriptions of a large number of instrument, survey, and target properties of interest. Statistical summaries of results can be obtained here. Some reference information can be described as well: the standard colour order used by MATLAB for plotting a sequence of outputs, channels or gates; the standard unit prefixes used in plots.

3.3 The Instrument menu

This allows instrument configuration file loading, reloading, editing, and describing. Reloading after editing and saving a configuration file can also be achieved by pressing the appropriate "reload" button on the GUI.

Many instruments collect information about a "normal" or reference reponse, for use in processing algorithms. For example, the desired output signal may be the difference between the survey point and a "normal" site. This is sometimes called "bucking". Clicking on the *Set bucking* instrument menu item enables the *Set bucking* mode, signalling this by changing the cursor to a large crosshair the first time the left mouse button is pressed. Clicking with this crosshair over a particular point in the output contour map defines that point as the reference point for bucking, after which UTemis and the cursor revert to ordinary operation. The reference point is then shown as a cross on the output contour map. The reference values (one for each output channel defined for the instrument) are then set to the values of the instrument channels (frequency or gate values depending on the mode of operation) *if* the instrument menu item *Enable bucking* is checked; otherwise the reference values are held at zero. The reference values are *not*, however, automatically subtracted subsequently from the output signals. They are made available to the user as formula variables *vr(1), vr(2), etc.* for use in the output algorithm formulae which are defined in the instrument configuration file.

3.4 The Survey menu

This allows survey configuration file loading, reloading, editing, and describing. Reloading after editing and saving a configuration file can also be achieved by pressing the appropriate "reload" button on the GUI.

3.5 The Targets menu

This allows target(s) configuration file loading, reloading, editing, and describing. Reloading after editing and saving a configuration file can also be achieved by pressing the appropriate "reload" button on the GUI.

3.6 The Run menu

This controls when UTemis calculates responses. If *Auto-recalculate* is on, it does so immediately after every change to the system description (convenient if the recalculation is fast). Otherwise (useful if calculations take a long time) it does so only when the *Calculate* item is clicked. Calculated responses can be cleared with the *Reset* item. Debug mode (see the Debug menu below) can be toggled on or off.

3.7 The View menu

This menu has 5 sections, variously involved with graphical and audio displays of the data.

3.7.1 Refresh and Clear

The top section of the menu list allows refreshing the plot displays, or clearing them.

3.7.2 Overlay Gates

For a time-domain instrument, this overlays the time gates (in colour, as per the standard MATLAB colour order) on any waveform plots.

3.7.3 Show Colorbar

This adds a color bar for the Output Contour plot.

3.7.4 Define Map Variable

Define Map Variable selects which of the output voltages defined for the instrument will be used to produce contour maps using the *Output Contour* selection.

3.7.5 Custom Profiling

The *Custom Profiling* item, in section 3, has a number of functions. If selected, it allows the the mouse to draw custom paths on the *Output Contour*

plot, either straight (using the left mouse button) or curved (using the the right mouse button). The output response as seen along this path is then plotted in the *Output Profiles* plot, if present.

3.7.6 Sound

The *Sound* item, if selected, simulates the audio response of an instrument along the defined custom profile, using the computer sound system. The conversion of the selected map output voltage to sound is done by a default routine built into UTemis; however, by specifying the instrument entity *speaker* with attribute *function* given the name of a user provided function[1], any conversion can be done. This function must take two input arguments: audio sampling rate (in Hertz), and the output voltage time series as sampled at that rate; it must provide the time series of the desired audio signal, samples at the same rate.

3.7.7 Plotting

The primary purpose of fourth section is to toggle on or off the display of selected plots of target responses and instrument and survey characteristics. Only 4 plots can be concurrently displayed. If more are requested, only the first 4 are shown. If a plot cannot be shown (the response has not yet been calculated, or it has been invalidated by loading a new configuration file or selecting a new current site with a mouse click on the survey map view), an empty space is left where it would be plotted, but no warning is issued. Most plots are self-explanatory; note that selecting *Output Profiles* plots the survey results as obtained along a *profile* type survey, or along a custom profile if that has been defined; if the survey type is *grid* and a custom profile has not been selected, the Output Profile plot links each line of the grid into a continuous path and plots the results obtained along it. The *Survey Map*, a plan view of the survey, shows the locations of any localized targets with filled red diamonds, and the currently selected site (to which any plotted receiver signals will correspond) as a filled green circle. Clicking on any survey site (shown as an open black circle) moves the current selection to that point. The *3D Survey View* shows a 3D view (to permit assessment of

[1]Which must be available to UTemis on the MATLAB path.

localized target depths, for example, by detaching the plot and viewing it from different angles), but is not interactive in the same way.

Plot Rx Signal and *Plot Rx Spectrum* give plots associated with the "current site". For frequency domain systems, the response at each frequency is plotted. For time domain instruments, the receiver voltage waveform is plotted. For frequency domain instruments, amplitudes for each frequency are plotted.

The voltage is as calculated after all receiver gains have been applied. Note that a cosine bell taper in the frequency domain is used to prevent ringing in the Fourier synthesis of the receiver waveform. This slightly smooths the computed receiver voltage timeseries, with the filter [0.25, 0.5,.0.25].

3.7.8 Detaching plots

The fifth part of the menu list allows the "detaching" of plots as full MATLAB graphics windows, for subsequent editing, printing, or saving. All detached plots can be closed simultaneously by clicking on the *Close detached figures* item. Note that detached plots are not guaranteed to survive indefinitely. If saved plots are desired, they should be saved immediately.

3.8 The Report menu

No reporting of any sort is done unless one of the top three options is checked, so that a reporting target is defined. Reporting on calculations can be done to any combination of the (1) MATLAB console (if available), (2) a file, or (3) by assignment in the main MATLAB workspace (if available). Choosing the "Report to Workspace" option means that reported information is immediately assigned in the workspace for interactive use and processing by the UTemis user. Names used for these assignments begin with an uppercase letter, as in *Acquisition*, *Output*, *Sensor*, *Source*, *Survey*, *Target*, *Waveform*, *Channels*, *Dt*, *Locations*, *Outputs*, *RXwaveform*, *TXwaveform*, and *SampleTimes*. Text output reported to a file is legal MATLAB code, and if cut, pasted into and executed in the MATLAB console, will produce the same results as having the "Report to Workspace" option on.

When reporting to a file, a timestamp is printed every time the file is (re)opened. The user-defined configuration information for instrument, targets, or survey can be reported. If a configuration file is reloaded while

reporting is on, a report on the new configuration is automatically written to the reporting device(s). In addition to this configuration information, the transmitter and receiver waveform time series, and the output map, and the survey locations can be reported.

When opening, as a report file, a file that already exists, the MATLAB-provided dialog box implies that the existing file will be replaced if you proceed. This is not true; the file will be appended to. If you want to replace it, you will have to delete it by hand first. In any case, since each appended reporting gets its own timestamp, separate reporting episodes are distinguishable even if they are in the same file.

3.9 The Debug menu

Although originally added to assist in program development, this menu was retained to facilitate interaction with other MATLAB programs. Use of any of the *dump* commands will write the corresponding UTEMIS internal variable into the MATLAB workspace, where it can be inspected, parsed, and otherwise processed by end user codes. This is a more primitive form of the *report*ing facility described above.

The *describe last error* option sometimes provides, for MATLAB programmers, more detailed information on errors.

Chapter 4

Configuration Files

4.1 Introduction

The need to model a variety of instruments, targets and survey configurations suggests that details of particular instruments, targets and survey geometries should not be built into the code, but rather described in user-editable configuration files which will be read by the simulation software at run time. The GUI organizes the use of these files in a user-friendly manner. This manual describes the syntax and options available for specifying properties of instruments, targets, and survey configurations in those configuration files which are used by UTemis.

4.2 Conventions

The configuration files are all text files, and editable by any text editor. There are three types, survey files (*.svy), target files (*.tgt) and instrument files (*.int). The format is the same in all: each line names some entity of interest, and follows that name with property name - property value pairs. Generically, a line is of the form

```
entityName propertyName1=valueString1 propertyName2=valueString2
```

where as many propertyName/valueString pairs as needed can be specified on a line.

Lines can be continued by using the standard MATLAB continuation operator ... and the end of the line to be continued (a blank must precede

...).

Configuration files can also "include" other configuration file fragments stored as separate files, using a line like

```
include      righthandscrew.tgt
```

which simplifies describing standard parts of configurations. Only one level of including is possible (to avoid accidental recursive includes).

If a property is to be assigned to a number of following entities (for example, a composite target is to have all of its components shifted together to a new location using the "offset" property), one precedes these lines with an "apply" statement, like

```
apply      offset=[0.5,.7,-.03]
```

An apply statement on its own without a following property cancels all previous apply statements.

No blanks are permitted *within* the propertyName/valueString groups. ValueString can be any valid MATLAB expression (numeric, array, string or a combination) but with no embedded blanks. Embedded blanks are forbidden, since they are used by the Utemis GUI to separate one property name-value pair from another. MATLAB arrays should use (MATLAB legal) commas as element separators rather than blanks,*i.e.* [1,2,3] rather than [1 2 3]). For strings, underscores can be used to replace blanks. Forgetting this rule is likely to be the commonest cause of syntax errors in making configuration files. If unusual characters are included in strings, it may be necessary to enclose them in single quotes.

Following these rules, an instrument configuration file might look like this:

```
information      name=Test_Instrument    date='15/03/07'
source type=coil shape=circle location=[0,0,0] radius=0.1 pole=[0,0,1] turns=10
sensor type=coil shape=circle location=[0,0,1] radius=0.1 pole=[0,0,1] turns=10
waveform shape=sine frequencies=[5000,30000] current=[.5,.02]
acquisition method=frequency  gain=1.0e7 noise=0.01
output algorithm='abs(real(v(1)-vr(1)))>0.001'
```

As noted above, MATLAB expressions are permitted for property values; the frequencies and currents in the above expression for the waveform are given as 2-element arrays. "turns" is the multiple of the transmitter current (as defined in the "waveform") that a transmitter coil ("txcoil") has when

Variable	Type	Description
f	scalar	Frequency (Hertz)
w	scalar	Angular frequency (radians/second)
v	array	Receiver voltage channels (these will correspond to frequencies in a multi-frequency instrument, and to time windows or samples in a time-domain instrument).
vr	array	Receiver voltage channels at the reference point, as defined with the Set Bucking operation.
x,y,z	scalar	Spatial location (in survey coordinates)

Table 4.1: Available variables for use in MATLAB expressions.

regarded as a single turn. Multiple coils, for both receiver and transmitter are allowed. The example detection entry describes the condition that must be met for a detection alarm to be triggered, for instruments that work this way. Note that the detection algorithm above uses a MATLAB evaluated formula referring to an array variable "v"; this refers to an internal array "v" in which the instrument response voltages for the various channels is stored (for the frequency domain instrument above, the two channels correspond to the two frequencies, and contain complex numbers in general). Similarly, "vr" refers to the channel voltages defined at some reference point, as defined during the *Set Bucking* operation. The acquisition gain is a simple number above. It may be any MATLAB evaluable formula containing numbers and either "f" (for frequency in Hertz) or "w" (for angular frequency in radians/second); expressions which are not purely numeric will require use of the MATLAB "eval" function within the GUI, and should be entered as singly-quoted strings, again without embedded blanks.

4.3 Formula variables

As noted above, MATLAB formulae can be used for some configuration property values. Formulas, unlike numeric values, must be enclosed (as per the MATLAB string convention) in single quotes, to permit them to be arguments to the MATLAB eval function. Aside from builtin MATLAB names like pi or cos, these formulae can use only the variable names in Table 4.1.

4.4 Attribute Descriptions

Although UTemis will read any attribute from any configuration file, it is customary to keep instrument, target, and survey information in different configuration files with file extensions *.int*, *.tgt*, and *.svy* respectively. Accordingly, these three categories are discussed separately below. Note that literally given values below are given as italicised words, and must be spelled exactly as shown if used. Where a legal entry is described as a MATLAB formula, it must use only variable names understood by UTemis as noted above. Asterisks denote options which may not be implemented yet. The abbreviation "w.r.t." means "with respect to".

Two coordinate systems are used. One is the survey coordinate system, in which survey point locations and targets are described. The other is the instrument coordinate system, in which the instrument features (in particular its coils) are described. The orientation of the instrument with respect to the survey coordinate system is described as part of the survey configuration.

4.5 Instrument

For each entity used in a configuration file, property names and values are described below. These entities are *information, waveform, source, sensor, acquisition* and *output*.

4.5.1 Information

Since these values are not used in computation, but merely reprinted or described if requested, they can be any property-value pairs desired. Typical entries might be instrument *name* or *date*.

4.5.2 Source

Type

This can currently be *coil*, *electrodes*, or *mdipole* (magnetic point dipole).

Coil Type

If the type is *coil*, *shape* must be specified as *circle* or *polygon*. If a circle, the *radius* is required. The number of *turns* in the coil, and the *pole* direction (3-vector)of the axis of the coil must also be specified. If the shape is *polygon*, an atribute *nodes* (an N by 3 array) is required to describe the node locations of the polygonal loop (relative to the instrument coordinate origin), whose nodes are described by the row vectors in the matrix nodes. The first and last nodes are not connected; if a closed circuit is desired, the last node must duplicate the first. If the type is *mdipole*, a point dipole source, the effective area is required as an attribute *area*, so that the magnetic moment of the dipole will be this area times the transmitter current.

Electrode Type

If the type is *electrodes*, *location* of the midpoint must be specified as a triplet, and the vector (plus to minus) *separation* (one or more).

4.5.3 Sensor

Type

This can currently be *coil*, *electrodes*, *mdipole*, or *bfield*. The *coil* and *electrodes* are parameterized as for the *source*. An *mdipole* sensor is actually a point coil with an effective area specified by *area*. The *bfield* sensor is actually the same as an *mdipole* coil sensor with unit effective area, but with an inverting voltage integrator included, so that it is a direct B field sensor with a sensitivity of one volt per Tesla.

4.5.4 Waveform

Shape

This is a string. Recognized types are *sine, square, bipolar, input*[1], *protem*[2], and *triangle*. If not one of these, the value is assumed to be a filename

[1]A once common geophysical waveform, consisting of alternating sign half-sines separated by off-periods of the same length.

[2]Another geophysically-used waveform, consisting of an upward-decaying exponential turn-on followed by a fast linear turnoff, followed by an off period, the whole sequence then repeated with opposite polarity. Input properties are *riserate, risetime*,and *droptime*.

in which is found a column of custom waveform values sampled at equal intervals. If *samples* is specified in the *acquisition* entity, the number of samples and the length of this custom transmitter waveform must agree.

4.5.5 Acquisition

Method

This is the method by which channel voltages are to be obtained from the receiver waveform. If "frequencies" a frequency-domain instrument is assumed, and channel voltages are simply the receiver output voltage (complex) amplitude at each frequency.

Method "Gates" utilizes the weighted gate approach of a time-domain instrument. It is an error to specify this method if the waveshape is specified as "sine".

Samples

This is the number of samples into which the waveform is divided for numerical processing. If not specified, it defaults to 4096. An even number greater than 3 must be used. If a custom transmitter waveform is used, its length will be used instead. In the interests of speed, lengths which are integer powers of 2 are recommended.

Gain

The instrument receiver gain can be specified as a single scalar number, or as a legal MATLAB formula (but with no embedded blanks) in terms of the frequency variable f, or as a vector of numerically specified gains at every discrete frequency up to one less than the Nyquist frequency (other terms will be ignored). The number of such frequency samples needed can be viewed in the *Describe* menu. Note that the default gain is unity all the way to the Nyquist. This (implausible for a real instument) sharp cutoff at the Nyquist frequency can lead to ringing in the calculation of steps and impulses. *Note: the gain must be entered as a true complex quantity, i.e. incorporating phase information, e.g. like* $1/(if + 1000)^2$ *rather than just a magnitude. Filters with purely real gains are not causal.*

4.6 Survey

For each entity used in a configuration file, property names and values are described below. These entities are *type, first, last, sites* (mandatory) and *currentsite* (optional). Note that a grid survey is always horizontal, with height taken from the height of the first point, regardless of the value specified for the height of the last point.

4.6.1 Type

This can be *grid*, or *profile*. Note that with vertical profiles, the survey map view will plot all locations on top of each other, making it difficult to graphically select a particular site for analysis. Adding a slight tilt to the survey solves this problem.

4.6.2 First

The [x,y,z] coordinates of the first survey point.

4.6.3 Last

The [x,y,z] coordinates of the last survey point. In the current version, this z value must be the same as for the first point. Note that some target computations may insist on all survey points being at the same height.

4.6.4 Sites

A number (or 2-vector) giving the number of points (equally spaced) along the profile (or grid) survey.

4.6.5 Currentsite

The sitenumber to be initially used for location-dependent plots such as the receiver waveform.

4.7 Targets

4.7.1 Introduction

There are a large number of possible target types, some of which are realistic field targets, and others of which are useful for instrument calibration and testing. Detailed descriptions of the attributes are to be found in the code validation chapter below. Utemis is extensible to new targets by adding "plug-in" functions to handle target preparation and response calculation in accordance with Utemis interface specifications (described elsewhere). This means that target descriptions are not themselves part of the Utemis specification, since they are passed, as MATLAB structuure, without change or usage, through utemis to the plug-in functions, and can be anything the plug-in write desires. For those plug-ins which are available currently, the attributes are described in the chapter on particular targets.

Chapter 5

A Tutorial Example

5.1 Startup

A demonstration case is provided with UTemiS as an example. Get started as follows:

1. Copy the demonstration configuration files *demo.int*, *demo.svy*, *demo.tgt*, to the working directory you will use. You do not want to work with the original copies of these, since they may be overwritten by UTemis during use.

2. Start MATLAB, and set the MATLAB directory to your working directory.

3. Start UTemis by typing *utemis* at the MTALAB command line. (This will fail unless your MATLAB path includes the utemis code installation directory.)

4. Select *Run* and then the subitem Plot RX Signal to toggle auto-recalculation off (the check mark will disappear from this submenu item).

5. Load the demonstration instrument by selecting the menu item *Instrument*, and clicking on *load*. You will get a dialog box permitting you to select the file *demo.int*. Similarly load the demonstration survey and target configuration files by clicking on the *Survey* and *Target* menu items respectively.

In what follows, shorthand notation like *Run* ⇒ *Auto-recalculate* will be used to denote actions like the above involving a main menu selection followed by a submenu selection.

If at any point, you wish to stop, but later resume from the same point, use *File* ⇒ *Save As* to save a *session* file. You can then close *utemis* using *File* ⇒ *Exit* (or *File* ⇒ *Exit Closing* if you wish to close all associated figures besides the main *UTemiS* GUI). Reloading this session file later with *File* ⇒ *Load* will restore your session at the point you left it (*if* you are working in the same directory with the same version of *UTemiS*).

5.2 The Describe Menu

The simulation configuration can be examined at this time if desired. Among the possibilities are:

1. Select the *Describe* menu, and click on any of the *Instrument*, *Survey*, or *Target* subitems. This generates a message box with the entities and their attributes of the object being described.

2. Sub-sections of the instrument, such as *Waveform*, *Acquisition*, *Instrument Name* can also be "described" individually.

3. The instrument coil configuration and primary magnetic and vector potential fields can also be seen with the *Describe* menu subitems *Draw Instrument*, *Draw B Field* and *Draw A Field*, respectively.

Describe subitems with the same functionality are also available under the *Instrument*, *Survey*, or *Target* main menu items.

Note that describe message boxes for complex targets in particular may lie partly offscreen. If the "ok" button is obscured, all describe boxes can be closed using *Describe* ⇒ *Kill Describe Windows*. The same information can be seen more compactly using the *Edit* subitem under the *Instrument*, *Survey*, or *Target* main menu items, as we shall see below.

5.3 Plots Which Are Available Before Response Calculations

1. Click on the *View* menu, and select the *Plot Survey Map* subitem.You can see all the survey points as open circles (which may be so close together as to obscure each other. The three localized targets are shown as red diamonds. The current instrument site is shown as a green circle. The green circle can be moved to any other survey point by (left) clicking with the mouse on the desired point.

2. The *Survey Map* plot gives no depth information. *View* $\Rightarrow$ *Plot Survey 3D View* providesa three-dimensional view of the survey. To get better 3D information, detach this plot by selecting *View* $\Rightarrow$ *Detach Survey 3D View* to make a copy in a separate figure window, which will have the satndard MATLAB figure menu rather than the UTemiS menu. Click on the Rotation Tool Button on this detached figure. The mouse and left mouse button can now be used, in normal MATLAB fashion, to grad and rotate this figure in three dimensions. When finished with this detached figure, either close the detached figure explicitly, or choose *View* $\Rightarrow$ *Close Detached Figures.* (This will close all open Describe Boxes as well.)

3. Click on the *View* menu, and select the *Plot TX I Waveform* subitem. This displays the transmitter waveform, in amperes as a function of time. How many cycles are displayed depends on the value of the *plotcycles* attribute of the instrument. Note that the timing of the receiver channel averaging windows ("gates") is superimposed on this waveform (if not, toggle the *Overlay Gates* subitem under the *View* menu.) Selecting the *Plot TX dI/dt Waveform* subitem displayed the time-derivative of the transmitter current.

4. Examine the instrument receiver gain as a function of frequency by selecting *View* $\Rightarrow$ *Plot Gains.* You will get a message that only 4 plots can be shown simultaneously. Press OK on this message, and note that the Gains plot is not present. Select *View* $\Rightarrow$ *Plot Survey 3D View* to toggle off the *Survey 3D* Plot. The *Gain* plot should now be visible, but is not very interesting, since it shows the (unrealistic) constant gain right up to the Nyquist frequency associated with the

time sampling. Toggle this plot off by selecting *View* ⇒ *Plot Gains* again. (The receiver time gates can also be explicitly displayed in a plot of their own by selecting *View* ⇒ *Plot Gates*).

In what follows, instructions to close un-needed subplots in excess of four will not always be explicitly given.

5.4 Viewing Receiver Responses

1. Select *View* ⇒ *Plot RX Signal*. No receiver plot will be shown, because no receiver responses have been calculated yet. Select *Run* ⇒ *Calculate* to force such a calculation, or, more easily, click the large *Recalculate* button at the upper right; a plot of the receiver signal will appear. It is a time domain waveform, with superposed receiver gates (toggling *View* ⇒ *Overlay Gates* will make these disappear. For a frequency domain waveform, the receiver amplitudes for each frequency channel would be plotted instead,as a function of frequency, on a linear scale. The *View* ⇒ *Plot RX Spectrum* provides a log-log plot of response for either type of instrument.

2. On the *Survey Map* plot, click to move the "current survey point" around, and watch how the receiver signal changes (mainly in amplitude). To avoid the annoyance of having to press the *Recalculate* button every time, toggle *Run* ⇒ *Autorecalculate* on.

3. Close the *Transmitter dI/dt* plot to make room for a map of the receiver output over the entire survey region using *View* ⇒ *Plot Output Contour*. A two-lobed response is seen for The lower left target is a wire loop lying in a north-south vertical plane, so its response maximizes just to the east and just to the west of the actual target location, because this is where maximum flux coupling to the target is achieved. The upper left target is a penny lying horizontally, so its peak response lies directly over the target, as does that of the small sphere to the upper right. To calibrate the values, draw a colour bar using *View* ⇒ *Show Colour Bar* (this needs to be redrawn after recalculation).

4. These patterns may not be obvious. Click the *Recalculate* button several times, noting that the pattern changes somewhat each time. One

of the global targets here is a randomly irregular dispersive magnetic halfspace. The irregularity is controlled by two attributes in the target description in the target configuration file, *varyfraction* and *varylength*, here set equal to 0.5 and 0.3 respectively. This means a fractional variability of magnetic susceptibility of 50%, and a characteristic wavelength of 0.3 meters (30 centimeters). The random realization of this irregularity is chosen anew each time a recalculation button is requested.

5. Choose one of the other instrument outputs (from a different time gate) by selecting *View* ⇒ *Select Map Variable* and choosing $v(3)$ (this is the red gate output, which although earliest, is defined as gate 3 by its color; verify this by examining the information box that results from *Describe* ⇒ *Colour Order*, or by examining the time gates as described in the instrument description). Recalculate. The localized targets are much less visible because of the strong masking by the magnetic response of the soil during the transmitter on-time. Examine the range of mapped values with *Describe* ⇒ *Output Statistics* or *Describe* ⇒ *Map Statistics*.

6. Deselect the transmitter current plot by toggling *View* ⇒ *Plot TX I Waveform*, to make room for a profile plot selected by *View* ⇒ *Plot Output Profiles*. The profile looks odd because it is the linked-together response of the instrument as it would be seen traversing the entire survey grid one line at a time[1]. Note how much higher the gate 3 (red) response is than the others.

7. Choose the blue gate (output 1) again for mapping using *View* ⇒ *Select Map Variable*. Turn on custom profiling with *View* ⇒ *Custom Profiling*. Individual survey points are now visible on the map for reference. With the left mouse button, click on a starting position on the *Output* map, move the mouse to a finishing point, and release the mouse button. A profile of the output along this straight line will now be visible in the output profile subplot. Only the mapped output will be shown.

8. Using the right mouse button similarly, a curved profile can be drawn on the map (if your computer is not very fast, move the mouse slowly in order to get a sufficiently dense set of sampled points along the profile).

[1]This survey is a *grid* survey. For a *profile* survey, this plot would simply be the response measured along the defined profile.

9. Toggle on the instrument audio output using *View* ⇒ *Sound* (make sure your computer speakers are on). Draw another custom profile, straight or curved, through an anomaly or anomalies on the map, and release the mouse button. Listen.

5.5 Reporting and Exporting UTemis Data

1. Toggle on *Report* ⇒ *To Console*. Click *Report* ⇒ *Receiver Waveform*. Return to the MATLAB command console and note that the receiver waveform at the selected site has been printed for your inspection. It has probably scrolled off the top of your console window.

2. Now type *clear all* into the MATLAB console, in case you have leftover work there. A more useable form of this information can be obtained by toggling on *Report* ⇒ *To Workspace* followed by *Report* ⇒ *Receiver Waveform* as before. Return to the MATLAB command console and type the MATLAB command *whos*. MATLAB reveals two new variables in the MATLAB workspace: *RXWaveform*, a list of the receiver waveform voltage samples, and *Dt*, the sampling interval in seconds. You can use these, save these, or calculate with them in MATLAB, completely outside of UTemiS.

3. To illustrate reporting to a file, toggle on *Report* ⇒ *To File* and define the desired output file name with the resulting dialog box. Now, select *Report* ⇒ *Receiver Waveform* as before. Toggle off *Report* ⇒ *To File*. Outside of UTemiS and MATLAB, check for the existence of the file you named. If you open it, you will see that the saved data is written as a MATLAB-legal m-file. Running it as an m-file from MATLAB on some subsequent occasion will load the saved variables into the workspace.

5.6 Engaging in design: editting configuration files

The designing of instruments or surveys with UTemis involves changing their description and re-running the response calculation for targets of

interest. We illustrate that process here by modifying the target configuration file. *Remember to make sure you are not using the original copies of the configuration files, as they will be overwritten during this part of the tutorial.*

5.6.1 Turning targets on and off

Select *Targets* ⇒ *Edit*. Your default MATLAB file editor will open with the target configuration file, *demo.tgt*, in front of you. It describes a number of targets, some of which have been commented out. This file describes some targets explicitly (*e.g.* the ring target), but uses *include* statements to include other files in which all the statements describing a particular target have been grouped together. All the descriptions can be included explicitly in *demo.tgt*, but this would be less clearly organized. Note that a file *penny.tgt* is included on or about line 19 of *demo.tgt*. Using the MATLAB editor, separately open the file *penny.tgt*. You will see that the penny is actually described as the sum of three more basic targets, of type *singleaxis*. The penny has one response to magnetic fields perpendicular to its plane, and a different response to magnetic fields in each of the two orthogonal directions that lie in its plane. The penny is oriented vertically in the y-z plane (the axis [1,0,0] is the one with a large response). The response parameters for each of these axes have been obtained experimentally, which is the only really safe way of characterizing objects whose physical properties are not well known[2]. In fact, these descriptions are slightly modified versions of the output files from the program utemispolefit, described in a later chapter. There is no reason why you can't put theoretical responses here, however, as long as they have the proper configuration file format.

Note that the *location* parameter for each *singleaxis* target is [0,0,0]. The actual location of the penny in the simulation would therefore be at the origin if it were not for the *apply offset* statement just before the *include penny.tgt* statement in the "master" target configuration file *demo.tgt*. This statement has the effect of offsetting all localized targets

[2]land mine manufacturers do not quality control for consistent magnetic permeability or conductivity in their batches of metal parts, since these properties are irrelevant to their function

subsequently described in *demo.tgt*, until another apply statement is encountered (which will cancel the previous *apply* statement). To move the penny from [0.25,0.25,-.2] to a greater depth (50 cm), edit the *apply offset* statement to become *apply offset=[0.25,0.25,-0.50]*. Save the file *demo.tgt*. Click the *recalculate* button in the UTemis GUI window. You will get a warning that the target configuration file on disk has been modified, and asked if you want to reload. Click yes. Note that configuration file changes are not imported immediately into UTemis, only saved to disk. Note also that *included* configuration files, such as *penny.tgt*, when modified and saved, will produce no such warning; it is only the "master" configuration file whose timestamp is checked when recalculating. If you make changes to configuration files which seem to have no influence on the result, check that you have actually reloaded all the modified information into UTemis. To be safe, make a habit of always explicitly using the *Reload* buttons after editing configuration files.

After the recalculation has completed, you will no longer see the characteristic east-west bilobate response of the penny under [0.25,0.25]; it is now too deep to be seen in the presence of the variable magnetic Bosnian soil. Edit *demo.tgt* by turning off the Bosnian soil by prepending the MATLAB comment marker (a percent sign) to the line. Recalculate. The penny is visible again, but at a much lower amplitude, as shown by the color bar invoked with *View* $\Rightarrow$ *Show Colorbar*.

Turn on the last target in *demo.tgt* by removing the percent sign in front of *include brine.tgt*. This is a highly porous earth saturated with super-saturated brine (salt water). Save *demo.tgt*. Recalculate. You will see at first almost no change, because the decay time of the step response of brine (with a conductivity of 30 s/m) is only about 2.5 microseconds for coils of this size (about 10 cm radius). To see the brine eddy current decay, detach the receiver signal plot using *View* $\Rightarrow$ *Detach Rx Signal*. On the detached figure, use the MATLAB zoom tool to magnify the decay between about 100 and 120 microseconds.

Alternatively, you can use the context menu available for each plot by right-clicking on the plot background. Choose the *Y Zoom* sub-item to magnify.

You will notice some ringing in the response caused by the (unrealistic)

uniform gain all the way up to the Nyquist cutoff frequency. To simulate a more realistic instrument design, open the instrument file with *Instrument* ⇒ *Edit*. Replace the uniform acquisition gain of 1000 with the MATLAB formula 1/(1+(i*f/1e6))^4 (*without embedded spaces*). Reload *demo.int*. Replace the survey map view with the receiver gains view, and recalculate. As above, detach the receiver response and magnify. The ringing is greatly reduced. The gains plot shows explicitly how the gain (in-phase, quadrature and magnitude) depends on frequency.

Chapter 6

Guide to UTEMIS Code Structure

6.1 Introduction

The first part of this Chapter is devoted to the theoretical representations of the various parts of the simulation calculation. The second part is a description of the actual code structure.

6.2 Theoretical representation of the instrument

The transmitter provides a current $i_T(t)$ to the source sensor (usually a coil, but possibly a grounded pair of electrodes), and the receiver obtains a voltage $v_R(t)$ from a receiving sensor (again, usually a coil, but possibly a grounded pair of electrodes). The most general relation between $i_T(t)$ and $v_R(t)$ for a linear system (*i.e.* the earth and any embedded targets, if the fields are not too high) is

$$v_R(t) = \int_{-\infty}^{\infty} z(\tau)\ i_T(t-\tau)\ d\tau \tag{6.1}$$

where the impulse response z has the dimensions of an impedance. In the frequency domain, this relation becomes

$$V_R(\omega) = Z(\omega)\ I_T(\omega) \tag{6.2}$$

where the complex function Z is called the transimpedance; it could equally well be called the mutual impedance.

For many situations, it is possible to calculate the response $Z(\omega)$ of the Earth with adequate accuracy as the sum of responses of each of a number of separate components $Z_k(\omega)$ from separate targets. For example, for relatively resistive and non-magnetic soils, the response of a point target such as a mine detonator, and the Earth in which it is embedded can be calculated separately, and then added to give the total response $Z(\omega) = \Sigma_k \; Z_k(\omega)$.

The central computational engine (CCE) in UTemis therefore has the task of computing the transimpedance of each target for the particular instrument and summing these contributions. However, this is not the entire task. Real electromagnetic induction (EMI) detectors do not output transimpedance to the operator, but rather amplitudes of some derived quantity, such as (for frequency domain systems) the magnitude of the transimpedance, or some ratio of transimpedances at different frequencies, or (for time domain systems) the mean amplitude of the received voltage within a specific time gate after the onset of the transmitter pulse.

For frequency domain systems, the CCE's job is simple: to compute the (complex) transimpedance at each of the operating frequencies of the instrument. This approach could be used for time domain systems as well, but time-domain systems are wideband, and computation of Z at many closely spaced frequencies over a wide frequency range is necessary to then synthesize, by Fourier transformation, the time-domain receiver voltage from which a single time-gate amplitude might be derived. This approach is inefficient.

Typically, it is not the entire receiver voltage waveform that is analysed, but a number of filtered or integrated sections of it as detected "channel voltages" c_n (V_C in West and Bailey[3], 2006), weighted integrals of the form

$$c_n \;\; = \;\; \int_0^T w_n(t) V_R(t)\, dt$$

Often the weight is simply unity between a start and a stop time.

To what type of voltage responses will equation (6.3) be applied? Real EMI targets have responses which can be represented much more simply than as a general function of frequency. Specifically, extending the results noted by West and Bailey[3], 2006, and Bailey and West[1], 2006, one can write the step response $S(t)$ of the Earth, in general,

$$s(t) \cong \sum_{k=0}^{K} N_{k+1} \; \delta^{(k)}(t) + N_0 H(t) + \sum_{m=1}^{M} \; D_m \, H(t) \, e^{-p_m t} \qquad (6.3)$$

where $\delta^{(k)}(t)$ is the k'th derivative of a Dirac delta function.

The fourier transform[1] of this is

$$S(\omega) \cong \sum_{k=0}^{K} N_{k+1} \, (i\omega)^k + \frac{N_0}{j\omega} + \sum_{m=1}^{M} \frac{D_m}{j\omega + p_m} \tag{6.8}$$

The impulse response $Z(\omega)$ is therefore obtained by multiplying this by $j\omega$:

$$Z(\omega) \cong \sum_{k=0}^{K} N_{k+1} \, (j\omega)^{k+1} + N_0 + \sum_{m=1}^{M} \frac{j\omega D_m}{j\omega + p_m} \tag{6.9}$$

or (the working equation for defining the frequency-domain transimpedance representation here)

$$Z(\omega) \cong \sum_{k=0}^{K} N_k \, (j\omega)^k + \sum_{m=1}^{M} \frac{j\omega D_m}{j\omega + p_m} \tag{6.10}$$

The time-domain transimpedance representation is therefore

$$z(t) \cong \sum_{k=0}^{K} N_k \, \delta^{(k)}(t) + \sum_{m=1}^{M} D_m \delta(t) + \sum_{m=1}^{M} D_m H(t) \, e^{-p_m t} \tag{6.11}$$

In general, relatively small numbers K and M of terms are required for an adequate representation.

---

[1]The Fourier transform convention used here is

$$Y(\omega) = \int_{-\infty}^{+\infty} y(t) \, e^{-j\omega t} \, dt \tag{6.4}$$

$$y(t) = \frac{1}{2\pi} \int_{-\infty}^{+\infty} Y(\omega) \, e^{+j\omega t} \, d\omega \tag{6.5}$$

The MATLAB equivalent commands for a time series of length N sampled every dt are

$$Y = fft(y) * dt \tag{6.6}$$

$$y = N * ifft(Y) * df \tag{6.7}$$

where $df = 1/(N * dt)$

6.2.1 Special cases

Inductively coupled systems

For a coil-coil system with purely inductive coupling, like most mine detectors, the step response simplifies to

$$s(t) \cong N_1\ \delta(t) + \sum_{m=1}^{M} D_m\, H(t)\, e^{-p_m t} \tag{6.12}$$

(there is no long-term response). This corresponds to a transimpedance

$$Z(\omega) \cong j\omega N_1 + \sum_{m=1}^{M} \frac{j\omega D_m}{j\omega + p_m} \tag{6.13}$$

For such purely inductively coupled systems, it is common to discuss the Earth response in terms of the *mutual inductance* $M(\omega)$ where $Z(\omega) = j\omega M(\omega)$, so that for the coil-coil systems,

$$M(\omega) \cong N_1 + \sum_{m=1}^{M} \frac{D_m}{j\omega + p_m} \tag{6.14}$$

As a further simplification of this example, consider a coil-coil system and a target in free space consisting of a ring of thin wire, of inductance L and resistance R, only one exponentially decaying mode with time constant $\tau = L/R = p_1^{-1}$ is important, so that

$$Z(\omega) \cong\ j\omega N_1 + \frac{j\omega D_1}{j\omega + p_1} \tag{6.15}$$

or

$$M(\omega) \cong\ N_1 + \frac{D_1}{j\omega + p_1} \tag{6.16}$$

Electrically coupled systems

A rather different example is offered by resistivity sounding, in which electric bipoles are used for the transmitter and receiver sensors. Here, there is a long term (DC) response, but no sharp inductive transient at the beginning, and the step response looks like

$$s(t) \cong N_0 H(t) + \sum_{m=1}^{M} D_m\, H(t)\, e^{-p_m t} \tag{6.17}$$

so that the general case (6.10)

$$Z(\omega) \cong \sum_{k=0}^{K} N_k \, (j\omega)^k + \sum_{m=1}^{M} \frac{j\omega D_m}{j\omega + p_m} \tag{6.18}$$

becomes

$$Z(\omega) \cong N_0 + \sum_{m=1}^{M} \frac{j\omega D_m}{j\omega + p_m} \tag{6.19}$$

Network connections

For the singular case[2] where the target is just a impedance (single or network) connected between both transmitter and receiver, the response is just the transimpedance $Z(\omega) = N_0$. For example, a parallel resistor-capacitor as the target yields a step response to a current I_0 of

$$V(t) = I_0 R(1 - e^{-t/RC}) \tag{6.20}$$

and a corresponding transimpedance (which is here the same as the impedance)

$$Z(\omega) = \frac{1}{\frac{1}{R} + j\omega C} = R - \frac{j\omega R}{j\omega + \frac{1}{RC}} \tag{6.21}$$

which, in the canonical form (6.10), requires $N_0 = R$, $D_1 = R$, and $p_1 = 1/(RC)$.

6.2.2 Generalization to resonant targets

The above formulation will handle resonant (non-diffusive) responses as well if we allow the poles p_m to be complex, as complex conjugate pairs. Thus, (6.10) can be re-written as

$$Z(\omega) \cong \sum_{k=0}^{K} N_k \, (j\omega)^k + \sum_{m=1}^{M} \frac{1}{2} D_m \left(\frac{j\omega}{j\omega + p_m} + \frac{j\omega}{j\omega + p_m^*} \right) \tag{6.22}$$

This evaluates to (6.10) if the poles p_m are real, but handles the more general resonant case also.

[2]Perhaps useful only in a lab calibration of an instrument with sensors removed.

An example

As an example, useful for calibrating the code, consider as a target a parallel RLC circuit connected directly across transmitter and receiver terminals (a generalization of the RC case above). The (trans)impedance of this is

$$Z(\omega) = \frac{1}{j\omega C + \frac{1}{R+j\omega L}} \tag{6.23}$$

$$= \frac{1}{LC}\left(\frac{R+j\omega L}{-\omega^2 + j\omega/\tau + \omega_0^2}\right) \tag{6.24}$$

where $\tau = L/R$ and $\omega_0^2 = 1/\sqrt{LC}$. This can be expanded in partial fractions as

$$Z(\omega) = \frac{a}{(j\omega + p_1)} + \frac{b}{(j\omega + p_2)} \tag{6.25}$$

where the roots p_1 and p_2 of the denominator are given by

$$p_{1/2} = \frac{1}{2\tau}\left(1 \pm j\sqrt{4\omega_0^2\tau^2 - 1}\right) \tag{6.26}$$

and a and b must satisfy

$$a + b = \frac{R}{LC} \tag{6.27}$$

$$p_2 a + p_1 b = \frac{1}{C} \tag{6.28}$$

or

$$a = \frac{1}{C}\left(\frac{R - Lp_1}{p_2 - p_1}\right) \tag{6.29}$$

$$b = \frac{1}{C} - a \tag{6.30}$$

Thus, the representation of this in the canonical form (6.10), requires $D_1 = 2a$, $D_2 = 2b$, and p_1 and p_2 as given by (6.26).

6.2.3 Computing channel responses

As noted, it is specific channel responses of the form (6.3) that are required. Equations (6.1) and (6.3) together give

$$c_n = \int_0^T w(t) \int_{-\infty}^{\infty} z(\tau)\, i_T(t-\tau)\, d\tau\, dt \tag{6.31}$$

Using the convolution theorem converts this to

$$c_n = \frac{1}{2\pi} \int_0^T \; w(t) \; \int_{-\infty}^{\infty} \; Z(\omega) \; I_T(\omega) \; e^{j\omega t} \; d\omega \; dt \tag{6.32}$$

Because $w(t)$ is zero outside the range $[0, T]$, extending the time range of the integration changes nothing, and this can be written as

$$c_n = \frac{1}{2\pi} \int_{-\infty}^{\infty} \; w(t) \; \int_{-\infty}^{\infty} \; Z(\omega) \; I_T(\omega) \; e^{j\omega t} \; d\omega \; dt \tag{6.33}$$

Performing the time integral yields

$$c_n = \frac{1}{2\pi} \; \int_{-\infty}^{\infty} \; W^*(\omega) \; Z(\omega) \; I_T(\omega) \; d\omega \tag{6.34}$$

where * denotes complex conjugate.

If we now use the special form (6.10) for $Z(\omega)$, this becomes

$$c_n = \sum_{k=0}^{K} \; C_{nk}^{(Z)} N_k + \sum_{m=1}^{M} \; C_{nm}^{(P)} D_m \tag{6.35}$$

where the coupling coefficients for the zeros and poles of the transimpedance are

$$C_{nk}^{(Z)} = \frac{1}{2\pi} \; \int_{-\infty}^{\infty} \; W^*(\omega) \; I_T(\omega) \; (j\omega)^k \; d\omega \tag{6.36}$$

and

$$C_{nk}^{(P)} = \frac{1}{2\pi} \; \int_{-\infty}^{\infty} \; W^*(\omega) \; I_T(\omega) \; \frac{j\omega}{j\omega + p_m} \; d\omega \tag{6.37}$$

For some targets (such as multiply coupled inductive loops), the integrand in (6.36) could apparently diverge, leading to evaluation difficulties. However, if $w(t)$ and $i_T(t)$ are bounded, the product $W^*(\omega) \; I_T(\omega)$ must fall off at least as fast as ω^{-2}, so that all the particular cases in section (6.2.1) must converge.

The time domain computation can thus be simplified as follows: for each target, which will have specified imaginary excitation frequencies p_m, using (6.36) and (6.37), compute the transmitter-receiver channel coupling coefficients in advance. Then, compute for each instrument location, the transimpedance amplitudes N_k and D_m, and make them this target's contributions to the total transimpedance for that location. Further efficiency can be obtained by using common p_m's for all targets if the physics of all the targets can be represented adequately in this way, but the bulk of the efficiency has already been obtained.

6.3 The central algorithm

The central response calculation is in a function m-file called *zgo* , previously called *calculate*. Its formal input argument is *handles* from which the desired survey locations (*xyz*), and the instrument and target properties are extracted.

After some initializations, *zgo* runs an outer loop over the *nTargets* targets described in *handles.work.targets.target*, computing the response contribution of each target and adding it to each output channel in the array *channels(nLocations,nChannels)*. Each target is either a single target as described in the target configuration file, or a sub-target for composite targets (such as the three sub-targets representing a point target with different frequency dependencies along each of three principal axes).

Once the channel voltages c_n have been calculated, they are converted to output signals by whatever algorithms the user has specified as legal MATLAB code[3] in the *output* specifier in the instrument configuration file. It is intended that all outputs be real, so that any imaginary part of the output is dropped before storage.

6.4 Localized targets for coil-coil systems

Consider a small localized target. Let the magnetic field induced by a unit current in the transmitter coil, at the location of the target, be $\hat{\mathbf{H}}^t$. The induced magnetic moment $\mathbf{m}$ in the target can be described by

$$m_i(\omega) = \sum_{j=1}^{3} S_{ij}(\omega)\, \hat{H}_j^t(\omega) I_t(\omega) \tag{6.38}$$

where $\mathbf{S}$ is the *magnetance* tensor of the target (typically the volume of the target times the geometric demagnetizing factor times the susceptibility of the target material). This moment induces a voltage in the receiver coil. Reciprocity tells us that the receiver voltage per unit rate of change of target magnetic moment is equal to the component, in the direction of that moment, of the magnetic induction $\hat{\mathbf{B}}^r$ at the target that would be generated by a unit

[3]With all embedded blank spaces removed.

current in the receiver coil. That is, the receiver voltage is

$$V_r(\omega) = j\omega(\hat{\mathbf{B}}^r \cdot \mathbf{m}) = \sum_{i=1}^{3} \sum_{j=1}^{3} S_{ij}(\omega)\, \hat{H}_j^t(\omega) \hat{B}_i^r(\omega)\, I_t(\omega) \tag{6.39}$$

or, more succinctly

$$V = j\omega I \sum_{i=1}^{3} \sum_{j=1}^{3} \hat{H}_i^t S_{ij}\, \hat{B}_j^r \tag{6.40}$$

Note that (6.40) gives only that portion of the receiver coil voltage resulting from the presence of the target, and includes neither the direct coil-coil coupling or the response of any host medium other than free space.

Thus the frequency-dependent transimpedance is

$$Z(\omega) = j\omega \sum_{i=1}^{3} \sum_{j=1}^{3} \hat{H}_i S_{ij}(\omega)\, \hat{B}_j \tag{6.41}$$

The description of local targets therefore involves computing the tensor relationship of the vector magnetic moment to an inducing field, as $S_{ij}(\omega)$, and finding a representation of $i\omega S_{ij}(\omega)$ of the same form as that for the transimpedance in (6.10), namely (for each element of the magnetance tensor)

$$S(\omega) \cong \sum_{k=0}^{K} N_k^S\, (j\omega)^k + \sum_{m=1}^{M} \frac{j\omega D_m^S}{j\omega + p_m} \tag{6.42}$$

6.5 Composing Responses

Sometimes the net response of a target is the product of two responses, for example of the host-target coupling and the taget response. This obliges us to clarify the procedure for the product of two responses, each described by an NPD response parameters of the representation

$$R(\omega) = \sum_{k=0}^{K} N_k\, (j\omega)^k + \sum_{m=1}^{M} \frac{j\omega D_m}{j\omega + P_m} \tag{6.43}$$

Let one factor's representation be described by (6.43), and the other's by

$$r(\omega) = \sum_{k=0}^{K} n_k\, (j\omega)^k + \sum_{m=1}^{M} \frac{j\omega d_m}{j\omega + p_m} \tag{6.44}$$

What is the joint or composite NPD representation of

$$r(\omega)R(\omega) = \left(\sum_{k=0}^{K} n_k\ (j\omega)^k + \sum_{m=1}^{M} \frac{j\omega d_m}{j\omega + p_m}\right)\left(\sum_{i=0}^{K} N_i\ (j\omega)^i + \sum_{t=1}^{M} \frac{j\omega D_t}{j\omega + P_t}\right) \tag{6.45}$$

in the form

$$J(\omega) = \sum_{k=0}^{K} c_k\ (j\omega)^k + \sum_{m=1}^{M} \frac{j\omega a_m}{j\omega + s_m} \tag{6.46}$$

Consider the product terms like

$$d_m D_t\, \Pi_{mt} = d_m D_t\, \frac{j\omega}{j\omega + p_m}\, \frac{j\omega}{j\omega + P_t} \tag{6.47}$$

Aiming at a partial fraction expansion, these can be written as

$$\Pi_{mt} = \frac{\alpha + j\omega a}{j\omega + p_m} + \frac{\beta + j\omega b}{j\omega + P_t} = \frac{(\alpha + j\omega a)(j\omega + P_t) + (\beta + j\omega b)(j\omega + p_m)}{(j\omega + p_m)(j\omega + P_t)} \tag{6.48}$$

$$= \frac{\alpha P_t + a(j\omega)^2 + j\omega(aP_t + \alpha) + \beta p_m + b(j\omega)^2 + j\omega(bp_m + \beta)}{(j\omega + p_m)(j\omega + P_t)} \tag{6.49}$$

from which

$$\begin{aligned} 1 &= a + b \\ 0 &= aP_t + \alpha + bp_m + \beta \\ 0 &= \alpha P_t + \beta p_m \end{aligned} \tag{6.50}$$

Choose $\alpha = \beta = 0$. Then (6.50) become

$$1 = a + b \tag{6.51}$$

$$0 = aP_t + bp_m \tag{6.52}$$

or

$$a = \frac{-p_m}{P_t - p_m} \tag{6.53}$$

$$b = \frac{P_t}{P_t - p_m} \tag{6.54}$$

Alternatively, we could have factored (6.47) as

$$c+\frac{j\omega a}{j\omega+p_m}+\frac{j\omega b}{j\omega+P_t}=c(j\omega+p_m)(j\omega+P_t)+\frac{j\omega a(j\omega+P_t)+j\omega b(j\omega+p_m)}{(j\omega+p_m)(j\omega+P_t)} \tag{6.55}$$

or

$$c((j\omega)^2+j\omega(p_m+P_t)+p_mP_t)+\frac{(a+b)(j\omega)^2+j\omega(aP_t+bP_m)}{(j\omega+p_m)(j\omega+P_t)} \tag{6.56}$$

which yields the same result as before.

The contribution of Π_{mt} to the expansion is therefore nothing to N, and $\Delta d'_m = d_m D_t\, a = d_m D_t\, p_m/(p_m - P_t)$ to the pole at p_m and $\Delta D'_t = d_m D_t\, b = d_m D_t\, P_t/(P_t - p_m)$ to the pole at P_t.

Now consider product terms like

$$d_m N_i \pi_{mj} = d_m N_i \frac{(j\omega)^{i+1}}{j\omega+p_m} \tag{6.57}$$

We can write

$$\pi_{mj} = \frac{(j\omega)^{i+1}}{j\omega+p_m} = \frac{\rho^{i+1}}{1-\rho}\,{p_m}^i \tag{6.58}$$

where $\rho \equiv -j\omega/p_m$. Using the expression for the sum of an infinite geometric progression

$$\pi_{mj} = {p_m}^i\ \left(\frac{1}{1-\rho}-1-\rho-\rho^2-\rho^3...-\rho^i\right) \tag{6.59}$$

Recasting in terms of $j\omega$ yields

$$\pi_{mj} = {p_m}^i\ \left(\frac{1}{1+j\omega/p_m}-1-\left(\frac{-j\omega}{p_m}\right)-\left(\frac{-j\omega}{p_m}\right)^2-\left(\frac{-j\omega}{p_m}\right)^3...-\left(\frac{-j\omega}{p_m}\right)^i\right) \tag{6.60}$$

Chapter 7

Particular Targets and Code Validation

7.1 Introduction

In this chapter are described test cases used to validate the various capabilities of the UTemis code. The tests are grouped into three categories: those which test only the UTemis signal processing code, assuming that the transimpedance has been calculated correctly (easy to achieve with a simple target like a resistor connected between the transmitter terminals); those which test a number of important transimpedance calculations such as free space, a magnetic half-space, and a conductive half-space; and those which test the UTemis code handling of the instrument coupling to local targets whose magnetance is provided. In most cases, very simple waveforms are used (particularly the triangle, which drives constant inducing EMFs in targets).

7.2 Instrument and Signal Processing Code

This code tested here is contained within the main program utemis.m and the calculation driver zgo.m. The test targets are not real earth targets, but rather resistors or impedances connected directly across the transmitter output terminals . The receiver terminals are also connected directly across the same impedance, so that the transimpedance sensed by the instrument is that of the actual test impedance. The source and sensor type which describes this direct connection is the *bipole* source, also used for electrical

resistivity surveys.

7.2.1 Resistor Target #1

This tests simple averaging windows and the associated channel voltage calculations, the computation of the receiver waveform, and the gain calibration. The applied transmitter current waveform is a *bipolar* waveform, with amplitude 1A (2A peak to peak). Here a test target impedance of 10 ohms (resistive) is used, so that the receiver waveform is a direct copy of the transmitter waveform, but with amplitude 20V (since the receiver gain is 2).

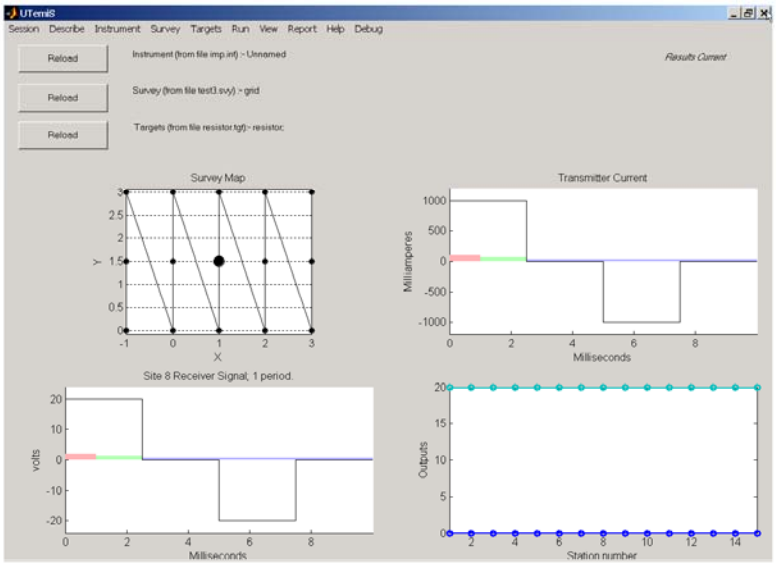

Figure 7.1: Screenshot for test case *Resistor1*.

Three averaging gates are defined, the first over the entire period, the second covering the first quarter period, and the third a short segment at the start of the period. These should yield 0V, +20V and +20V respectively as channel voltages. The configuration files are given below; the results are location-independent, but the survey file has more than one site just to exercise the plotting code.

Instrument file *imp.int*:

```
source       type=electrodes length=3  location=[0,0,0]  weighting=1
```

```
sensor       type=electrodes length=1  location=[0,0,0]  weighting=1
waveform     shape=bipolar period=.01 current=1 plotcycles=1
acquisition  method=Gates  gain=2 noise=0.0 ...
  windows=[0,0.01;0,0.0025;0,0.001] output
algorithm='[v(1),v(2),v(3),abs(v(3))]'
```

Target file *resistor1.tgt*:

```
target  name=calib type=resistor resistance=10
```

Survey file *test3.svy*:

```
survey      type=grid first=[-1,0,1] last=[3,3,1] sites=[5, 3]
```

7.2.2 Parallel Resistor-Capacitor

Target #2 This is identical to the resistor test case above, except that a 10 microfarad capacitor is placed across the resistor. It also tests simple averaging windows and the associated channel voltage calculations, the computation of the receiver waveform, and the gain calibration, but with an AC response as well as a DC response. The applied transmitter current waveform is a *bipolar* waveform, with amplitude 1A (2A peak to peak). Here a test target impedance of 10 ohms (resistive) in parallel with 10 microfarads is used, so that the receiver waveform has a transient decay at each edge tailing off to the pure resistor test case described above. The transient decay of the voltage after each current edge of size I_0 is the step response

$$V(t) = I_0 R(1 - e^{-t/RC}) \tag{7.1}$$

for which, in equation (6.10), implies $N_0 = R$, $D_1 = -R$, and $p_1 = (RC)^{-1}$.

The target configuration file is

```
target  name=RC_calib type=rc resistance=10 capacitance=0.00001
```

7.2.3 Custom waveforms, windows, and gains

In this test case, a R = 10 Ω resistor target is used, and a transmitter square wave (switching between 0 and +1 amp) with period $T = 0.01$ seconds. The instrument gain g is set to 1 at the third harmonic of the transmitter and zero at all other frequencies. The windows are non-zero over (1) the

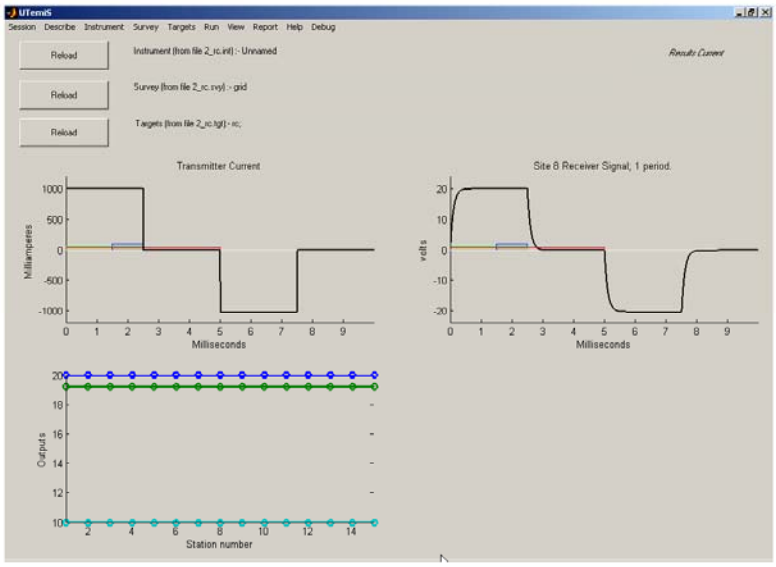

Figure 7.2: Screenshot for test case *rc*.

entire waveform (value $W = 100$) and (2) the first half of the waveform (value $W = 200$). However, the transmit waveform, the gains, and the windows are all read as custom time series from files generated by the script *customseriestest.m*.

The receiver waveform is pure third harmonic, with an amplitude of $2gR/(3\pi) = 2.12$ volts. The gate outputs are 0 and $2TWgR/(9\pi^2) = 0.450$. Note that the fractional error in this calculation are of order $1/n$, where n is the timeseries length as specified in *customseriestest.m*.

7.3 Global and host targets

Global targets are those where the support routines TPtargetname.m and TZtargetname.m handle the entire transimpedance calculation. The main UTemis code simply utilizes the result.

7.3.1 Free space

The free space target simply computes the direct coupling between transmitter and receiver in the absence of any material. For coil-coil systems, the

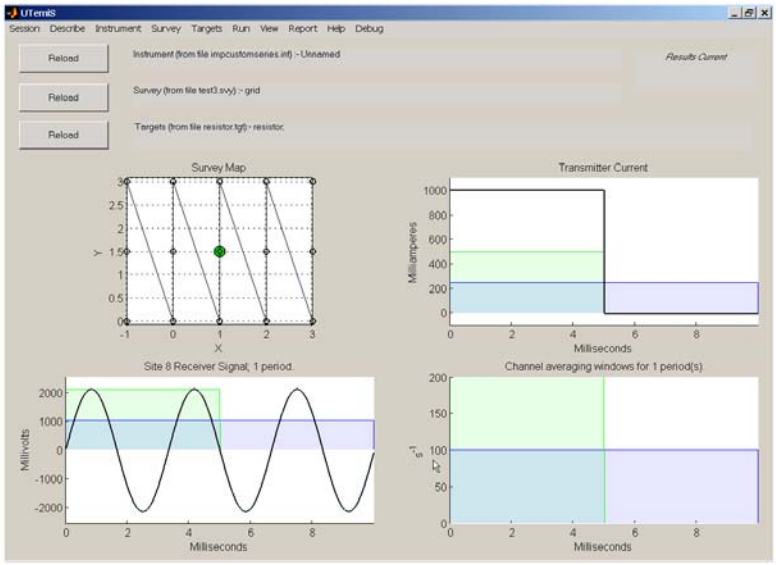

Figure 7.3: Screenshot for *customseries* test case.

transimpedance is simply $j\omega$ times the mutual inductance of the coils. As a simple test case, consider the mutual inductance of a large (single turn) loop of radius a and a small distant (single turn) coaxial loop of radius b at large distance $z \gg a \gg b$. The mutual inductance is

$$M = \frac{\pi\mu_0}{2}\frac{a^2b^2}{(a^2+z^2)^{3/2}} \tag{7.2}$$

For a coil-coil instrument described by the configuration file

```
information  name=freespaceTestInstrument
source type=coil radius=0.1   location=[0,0,0]  pole=[0,0,1] turns=1
sensor type=coil radius=0.01  location=[0,0,10]  pole=[0,0,1] turns=1
waveform     shape=triangle period=.01 current=1 plotcycles=1
acquisition  method=Gates  gain=1 noise=0.0 windows=[0,0.005;0.005,0.01]
output algorithm='[v(1),v(2)]'
```

the mutual impedance is $1.9736 \cdot 10^{-15}$ henries. Since $\dot{I}$ for this triangular waveform is 400 amperes/second, the expected voltage is $7.8945 \cdot 10^{-13}$ volts, as shown in Fig. (7.3.1).

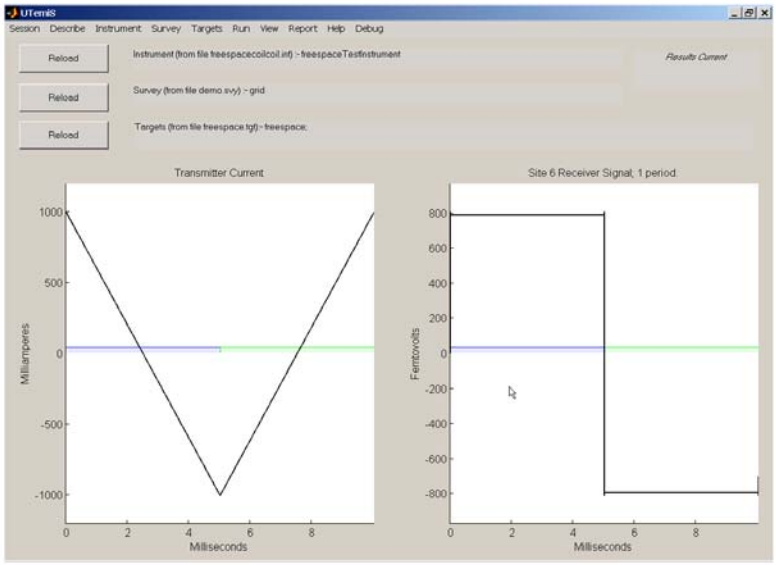

Figure 7.4: Screenshot for test case *Freespace*.

7.3.2 Uniform magnetic half-space

This response is based on an image solution [?]. If a source magnetic dipole is in free space a distance z above the (horizontal) surface of a magnetic half-space, the secondary fields of the magnetic half-space, as seen above the surface, are the same as those generated by an image dipole a distance z below the surface, whose horizontal components are reversed. This image has a strength α of the source strength. For observation points below the surface, the fields are those of the source attenuated by a factor β. These factors are given by

$$\alpha = \frac{\mu - \mu_0}{\mu + \mu_0} \tag{7.3}$$

and

$$\beta = \frac{2\mu_0}{\mu + \mu_0}; \tag{7.4}$$

where μ and μ_0 are the permeabilities of the magnetic half-space and free space respectively. The code to compute this response merely repeats the free-space target code, but with an added second source coil below the surface.

7.3.3 Conductive half-space

The type name for a conductive half-space is *conductivehalfspace* No zero conductivities are allowed. A sample configuration file is shown here:

```
target  name=halfspaceTest type=conductivehalfspace ...
 conductivity=0.01 scope=global
```

For a layered earth, the appropriate syntax would be:

```
target  name=halfspaceTest type=conductivehalfspace ...
 sigmas=[3,0.01] topdepths=[0,0.3] scope=global
```

Coaxial coil system

Following Ryu *et al* (1970), the tangential electric field $E_\phi(r,z)$ at height z of a circular coil of radius a at a height h above a layered Earth with wavenumber dependent reflection coefficient $R(\lambda)$ is the first order Hankel transform of

$$E_\phi(\lambda,z) = -\frac{j\omega\mu_0 a I(\omega)}{2}\, J_1(\lambda a)\frac{\lambda}{u_0}\left[\, e^{-u_0|z-h|} + R(\omega,\lambda)e^{-u_0(h+z)}\right] \qquad (7.5)$$

or

$$E_\phi(r,z) = -\frac{j\omega\mu_0 a I(\omega)}{2}\int_0^\infty J_1(\lambda r)\, J_1(\lambda a)\frac{\lambda}{u_0}\left[\, e^{-u_0|z-h|} + R(\omega,\lambda)e^{-u_0(h+z)}\right] d\lambda \qquad (7.6)$$

where r is the distance from the (vertical) coil axis, and $u_0^2 = \lambda^2 - \omega^2\mu_0\epsilon_0$. Neglecting displacement currents, which we will do, is equivalent to setting $u_0 = \lambda$.

A recursion approach is used to calculate the reflection coefficient R_0. Assume the Earth below the surface at $z = 0$ to have N layers (of which the basal layer $n = N$ has infinite thickness) with thicknesses d_n and physical properties σ_n, μ_n, and ϵ_n , and let

$$Y_n \equiv \frac{u_n}{j\omega\mu_n} \qquad (7.7)$$

and $\hat{Y}_n$ be the intrinsic and upper surface impedances of the n'th layer, where $u_n^2 = \lambda^2 - \gamma_n^2$, and $\gamma_n^2 = \omega^2\mu_n\epsilon_n - j\omega\mu_n\sigma_n$. For the basal layer,

$$\hat{Y}_N = Y_N = \frac{u_N}{j\omega\mu_N} \qquad (7.8)$$

Beginning with this, recursively calculate

$$\hat{Y}_n = Y_n \frac{1 - R_n e^{-2u_n d_n}}{1 - R_n e^{-2u_n d_n}} \tag{7.9}$$

where

$$R_n = \frac{Y_n - \hat{Y}_{n+1}}{Y_n + \hat{Y}_{n+1}} \tag{7.10}$$

is the reflection coefficient at the top of the $n+1$'th layer.

Care needs to be taken with the numerical evaluation using a finite sampling in λ at interval $\Delta\lambda$. For evaluation points high above or below the source coil, the exponential factor attenuates so fast that the entire significant part of the integral resides between the first two sampling points at $\lambda = 0$ and $\lambda = \Delta\lambda$. Similarly, if the height is zero, the integrand decays slowly, and may not be zero at the maximum sampled $\lambda = \lambda_M$. It is useful to separate the integrand into a part that handles these situations semi-analytically and a numerically better-behaved remainder that is tractable. As a function of λ, R varies from a complex constant (the magnetotelluric limit, -1 for a perfect conductor) to 0 as λ goes from 0 to infinity. The transition from one limit to the other occurs in a range of λ which we attempt to sample well in the numerical evaluation. It is therefore reasonable to represent R as

$$R(\lambda) = R_R(\lambda) + G(\lambda) \tag{7.11}$$

where $G(\lambda)$ is an analytic function chosen to match both the value of $R(\lambda)$ at $\lambda = 0$ and to decay towards zero as λ increases. A suitable G is therefore

$$G(\lambda) = -R|_{\lambda=0}\ e^{-\lambda s} \tag{7.12}$$

where s is a real constant (real because of the limitations of the subsequently required elliptic integral calculations below) best chosen to approximate the effective skin-depth[1] in the layered Earth. Substitution of equation (7.11) into (neglecting displacement currents) (7.6) yields

$$E_\phi(r,z) = -\frac{j\omega\mu_0 a I(\omega)}{2}\,\Gamma(r,z) - \tag{7.13}$$

$$\frac{j\omega\mu_0 a I(\omega)}{2}\int_0^\infty J_1(\lambda r)\,J_1(\lambda a)\,R_R(\omega,\lambda)e^{-\lambda(h+z)}\,d\lambda \tag{7.14}$$

[1]Because this will force G to decay in magnitude at about the same rate as R, so that R_R will go to zero at about the same rate as R. If s were much smaller R_R would not decay to zero in the range of sampling λ chosen on the basis of the problem geometry, and would be inaccurately Hankel-transformed. If s were much larger, G would be effectively zero by the first non-zero sampling λ value, and not solve the original large z large r problem.

where the term $\Gamma(r,z)$ can be expressed analytically as

$$\Gamma(r,z) = \int_0^\infty J_1(\lambda r)\, J_1(\lambda a)\, e^{-\lambda|z-h|}\, d\lambda \tag{7.15}$$

$$- \int_0^\infty J_1(\lambda r)\, J_1(\lambda a) e^{-\lambda(s+h+z)}\, d\lambda \tag{7.16}$$

Both terms in the expression for Γ can be evaluated using

$$\int_0^\infty J_1(\lambda r)\, J_1(\lambda a)\, e^{-cx} d\lambda = \frac{2}{\pi k\sqrt{ar}} \Big[(1-k^2/2)K(k) - E(k)\Big] \tag{7.17}$$

where

$$k^2 = \frac{4ar}{(a+r)^2+c^2} \tag{7.18}$$

and the elliptic integrals of the first and second kinds defined by

$$K(k) = \int_0^{\pi/2} \frac{d\phi}{\sqrt{1-k^2\sin^2\phi}} \tag{7.19}$$

$$\tag{7.20}$$

$$E(k) = \int_0^{\pi/2} \sqrt{1-k^2\sin^2\phi}\, d\phi \tag{7.21}$$

are available as standard functions in programming languages.

7.4 Localized targets

Localized targets are handled in a different way from global targets, since UTemis handles the calculation of the transducer-target coupling fields, requiring the support routines TPtargetname.m and TStargetname.m to be responsible only for the local (*e.g.* magnetance) response of the target. The following tests validate both the coupling code and the representations of some particular local target types.

7.4.1 Single-axis target with arbitrary frequency response

This is the most general localized target. Any other localized target can be made up as a superposition of such targets. If the principal axes of

a target are independent of frequency (as is often the case, either exactly or approximately), then only three *singleaxis* targets need be combined to make up a real target. An example is shown in the target configuration file listed below, which is actually simulating the response of a coin, which has two orthogonal but equivalent principle axes in the plane of the coin, and one perpendicular to the coin. In this example, the frequency response parameters were obtained experimentally using the UTEMI spectrometer, and the program utemispolefit described elsewhere in this manual.

```
% Generic frequency-dependent target written by POLEFIT
target name=A-05-02-17-Penny_at_90_degrees type=singleaxis ...
 zamps=[0.000001] pamps=[-0.002119,-0.000314,-0.000264,-0.000177] ...
 freqs=[28145.864259,60831.147430,120197.950332,419615.704960] ...
 axis=[1,0,0] location=[0,0,0]

% Generic frequency-dependent target written by POLEFIT
target name=A-05-02-17-Penny_at_0_degrees type=singleaxis ...
 zamps=[-0.000003] pamps=[-0.000019,-0.000248,-0.000168] ...
 freqs=[28443.914326,390242.273811,1288498.335013] ...
 axis=[0,1,0] location=[0,0,0]

% Generic frequency-dependent target written by POLEFIT
target name=A-05-02-17-Penny_at_0_degrees type=singleaxis ...
 zamps=[-0.000003] pamps=[-0.000019,-0.000248,-0.000168] ...
 freqs=[28443.914326,390242.273811,1288498.335013] ...
 axis=[0,0,1] location=[0,0,0]
```

7.4.2 Small distant spherical susceptible target in free space

Consider a small spherical (radius r) susceptible (susceptibility χ) target lying on the common vertical axis of a transmitter coil (of radius $a_t \gg r$) and a receiver coil (of radius $a_r \gg r$), at distances z_t ($z_t \gg a_t \gg r$) and z_r ($z_b \gg a_r \gg r$) respectively below the planes of the transmitter and receiver coils.

The magnetic field H of the transmitter at the target is vertical (axial)

and of magnitude

$$H = \frac{I}{2} \frac{a_t^2}{(z_t^2 + a_t^2)^{3/2}} \tag{7.22}$$

where I is the transmitter current. The (vertical) magnetic moment induced in the target is then

$$m = \frac{4\pi}{3} r^3 \chi_e H = \frac{2\pi}{3} r^3 \chi_e I \frac{a_t^2}{(z_t^2 + a_t^2)^{3/2}} \tag{7.23}$$

where the effective susceptibility χ_e is related to the true material susceptibility χ by

$$\chi_e = \frac{\chi}{1 + \frac{N_d}{4\pi}\chi} \tag{7.24}$$

and N_d is the demagnetizing factor of the target shape (for a sphere, $N_d/(4\pi)$ is $1/3$).

At the centre of the receiver coil, the (vertical) magnetic induction of this magnetic moment is

$$B = \frac{\mu_0 m}{2\pi z_r^3} = \frac{\mu_0}{3} r^3 \chi_e I \frac{a_t^2}{z_r^3 (z_t^2 + a_t^2)^{3/2}} \tag{7.25}$$

in the same direction as the inducing H. Assuming this field approximately constant across the area πa_r^2 of the receiver coil, the induced voltage in the receiver coil must be

$$V = -\frac{j\omega\mu_0 \pi r^3 I \chi_e}{3} \frac{a_t^2 a_r^2}{z_r^3 (z_t^2 + a_t^2)^{3/2}} \tag{7.26}$$

where ω is the frequency of the transmitter (as in $I = I_0\, e^{j\omega t}$). The minus sign is to be interpreted as meaning that this voltage would drive a current in the receiver coil in a sense *opposite* to the sense of circulation of the rate of change of current in the transmitter coil.

A more accurate formula (using the reciprocity which must exist between transmitter and receiver coils) is

$$V = -\frac{\mu_0 \pi r^3 \chi_e}{3} j\omega I \frac{a_t^2 a_r^2}{(z_r^2 + a_r^2)^{3/2} (z_t^2 + a_t^2)^{3/2}} \tag{7.27}$$

where $\dot{I}$ is the time derivative of the transmitter current. Equation (7.27) is valid for any z_t and z_r and requires only that the target be small (that $r \ll a_t$ and $r \ll a_r$).

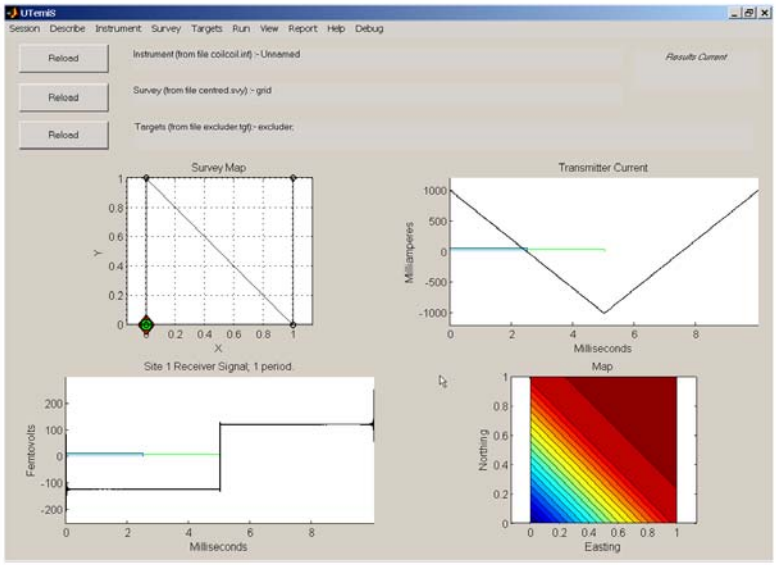

Figure 7.5: Screenshot for test case *Excluder*.

For the special case of coplanar coils, $z_r = z_t = z$ and

$$V = -\frac{\mu_0 \pi r^3 \chi_e}{3} \dot{I} \frac{a_t^2 a_r^2}{(z^2 + a_r^2)^{3/2}(z^2 + a_t^2)^{3/2}} \tag{7.28}$$

Further specializing to a target which completely excludes magnetic flux ($\chi_e = -1$) gives

$$V = \frac{\mu_0 \pi r^3}{3} \dot{I} \frac{a_t^2 a_r^2}{(z^2 + a_r^2)^{3/2}(z^2 + a_t^2)^{3/2}} \tag{7.29}$$

or

$$V = \frac{\mu_0 v}{4} \dot{I} \frac{a_t^2 a_r^2}{(z^2 + a_r^2)^{3/2}(z^2 + a_t^2)^{3/2}} \tag{7.30}$$

where v is the volume of the sphere.

Because this response is in phase with $\dot{I}$, it tests only the utilization of the N_1 term in (6.13).

7.4.3 Small distant inductive ring in free space

Frequency domain derivation

This is a small circular loop (radius b) of vanishingly thin wire of resistance R and self inductance L, oriented with axis in direction $\mathbf{n}$, lying on the

common vertical axis of a transmitter coil (of radius $a_t \gg r$) and a receiver coil (of radius $a_r \gg r$), at distances z_t ($z_t \gg a_t \gg r$) and z_r ($z_b \gg a_r \gg r$) respectively below the planes of the transmitter and receiver coils, as in section (7.4.2). Following this previous example, the magnetic field H of a unit current in the transmitter at the target is vertical and equal to

$$\hat{H}^t = \frac{1}{2} \frac{a_t^2}{(z_t^2 + a_t^2)^{3/2}} \tag{7.31}$$

Assume the transmitter current I varies sinusoidally as $I_0 e^{j\omega t}$. The current I_r in the ring induced by the transmitter current I is governed by the Kirchhoff's loop equation (summing voltages around the loop)

$$V_i - L\frac{\partial I_i}{\partial t} - I_i R = 0 \tag{7.32}$$

or

$$V_i - j\omega L I_i - R I_i = 0 \tag{7.33}$$

where n_z is the vertical component of the ring axis direction, and the inducing voltage is $V_i(\omega) = -j\omega\pi b^2 \mu \hat{H}^t n_z I_t(\omega)$, where $I_t(\omega)$ is the transmitter current, and μ is the permeability of the medium in which the target ring is embedded. The minus sign means the voltage drives a current so as to oppose the inducing field changes. The solution is

$$I_i(\omega) = \frac{V_i(\omega)}{R + j\omega L} = -\frac{j\omega\pi b^2 \mu \hat{H}^t n_z I_t(\omega)}{R + j\omega L} \tag{7.34}$$

Reciprocity tells us that the receiver coil voltage induced by a unit current in the ring is the same as the ring voltage induced by a unit current in the receiver coil. This latter is simply

$$-j\omega \hat{B}^r n_z \pi b^2 \tag{7.35}$$

where

$$\hat{B}^r = \frac{\mu}{2} \frac{a_r^2}{(z_t^2 + a_r^2)^{3/2}} \tag{7.36}$$

Thus the induced receiver voltage is

$$V_r(\omega) = -j\omega \hat{B}^r n_z \pi b^2 I_i(\omega) = -\frac{\omega^2 \pi^2 b^4 \mu \hat{B}^r \hat{H}^t n_z^2 I_t(\omega)}{R + j\omega L} \tag{7.37}$$

where ω is the frequency of the transmitter (as in $I_t = I_0\, e^{j\omega t}$). The minus sign is to be interpreted as meaning that this voltage would drive a current in the receiver coil in a sense *opposite* to the sense of circulation of the rate of change of current in the transmitter coil.

$$V_r(\omega) = -\frac{\omega^2\pi^2 b^4 I_t(\omega)}{R + j\omega L}\mu(\hat{\mathbf{H}}^t \cdot \mathbf{n})(\hat{\mathbf{B}}^r \cdot \mathbf{n}) \tag{7.38}$$

Canonical representation

The transimpedance of the ring target is therefore

$$Z(\omega) = \frac{V_r(\omega)}{I_t(\omega)} = -\frac{\mu\omega^2\pi^2 b^4}{R + j\omega L}(\hat{\mathbf{H}}^t \cdot \mathbf{n})(\hat{\mathbf{B}}^r \cdot \mathbf{n}) \tag{7.39}$$

The magnetance part of this, which we need for a local target representation of the form (6.40)

$$V = \dot{I}\sum_{i=1}^{3}\sum_{j=1}^{3} \hat{H}_i^t S_{ij}\, \hat{B}_j^r \tag{7.40}$$

is

$$S(\omega) = \frac{V(\omega)}{\dot{I}(\omega)(\hat{\mathbf{H}}^t \cdot \mathbf{n})(\hat{\mathbf{B}}^r \cdot \mathbf{n})} = \frac{j\mu\omega\pi^2 b^4}{R + j\omega L} = \frac{j\mu\omega\pi^2 b^4}{L}\frac{1}{j\omega + R/L} \tag{7.41}$$

This can be put into canonical form (6.42) for UTemis with all coefficients N_k^S and D_k^S zero except for

$$D_1^S = \frac{\mu\pi^2 b^4}{L} \tag{7.42}$$

with $p_1 = R/L$.

Time domain solution check

We can get the time domain step response to a step of size I_0 ($I_t(\omega) = -jI_0/\omega$) by Fourier transforming

$$V(t) = \mu\pi^2 b^4 I_0(\hat{\mathbf{H}}^t \cdot \mathbf{n})(\hat{\mathbf{B}}^r \cdot \mathbf{n})\frac{d}{dt}\left(\frac{1}{L}H(t)e^{-Rt/L}\right) \tag{7.43}$$

$$= \frac{\mu\pi^2 b^4}{L} I_0(\hat{\mathbf{H}}^t \cdot \mathbf{n})(\hat{\mathbf{B}}^r \cdot \mathbf{n})\left(\delta(t) - H(t)\frac{R}{L}e^{-Rt/L}\right) \tag{7.44}$$

where $H(t)$ is the Heaviside function.

The response to a time domain slope discontinuity of $\dot{I}_0$, (for a triangle waveform, $\dot{I}_0 = 8I_p/T$ where I_P and T are the peak current and period) for which $I_t(\omega) = -\dot{I}_0/\omega^2$

$$V(t) = \frac{\mu\pi^2 b^4}{L}\dot{I}_0(\hat{\mathbf{H}}^t \cdot \mathbf{n})(\hat{\mathbf{B}}^r \cdot \mathbf{n})H(t)e^{-Rt/L} \tag{7.45}$$

For the triangle wave coil-coil instrument described by

```
source       type=coil shape=circle radius=0.1 location=[0,0,0.01] ...
  pole=[0,0,1] turns=1
sensor       type=coil shape=circle radius=0.1  location=[0,0,0]  ...
  pole=[0,0,1] turns=1
waveform     shape=triangle period=.01 current=1 plotcycles=1
acquisition  method=Gates  gain=1 noise=0.0 ...
 windows=[0,0.0025;0,0.005]
output       algorithm='[v(1),v(2)]'
```

and ring target described by

```
 target  name=ring type=ring resistance=.03 inductance=0.000010 ...
radius=0.01 axis=[0.7071,0.7071,.5] location=[0,0,-1] scope=local
```

the expected response is an exponential decay from initial peak voltage of $6.05 \cdot 10^{-17}$ volts with a relaxation time of 1/3 millisecond (half-life of 0.231 milliseconds). The actual UTemis result is shown in Fig. (7.6). It differs by about 3%, presumably because of the inability of the program to perfectly numerically synthesize the discontinuity as the second time derivative of the transmitter waveform. The mean values of this in the two averaging windows over 1/4 and 1/2 cycle respectively are $0.80 \cdot 10^{-17}$ and $0.40 \cdot 10^{-17}$.

7.4.4 Excluder target with dipole transducers

This tests the free-space coupling of the *mdipole* source and the *bfield* sensor. Both are vertically oriented and at heights of z_t and z_r, and the excluder target is at height z_e. Using the standard formula for the axial field of a magnetic dipole, the H field at the target is $H = m_t/(2\pi(z_t - z_e)^3)$ where the source moment is $m_t = IA_t$, A_t being the effective area of the source dipole.

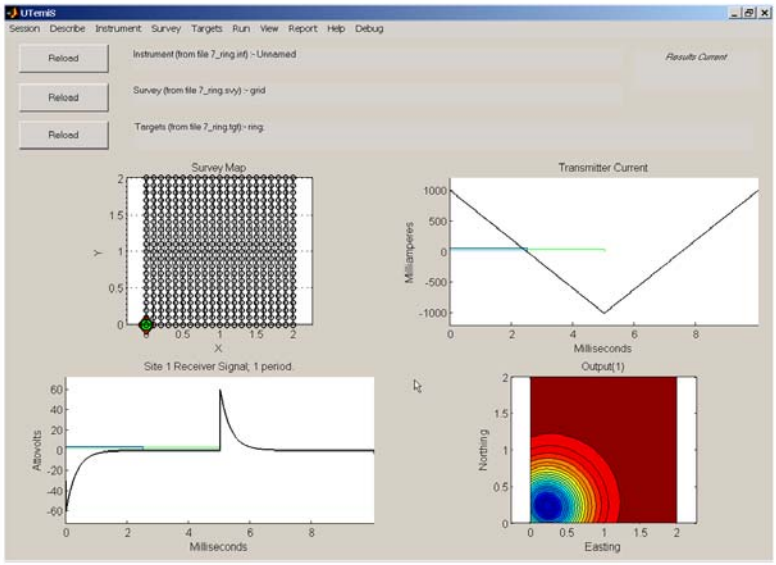

Figure 7.6: Screenshot for the ring target test case.

The induced moment is thus $m_i = VH = VIA_t/(2\pi|z_t - z_e|^3)$ where V is the excluder target volume. The B field this places at the sensor is

$$B = \frac{\mu_0 m_i}{2\pi|z_s - z_e|^3} = \frac{\mu_0 VIA_t}{4\pi^2|z_s - z_e|^3|z_t - z_e|^3} \tag{7.46}$$

The sensor voltage is thus

$$V = \frac{\mu_0 m_i}{2\pi|z_s - z_e|^3} = \frac{\mu_0 VIA_t A_r}{4\pi^2|z_s - z_e|^3|z_t - z_e|^3} \tag{7.47}$$

where A_r is the effective area of the *bfield* sensor.

7.4.5 Small homogeneous conductive permeable sphere with dipole transducers

From equations 17-13 and 17-14 in [2], the dipole moment of a homogeneous conductive permeable sphere or radius a, permeability μ, and conductivity σ, in a unit inducing H with angular frequency ω is

$$m(\omega) = -2\pi a^3(X(\omega) + iY(\omega)) \tag{7.48}$$

where

$$F(\omega) = X(\omega) + iY(\omega) = \frac{(2\mu + (a^2k^2+1)\,\mu_0)\sinh(ak) - ak\,(2\mu+\mu_0)\cosh(ak)}{ak\,(\mu-\mu_0)\cosh(ak) + ((a^2k^2+1)\,\mu_0 - \mu)\sinh(ak)} \tag{7.49}$$

where $k = \sqrt{i\sigma\mu\omega}$. Since it is the poles of this on the imaginary frequency axis (s-axis) that we wish to investigate, it is useful to let $\omega = is$, so that $k = \sqrt{-\sigma\mu s}$ and $ka = i\alpha$. In terms of α, this expression is

$$f(\alpha) = F(\omega) = \frac{\alpha\cos(\alpha) + (\alpha^2-1)\sin(\alpha) + 2(\alpha\cos(\alpha) - \sin(\alpha))\mu_r}{\alpha\cos(\alpha) + (\alpha^2-1)\sin(\alpha) + (\sin(\alpha) - \alpha\cos(\alpha))\mu_r} \tag{7.50}$$

where μ_r is the relative permeability μ/μ_0.

This is a meromorphic function of α, whose poles α_k lie on the real α axis, and which tends to 1 as α tends to infinity, and can therefore be represented in the form

$$f(\alpha) = 1 + \sum_{k=1}^{\infty}\left(\frac{r_k}{\alpha-\alpha_k} - \frac{r_k}{\alpha+\alpha_k}\right) \tag{7.51}$$

where we have taken advantage of the fact that $F(\alpha)$ is an odd function of α. No analytic expression for the pole locations α_k exists. However, it is possible to find them numerically by finding the zeros of the denominator of (7.50), that is, of

$$d(\alpha) = \alpha\cos(\alpha) + \left(\alpha^2-1\right)\sin(\alpha) + (\sin(\alpha) - \alpha\cos(\alpha))\mu_r \tag{7.52}$$

Once these pole locations are known, the residues r_k are easily calculated.

If α is near a pole, $\alpha = \alpha_k + \rho$ where ρ is small, and (7.52) can be written as

$$\begin{aligned} d(\rho) &= \left(\sin(\alpha_k)\alpha_k^2 + \cos(\alpha_k)\alpha_k - \cos(\alpha_k)\mu_r\alpha_k - \sin(\alpha_k) + \sin(\alpha_k)\mu_r\right) \\ &\quad + \left(\cos(\alpha_k)\alpha_k^2 + \sin(\alpha_k)\alpha_k + \sin(\alpha_k)\mu_r\alpha_k\right)\rho + O\left(\rho^2\right) \\ &= \left(\cos(\alpha_k)\alpha_k^2 + \sin(\alpha_k)\alpha_k + \sin(\alpha_k)\mu_r\alpha_k\right)\rho + O\left(\rho^2\right) \end{aligned} \tag{7.53}$$

The k' th residue r_k must therefore be the numerator of (7.50) divided by the coefficient of ρ in (7.53), or

$$r_k = \frac{\alpha_k\cos(\alpha_k) + (\alpha_k^2-1)\sin(\alpha_k) + 2(\alpha_k\cos(\alpha_k) - \sin(\alpha_k))\mu_r}{\cos(\alpha_k)\alpha_k^2 + \sin(\alpha_k)\alpha_k + \sin(\alpha_k)\mu_r\alpha_k} \tag{7.54}$$

Because the amplitudes of these closely spaced poles die away very slowly (thousands of poles can be needed for an accurate simulation), this is not very useful. A direct approximatiuon to a measure or computed frequency response using utemispolefit (see Chapter 8) is the appropriate approach.

Chapter 8

Creating a Pole-zero Description of a Target

Local targets and some global targets (*e.g.* a frequency dependent susceptible halfspace) have frequency responses which are intrinsic, that is, do not depend on the instrument, survey geometry or other targets. A MATLAB function *itrplot* is provided to plot these. It takes one argument (the target filename).

More useful is the interactive program *utemispolefit* which will read experimentally determined frequency response spectra using the University of Toronto spectrometer, and efficiently fit a sum of a small number of poles on the imaginary frequency axis to it (corresponding to a sum of decaying exponentials as the step response). This is the information required by Utemis for fast response calculations.

8.1 Using *utemispolefit*

This is a standalone MATLAB application. It uses the downhill simplex method as implemented in MATLAB's *fminsearch* function to obtain N_0, D, and P by fitting the following expansion to spectral response data as a function of frequency:

$$s(\omega) = N_0 + \sum_{k=1}^{m} \frac{j\omega}{j\omega + P_k} \tag{8.1}$$

8.1.1 Input data

To use, prepare an ASCII file with either three or four columns which contain, on each line, the frequency (actual, not angular), the real part of the spectral response, the imaginary part of the spectral response, and optionally, the estimated error in the response at that frequency. Comment lines beginning with % are ignored. An example of such a text file is shown here:

```
% Idealized Problem Soil; Format: freq  real(S)  imag(S)
      10.000000        8.900597       -0.750000
      17.782794        8.625746       -0.750000
      31.622777        8.350895       -0.750000
      56.234133        8.076044       -0.750000
     100.000000        7.801193       -0.750000
     177.827941        7.526342       -0.750000
     316.227766        7.251492       -0.750000
     562.341325        6.976641       -0.750000
    1000.000000        6.701790       -0.750000
    1778.279410        6.426939       -0.750000
    3162.277660        6.152088       -0.750000
    5623.413252        5.877237       -0.750000
   10000.000000        5.602386       -0.750000
   17782.794100        5.327536       -0.750000
   31622.776602        5.052685       -0.750000
   56234.132519        4.777834       -0.750000
  100000.000000        4.502983       -0.750000
```

Alternatively, this information can be contained in a MATLAB *.mat* file containing it as arrays *f* (frequency) , *sp*, (spectral response) and optionally *esr* (the (positive) error estimates). *sp* is complex. If *esr* is present and real, it will be assumed to apply equally to the real and imaginary parts of *sp*.

This data is loaded using *Spectrum* → *Load Spectrum* in the menu bar. The two types of input file above are distinguished by the program on the basis of their file types (either *.txt* or *.mat*, respectively). Once loaded, the spectrum will be displayed using blue circles (real) and red triangles (imaginary) as a function of frequency. Note that if a zero frequency spectral value is present, it will be loaded and fitted, but not displayed on the semilog plot used.

8.1.2 Choosing a fit target

Some applications do not use a representation of the frequency response defined by the data, but rather some function derived from the data. For example, in modelling the response of dispersive paramagnetic soils, the data represent , Utemis requires the pole-zero representation of the reflection coefficient

$$R(\omega) = \frac{\chi(\omega)}{2 + \chi(\omega)} \tag{8.2}$$

rather than a pole-zero representation for the directly measured frequency-dependent magnetic susceptibility. Although a pole-zero representation for χ could be analytically converted to one for R, this would be very tedious, and in the end, less accurate than directly fitting the representation for R. Accordingly, *utemispolefit* allows the user to specify a data transformation (of which (8.2) is just one example) of the raw data prior to fitting.

8.1.3 Fitting

To fit, press the *run* button. Fitting progress will be displayed by updating two plots. The upper shows the spectral data (points) and best-fitting representation of type (8.1) found so far. The lower shows the amplitudes D_k and locations P_k of the poles on the imaginary ω axis. The default starting representation has only one pole (or a minimum specified by the user); new poles are added (or deleted) during the iteration as appropriate. The iteration stops when the fit (as determined by the χ^2 based penalty function of the fit is small enough (comparable with unity), or when the number of iterations exceeds a user-specified number. Users can re-iterate to improve the fit, keeping or changing various fitting parameters.

These fitting parameters allow users to guide the fitting in several ways. The number of iteration blocks can be reduced (or increased) using the eponymous edit box. Similarly, the user can adjust the minimum and maximum number of poles allowed: *e.g.* 2 10 means a minimum of 2 (which will be the starting value) and a maximum of 10. If only one number is present it will be assumed to be a starting value. The user can choose to load, before starting, a previously saved representation which is thought to be a good starting point for fitting, with *Initialize* $\rightarrow$ *Load Representation.* Finally the *tolerance* edit box allows the desired degree of fitting accuracy to be specified. If no errors are specified for the spectral data, such errors are calculated as

tolerance times the median spectral amplitude, so that values of *tolerance* small compared with unity are sensible. If errors are specified in the spectral data file, this modifies the errors used by multiplying the original errors, so that values of *tolerance* comparable with unity are sensible. The errors thus calculated, for either case, are used in calculating a χ^2 statistic for the current which is displayed in the plot title. Because a size norm (mean square) for the fitting parameters N_0 and D (at a very small weight of 10^{-7} divided by the mean square spectral response) is also included in the fitting norm in addition to the fitting error norm, adjusting the tolerance well up or down can sometimes help the fit out of an undesired local minimum by changing the relative importance of the error and model norms. Negative values for P_k are absolutely precluded. The *reset* button restores the representation to the simple minimum-pole starting default.

8.1.4 Saving and Viewing

The plots showing spectral fit and the pole locations can be separately detached as regular MATLAB figures using the *View* $\rightarrow$ *DetachXXX* menu items. As normal MATLAB figures, these detached plots can be edited, manipulated, saved, and exported to other file formats using MATLAB's standard tools. The spectral plot is shown over a wider frequency range to give the viewer some idea of behaviour of the representation outside the fitting range.

Representation results can be saved using the menu item *Representation* $\rightarrow$ *Save Representation*. Users effectively choose among three save formats by choosing the extension of the save filename. If the extension is *.txt*, a text file is written. After some comment lines, a line containing N_0 and a zero follows (the zero pads the line so MATLAB's *load* function will later read it). Subsequent lines have $(P_k\, D_k)$ pairs. An example is shown here:

```
% Fit of function of spectrum x(frequency) from file junk.txt
% Pre-fit data transformation  f(x) of spectral data x was:
% x/(2+x)
% Fitted representation as f(x(w)) = N0 + sum_k D(k)*i*w/(i*w+P(k))
% where w = 2 pi frequency
% First line: [N0 0]; succeeding lines: [P D] pairs
    2.999990         0.000000
   20.000000     20000.000010
```

```
 1000.000004       8000.000016
 9999.999998      70000.000040
```

If the extension is *.mat*, variables $N0$, P, D and the original spectral file name *spname* are saved in a *.mat* file.

Finally, if the file extension is *.tgt*, a Utemis target description file will be written (or appended) to, making a target with the fields *name*, *zamps*, *pamps* and *freqs*[1], preceded by a comment line. Before this can be used as a legal target by Utemis, the user must edit it to provide it with any other necessary fields (such as *type* and any other parameters required by that target type). The entry in the file looks like this (although the target information is actually on a single line):

```
% Generic frequency-dependent target written by POLEFIT
target name=threepole zamps=[2.999990]
    pamps=[20000.000010,8000.000016,70000.000040]
    freqs=[20.000000,1000.000004,9999.999998]
```

[1] *zamps*, *pamps* and *freqs* are the Utemis target-file field names for N, D, and P.

Chapter 9

Batch Mode

9.1 Introduction

UTemis has a batch mode, whose original purpose was to facilitate automated testing of the code against a suite of test cases during development. The format of the required command in the MATLAB console is

```
utemis batch_mode instrumentFileName surveyFileName ...
      targetFileName reportingFileName > outputfilename
```

The word 'batch_mode' is obligatory as shown. The strings *instrumentFileName, surveyFileName* and *targetFileName* are the names of the instrument, survey, and target configuration files to be used. Text output is directed, in the same formats as used by the *reporting* mechanism in the GUI, to an output file *outputfilename* The filename *reportingFileName* (by convention with extension *.rcf*) tells UTemis what output is actually required, and replaces the use of the *reporting* menu in the GUI. It should contain the user's choice of strings from the GUI *Report* menu (*NOT* the *View* menu), exactly as they are spelled there. For example, to output the instrument description, the sample times, and the receiver waveform, the reporting file would have three lines as follows:

```
Instrument Configuration Waveform Sample Times Receiver Waveform
```

9.2 Automated code testing

A problem during code development or modification is that well-meant changes may 'break' some earlier part of the code. To detect such problems, automated code testing was used. The procedure used was to write a report file for a (correct and debugged!) test case as a 'reference file' (by convention with extension *.ref*). Subsequent code testing after further development then utilized a script (see Appendix 11, see Appendices) ran the same case using batch mode, and compared (character by character) the report file thus generated with the reference file, giving a 'failure' output if the files were not identical. The name of the batch testing file provided with UTemiS is *testUtemis.m*; users can write their own, with different or additional test cases.

Chapter 10

Incorporating new target types in UTemiS

UTemis is designed to accommodate new target types as they are added, without having to rewrite any of the main code. Any new target requires that two MATLAB functions be added to the UTemis code directory: a routine to calculate the target response to the various types of instrument and a target preparation routine to convert user specifications given in a target configuration (*.tgt) file to the form needed by the response routine. If the target type is to be called targetname in any configuration file, the response routine must be named TStargetname or TZtargetname, depending on whether the target is a local one with a magnetance response, or a global one with an transimpedance response, as described in the previous chapters. These must return the zero amplitudes, the pole locations, and the pole amplitudes [N,P,D] of the response that are described above. The input arguments to this routine must be (source, sensor, xyz, target), namely the source description structure, the sensor description structure, the set of survey locations as a N by 3 array, and the (sub-) target description structure. Because end-user descriptions of target properties may be different (and hopefully simpler) than the target properties required by the response calculation, the function TPtargetname must also be present. Its job is to take the target structure produced by reading the configuration file, and output a (cell array) list of (sub) targets with whatever fields and properties will be required by the response routine.

An example of a minimal target preparation routine is given by the freespace target. Properties *scope* must be set to *global* (for a transimpedance

target), or *local* (for a magnetance target).

```
function subtarget = TPfreespace(target)
% Prepares the magnetic half space  subtarget info from user input
% Since free space has no parameters, hardly any prep is needed
if(isfield(target,'scope'))
    subtarget{1}.scope = target.scope;
else
    subtarget{1}.scope = 'global';
end;
subtarget{1}.TZname = 'TZfreespace';
subtarget{1}.hHname='hHfreespace';
subtarget{1}.hEname='hEfreespace';
```

As a global target which may host local targets, freespace has to specify the two functions that will be used to calculate H and E fields at the locations of any local targets embedded within it. These field functions works as follows:

```
function [H,mu] = hHfreespace(transducer,r,f)
% H = freespaceCoupling(coil,f,r) returns vector H field and
% local absolute permeability  produced by  a transducer at
% frequency f (irrelevant here) for relative locations r
% (in true coords)  of the target point with respect to the
% instrument. r and H has dimensions (nLocations,3)
... ...
```

Not all target responses need to be implemented for every conceivable source type, sensor type, or survey, but these routines *must* throw an informative error message when an unhandled configuration is encountered.

Chapter 11

Automated code testing

An example of a script for automated code validation is given here, which uses four previously generated reference files for particular test cases:

```
function varargout  = testUTemis
% ok = testUTemis
% This Tests UTemis against prescribed test cases. If there is no output
% argument "ok", a detailed tests analysis is printed to the console.

ok = 1;
testcases = 0;
passedCases = 0;

%%%%%%%%%%%%%%%%%%%%%%%%%%%%%%%%%%%%%%%%%%%%%%%%%%%%%%%%%%%%%%%%%%%%%%%%%%%%%%%
%%%%%%%%%%%%%%%%%%%%%%%%%%%%%%%%%%%%%%%%%%%%%%%%%%%%%%%%%%%%%%%%%%%%%%%%%%%%%%%
%%%%%%%%%%%%%%%%%%%%%%%%%%%%%%%%%%%%%%%%%%%%%%%%%%%%%%%%%%%%%%%%%%%%%%%%%%%%%%%
%%%%%%%%%%%%%%%%%%%%%%%%%%%%%%%%%%%%%%%%%%%%%%%%%%%%%%%%%%%%%%%%%%%%%%%%%%%%%%%
%%%%%%%%%%%%%%%%%%%%%%%%%%%%%%%%%%%%%%%%%%%%%%%%%%%%%%%%%%%%%%%%%%%%%%%%%%%%%%%
%%%%%%%%%%%%%%  Place test cases below here

% Test number 1
testname = '1_resistor'; refFile = '1_resistor.ref';
surveyFile='1_resistor.svy'; instrumentFile = '1_resistor.int';
targetFile = '1_resistor.tgt'; reportingFile = '1_resistor.rcf';
thisOk = testThisCase(refFile, instrumentFile,  surveyFile,
targetFile, reportingFile,~nargout); ok = ok & thisOk; testcases =
```

```
testcases+1; if(thisOk) passedCases = passedCases  + 1; end;

% Test number 2
testname = '2_rc'; refFile = '2_rc.ref'; surveyFile = '2_rc.svy';
instrumentFile = '2_rc.int'; targetFile = '2_rc.tgt';
reportingFile = '2_rc.rcf'; thisOk = testThisCase(refFile,
instrumentFile,  surveyFile, targetFile, reportingFile,~nargout);
ok = ok & thisOk; testcases = testcases+1; if(thisOk) passedCases
= passedCases  + 1; end;

% Test number 3
testname = '3_freespace'; refFile = '3_freespace.ref'; surveyFile
= '3_freespace.svy'; instrumentFile = '3_freespace.int';
targetFile = '3_freespace.tgt'; reportingFile = '3_freespace.rcf';
thisOk = testThisCase(refFile, instrumentFile,  surveyFile,
targetFile, reportingFile,~nargout); ok = ok & thisOk; testcases =
testcases+1; if(thisOk) passedCases = passedCases  + 1; end;

% Test number 4
testname = '4_excluder'; refFile = '4_excluder.ref'; surveyFile =
'4_excluder.svy'; instrumentFile = '4_excluder.int'; targetFile =
'4_excluder.tgt'; reportingFile = '4_excluder.rcf'; thisOk =
testThisCase(refFile, instrumentFile,  surveyFile, targetFile,
reportingFile,~nargout); ok = ok & thisOk; testcases =
testcases+1; if(thisOk) passedCases = passedCases  + 1; end;

%%%%%%%%%%%%%%  Place test cases above here
%%%%%%%%%%%%%%%%%%%%%%%%%%%%%%%%%%%%%%%%%%%%%%%%%%%%%%%%%%%%%%%%%%%%%%%%%%%%%%%%%%
%%%%%%%%%%%%%%%%%%%%%%%%%%%%%%%%%%%%%%%%%%%%%%%%%%%%%%%%%%%%%%%%%%%%%%%%%%%%%%%%%%
if(~nargout)
    if(ok)
        disp(['testUTemis Success: ' num2str(passedCases) ' of ' ...
        num2str(testcases) ' cases passed successfully']);
    else
        disp(['testUTemis Failure:  only ' num2str(passedCases) ...
        ' of ' num2str(testcases) ' cases passed successfully']);
    end;
end; if(nargout) varargout{1} = ok; end;
```

```
function ok = testThisCase(refFileName, instrumentFileName,
surveyFileName, targetFileName, reportingFileName,level) ok = 1;
% Read the reference file
try
oldfile = textread(refFileName,'%s','delimiter','\n',...
'whitespace','','bufsize',250000);
catch
    warning(['Could not read the reference file ' refFileName]);
end; newfilename = ['temp_' refFileName '_try.txt'];
if(2==exist(newfilename)) delete(newfilename); end;
% Make the new file
feval('utemis', 'batch_mode', instrumentFileName, surveyFileName,
targetFileName, reportingFileName, '>', newfilename);
% Read the new file
newfile = textread(newfilename,'%s','delimiter','\n',...
'whitespace','','bufsize',250000);
% Read the new file
nreflines = length(oldfile); nnewlines = length(newfile);
if(level) disp(['testUTemis: case ' refFileName ': ']); end;
if(nreflines~=nnewlines)
    if(level) disp(['  error: ' num2str(nreflines) ...
    ' lines in reference file, ' num2str(nnewlines) ' in test file.']);
     end;
    ok = 0;
end;

for k=1:min(nreflines,nnewlines)
    lineok = strcmp(newfile{k},oldfile{k});
    if(~lineok)
    % If it is simply a different run date, ignore the difference
        if(strfind(newfile{k},'Report.date'))
        else
            if(level) disp(['  Files disagree at line ' num2str(k) ': ']); end;
            nshow = min(length(oldfile{k}),64);
            if(level) disp(['      Ref: ' oldfile{k}(1:nshow) '...' ]); end;
            nshow = min(length(newfile{k}),64);
```

```
            if(level) disp(['     Test: ' newfile{k}(1:nshow) '...' ]);  end;
            ok = 0;
        end;
    end;
end;
if(ok) delete(newfilename); end;  % leave for comparison if failed
```

Appendix A

Miscellaneous theory

A.1 Validation targets

A.1.1 Alternate ring response derivation

This is a small circular loop (radius b) of vanishingly thin wire of resistance R and self inductance L, oriented with axis in direction $\mathbf{n}$, lying on the common vertical axis of a transmitter coil (of radius $a_t \gg r$) and a receiver coil (of radius $a_r \gg r$), at distances z_t ($z_t \gg a_t \gg r$) and z_r ($z_b \gg a_r \gg r$) respectively below the planes of the transmitter and receiver coils, as in section (7.4.2).

Time domain response

Following this previous example, the magnetic field H of a unit current in the transmitter at the target is vertical and equal to

$$H_1 = \frac{1}{2} \frac{a_t^2}{(z_t^2 + a_t^2)^{3/2}} \tag{A.1}$$

Assume the transmitter current ($I_t = R(t)\dot{I}_0$ where R(t) is a unit slope causal ramp function (the integral of the Heaviside function), and $\dot{I}_0$ is the constant rate of change of the transmitter current) is increasing uniformly beginning at time zero (as with a long period triangular wave current excitation). The current $I_i(t)$ in the ring induced by the transmitter current $I_t(t)$ is governed

by the Kirchhoff's loop equation (summing voltages around the loop)

$$V_i - L\frac{\partial I_i}{\partial t} - I_i R = 0 \tag{A.2}$$

where n_z is the vertical component of the ring axis direction, and the inducing voltage is $V_i = \pi b^2 \mu H_1 n_z \dot{I}_0 = V_{i0} H(t)$, where $\dot{I} = \dot{I}_0 H(t)$ is a step function, and μ is the permeability of the medium in which the host is embedded. The solution is

$$I_r = \frac{V_{i0}}{R}\,(1 - e^{-Rt/L}) H(t) \tag{A.3}$$

The magnitude of the magnetic moment of the ring is its area times the current, or

$$m = I_r \pi b^2 = \frac{\pi^2 b^4 \mu H_1 n_z \dot{I}_0}{R}\, H(t)(1 - e^{-Rt/L}) \tag{A.4}$$

Only the vertical component m_z of this can induce a voltage in the receiver coil.

$$m_z = \mathbf{m} \cdot \mathbf{n} = m n_z = \frac{\pi^2 b^4 \mu H_1 n_z^2 \dot{I}}{R}\, H(t)(1 - e^{-Rt/L}) \tag{A.5}$$

At the centre of the receiver coil, the (vertical) magnetic induction of this magnetic moment is

$$B = \frac{\mu_0 m_z}{2\pi z_r^3} = \frac{\mu_0}{2\pi z_r^3} \frac{\pi^2 b^4 \mu H_1 n_z^2 \dot{I}_0}{R}\, H(t)(1 - e^{-Rt/L}) \tag{A.6}$$

in the same direction as the inducing H. Assuming this field approximately constant across the area πa_r^2 of the receiver coil, the induced voltage in the receiver coil must be

$$V_r = -\pi a_r^2 \frac{d}{dt}\left(\frac{\mu_0}{2\pi z_r^3} \frac{\pi^2 b^4 \mu H_1 n_z^2 \dot{I}_0}{R}\, H(t)(1 - e^{-Rt/L}) \right) \tag{A.7}$$

The minus sign is to be interpreted as meaning that this voltage would drive a current in the receiver coil in a sense *opposite* to the sense of circulation of the rate of change of current in the transmitter coil. Again, we can use reciprocity to replace z_r^3 by the more accurate $(z_r^2 + a_r^2)^{3/2}$ to give

$$V_r = -\pi a_r^2 \frac{\mu_0}{2\pi (z_r^2 + a_r^2)^{3/2}} \frac{\pi^2 b^4 \mu H_1 n_z^2}{R}\, \dot{I}_0 \frac{d}{dt}\left(H(t)(1 - e^{-Rt/L}) \right) \tag{A.8}$$

where the magnetic induction at the target generated by a unit current in the receiver coil is

$$B_1 = \frac{\mu}{2} \frac{a_r^2}{(z_r^2 + a_r^2)^{3/2}} \tag{A.9}$$

so that

$$V_r = -\frac{\mu_0 \pi^2 b^4 B_1 H_1 n_z^2}{R} \dot{I}_0 \frac{d}{dt} H(t) \left((1 - e^{-Rt/L}) \right) \tag{A.10}$$

In terms of the formalism in section (6.4), this can be written as

$$V = -\frac{\mu_0 \pi^2 b^4 \dot{I}_0}{L} e^{-Rt/L} (\mathbf{H}_t \cdot \mathbf{n})(\mathbf{B}_r \cdot \mathbf{n}) \, H(t) \tag{A.11}$$

where $\mathbf{H}$ and $\mathbf{B}$ are unit current transmitter field and receiver induction at the target, and $\dot{I}_t$ is the slope of the triangular transmitter current waveform. Fourier transforming this yields

$$V(\omega) = -\frac{\mu_0 \pi^2 b^4 \dot{I}_0}{j\omega L + R} (\mathbf{H}_t \cdot \mathbf{n})(\mathbf{B}_r \cdot \mathbf{n}) \tag{A.12}$$

This is the response to a transmitter current waveform whose slope goes from zero to $\dot{I}_0$ at time zero, whose Fourier transform is therefore

$$I(\omega) = -\frac{\dot{I}_0}{\omega^2} \tag{A.13}$$

The transimpedance of the ring target is therefore

$$Z(\omega) = -\frac{\omega^2 \mu_0 \pi^2 b^4}{R + j\omega L} (\mathbf{H}_t \cdot \mathbf{n})(\mathbf{B}_r \cdot \mathbf{n}) \tag{A.14}$$

Bibliography

[1] R.C. Bailey and G.F. West. Characterizing mine detector performance over difficult soils. In *Detection and Remediation Technologies for Mines and Minelike Targets XI, DSS06 Defense and Security Symposium*, 2006.

[2] F.S. Grant and G.F. West. *Interpretation theory in applied geophysics.* McGraw-Hill, 1965.

[3] G.F. West and R.C. Bailey. Spectral representation, a core aspect of modelling the response characteristics of time-domain emi mine detectors. In *Detection and Remediation Technologies for Mines and Minelike Targets XI, DSS06 Defense and Security Symposium*, 6217-3, 2006.

Index

DOCUMENT CONTROL DATA

(Security classification of title, body of abstract and indexing annotation must be entered when the overall document is classified)

1. ORIGINATOR (the name and address of the organization preparing the document. Organizations for who the document was prepared, e.g. Establishment sponsoring a contractor's report, or tasking agency, are entered in Section 8.)

Department of Physics, University of Toronto
60 Saint George Street
Toronto ON M5S 1A7

2. SECURITY CLASSIFICATION
(overall security classification of the document, including special warning terms if applicable)

Unclassified

3. TITLE (the complete document title as indicated on the title page. Its classification should be indicated by the appropriate abbreviation (S, C or U) in parentheses after the title).

Project to Study Soil Electromagnetic Properties – Final Report (U)

4. AUTHORS (Last name, first name, middle initial. If military, show rank, e.g. Doe, Maj. John E.)

Bailey, Richard C. and West, Gordon F.

5. DATE OF PUBLICATION (month and year of publication of document)

September 2007

6a. NO. OF PAGES (total containing information, include Annexes, Appendices, etc) 206

6b. NO. OF REFS (total cited in document) 17

7. DESCRIPTIVE NOTES (the category of the document, e.g. technical report, technical note or memorandum. If appropriate, enter the type of report, e.g. interim, progress, summary, annual or final. Give the inclusive dates when a specific reporting period is covered.)

Contract Report

8. SPONSORING ACTIVITY (the name of the department project office or laboratory sponsoring the research and development. Include the address.)

9a. PROJECT OR GRANT NO. (If appropriate, the applicable research and development project or grant number under which the document was written. Please specify whether project or grant.)

9b. CONTRACT NO. (If appropriate, the applicable number under which the document was written.)

W7702-03-R942

10a. ORIGINATOR'S DOCUMENT NUMBER (the official document number by which the document is identified by the originating activity. This number must be unique to this document.)

DRDC Suffield CR 2009-051

10b. OTHER DOCUMENT NOs. (Any other numbers which may be assigned this document either by the originator or by the sponsor.)

11. DOCUMENT AVAILABILITY (any limitations on further dissemination of the document, other than those imposed by security classification)

(x) Unlimited distribution
( ) Distribution limited to defence departments and defence contractors; further distribution only as approved
( ) Distribution limited to defence departments and Canadian defence contractors; further distribution only as approved
( ) Distribution limited to government departments and agencies; further distribution only as approved
( ) Distribution limited to defence departments; further distribution only as approved
( ) Other (please specify):

12. DOCUMENT ANNOUNCEMENT (any limitation to the bibliographic announcement of this document. This will normally corresponded to the Document Availability (11). However, where further distribution (beyond the audience specified in 11) is possible, a wider announcement audience may be selected).

Unlimited

13. ABSTRACT (a brief and factual summary of the document. It may also appear elsewhere in the body of the document itself. It is highly desirable that the abstract of classified documents be unclassified. Each paragraph of the abstract shall begin with an indication of the security classification of the information in the paragraph (unless the document itself is unclassified) represented as (S), (C) or (U). It is not necessary to include here abstracts in both official languages unless the text is bilingual).

The research covered in this contract is directed to improving the effectiveness of EMI mine detectors of the kinds typically used in humanitarian demining. More specifically, it focuses on the effect of "difficult" (ferromagnetic mineral containing) soils on performance of the detectors. It began with a period of exploratory studies and goal identification; with the objectives then being specified more clearly. Originally, the main objective was a computer modelling code which could also model the problematic soils. The chief variation from that plan was inclusion of an instrument development and a sample measurement phase. Originally, the program was intended to finish by 31 March 2006, but because of the success of the instrument phase, it was extended an additional year to allow for construction of two additional instruments for delivery to the Scientific Authority, and also to allow results of earlier phases to be incorporated into the modelling code.

The overall purpose of the project is to facilitate the design of electromagnetic induction (EMI) mine detectors for humanitarian demining purposes. The specific aim is to help designers optimize the ability of these devices to detect low metal, anti-personnel mines in what are called "difficult" soils (considered here mainly to be those soils that contain appreciable quantities of electromagnetically lossy ferromagnetic minerals).

Present day EMI mine detectors are already very refined devices. If one is to improve them appreciably, one must not only be able to simulate a hypothetical instrument's response to typical target objects but also be able to simulate typical kinds of interference arising from the earth environment. From a theoretical point of view, creation of the simulation code is a technically complicated but feasible task. However, the code can only serve its purpose if enough quantitative information is available not only to describe the metal objects typically found in anti-personnel mines but also the electromagnetic properties of the soils in which they are found. It was to get some initial observational data for this that an instrument development part was included in the project.

14. KEYWORDS, DESCRIPTORS or IDENTIFIERS (technically meaningful terms or short phrases that characterize a document and could be helpful in cataloguing the document. They should be selected so that no security classification is required. Identifies, such as equipment model designation, trade name, military project code name, geographic location may also be included. If possible keywords should be selected from a published thesaurus, e.g. Thesaurus of Engineering and Scientific Terms (TEST) and that thesaurus-identified. If it is not possible to select indexing terms which are Unclassified, the classification of each should be indicated as with the title.)

Electromagnetic Induction, metal detector, land mines, demining, induction spectrometer, complex magnetic susceptibility soil

Defence R&D Canada

Canada's Leader in Defence
and National Security
Science and Technology

R & D pour la défense Canada

Chef de file au Canada en matière
de science et de technologie pour
la défense et la sécurité nationale

www.drdc-rddc.gc.ca